STUDY OF HEAT PIPE HEAT EXCHANGER FOR LOW TEMPERATURE WASTE HEAT RECOVERY APPLICATION

By

Sakil Hossen
Student No. 0416102087

MASTER OF SCIENCE IN MECHANICAL ENGINEERING

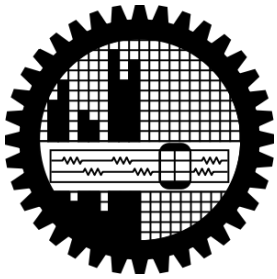

Department of Mechanical Engineering
Bangladesh University of Engineering and Technology

January 2019

The thesis titled 'STUDY OF HEAT PIPE HEAT EXCHANGER FOR LOW TEMPERATURE WASTE HEAT RECOVERY APPLICATION', submitted by **Sakil Hossen**, Student no: **0416102087**, Session: April 2016 has been accepted as satisfactory in partial fulfillment of the requirement for the degree of **Master of Science in Mechanical Engineering** on January 26, 2019.

BOARD OF EXAMINERS

1. _____
Dr. A. K. M. Monjur Morshed — **Chairman**
Associate Professor
Department of ME, BUET, Dhaka.

2. _____
Dr. Md. Ashraful Islam — **Member**
Professor and Head (Ex-Officio)
Department of ME, BUET, Dhaka.

3. _____
Dr. Md. Zahurul Haq — **Member**
Professor
Department of ME, BUET, Dhaka.

4. _____
Dr. Mohammad Nasim Hasan
Professor — **Member**
Department of ME, BUET, Dhaka.

5. _____
Dr. A. K. M. Sadrul Islam
Former Professor — **Member**
Department of ME, BUET, Dhaka. (External)
Apt. No. 4, House No. 110
Road No. 9/A, Dhanmondi, Dhaka.

CANDIDATE'S DECLERATION

This is to certify that this thesis titled "Study of Heat Pipe Heat Exchanger for Low Temperature Waste Heat Recovery Application" is carried out by the author Sakil Hossen under the supervision of Dr. A. K. M. Monjur Morshed, Associate professor, Department of Mechanical Engineering, BUET.

This is hereby declared that this thesis or any part of it has not been submitted elsewhere for the award of any degree or diploma.

_____

Sakil Hossen
Student No. 0416102087

ACKNOWLEDGEMENTS

First of all I am grateful to the Almighty for giving me the patience and strength to complete this work. This thesis is prepared under constant and keen supervision of Dr. A. K. M. Monjur Morshed, Associate Professor, Department of Mechanical Engineering, BUET. I would like to express my deep and sincere gratitude to him. His wide knowledge and logical way of thinking have been of great value for me. His understanding, encouraging and personal guidance have provided a good basis for the thesis.

I would like to express my gratefulness to the instructor of Welding and Sheet metal shop, Machine shop, Heat transfer laboratory, Fuel testing laboratory, Instrumentation and Measurement laboratory, Production process laboratory for their constructive assistance and advice that inspired to achieve the goal.

I also like to express my gratitude to the Departmental Library of Mechanical Engineering for its copious collection of Books, Journals and Research papers.

Finally, I owe my warm thanks to my friends and family. Without their encouragement and understanding, it would have been impossible for me to finish this work.

ABSTRACT

Due to environmental concern and high price of fuel, waste heat recovery has become a very crucial issue for the industrial and commercial energy users. As a large portion of this waste heat comes out as a low-grade energy, conventional energy recovery technology can't be employed to recover this waste energy economically. Heat pipe heat exchanger (HPHE) is an alternative technology that can be employed to recover this low grade waste energy. In this study, performance of an air-to-air HPHE has been studied experimentally. The HPHE consisting of number of heat pipes (thermosyphon) was constructed in a shop without any sophisticated equipment using copper tube and distilled water as the working fluid.

Performance of the heat pipe was experimentally investigated for different working fluid, filling ratio and adiabatic length. Among the studied parameters, water was found superior over ethanol as the working fluid and heat pipe with 50% filling ratio shows better performance compared to that of other filling ratios. Shorter adiabatic length enhances heat transfer performance and the best performance was found for the heat pipe without adiabatic section. The best performer heat pipe with optimized parameters was selected for the construction of air-to-air HPHE. The constructed HPHE was placed between two ducts carrying hot and cold air.

Temperature of the hot and cold air was varied to resemble two types of waste heat recovery applications: (i) low grade waste heat recovery applications where hot air was at □70°C and cold air was at atmospheric temperature of □35°C (ii) HVAC waste heat recovery application where hot air was at atmospheric temperature of ~35°C and cold air was at □25°C. Performance of the HPHE was evaluated by analyzing heat transfer rate, heat transfer coefficient, effectiveness and NTU under different mass flow rate of air. The results indicate that HPHE can recover waste heat from a small temperature difference in both low and moderate temperature applications. At moderate temperature application, about 800W energy was recovered by HPHE when hot fluid temperature was 70°C and cold fluid temperature was at 30°C and at low temperature application, about 200W energy was recovered when hot fluid temperature was at 40°C and cold fluid at 22°C. Financial analysis also has been conducted for the HPHE and average payback period has been estimated with the current energy prices as 3.3 years for the moderate temperature application and 8.2 years for the HVAC waste heat recovery application.

Table of Contents

Abstract v
List of Figures ix
List of Tables xii
Chapter 1 Introduction 1
1.1 Motivation 2
1.2 Objectives 3
1.3 Scope of the Thesis 3
Chapter 2 Literature Review 5
2.1 Introduction 6
2.2 Heat Pipe Technology 6
2.3 Different Types of Heat Pipes 7
2.3.1 Conventional Heat Pipe (CHP) 7
2.3.2 Two-Phase Closed Thermosyphon (TPCT) 7
2.3.3 Oscillating Heat Pipe (OHP) or Pulsating Heat Pipe (PHP) 8
2.4 Some Other Types of Heat Pipes 10
2.4.1 Vapor Chamber or Flat Heat Pipes 11
2.4.2 Variable Conductance Heat Pipes (VCHPs) 11
2.4.3 Pressure Controlled Heat Pipes (PCHPs) 12
2.4.4 Diode Heat Pipes 13
2.4.5 Rotating Heat Pipes 14
2.4.6 Loop Heat Pipe 15
2.5 Heat Pipe Characteristics Analysis 16
2.5.1 Study on the effect of heat pipe material 17
2.6.1 Cooking 23
2.6.2 Spacecraft 23
2.6.3 Computer and Electronic Device 24
2.6.4 Solar Thermal 24
2.6.5 Heat Pipes in Air-Conditioning and Waste Heat Recovery Systems 25
2.7 Present Work 27
Chapter 3 Performance Assessment of Heat Pipe (Thermosyphon) 28
3.1 Factors Affecting the Thermal Performance of Heat Pipe (Thermosyphon) 29

3.2 Selection of Heat Pipe Material and Working Fluid 29
3.3 Design and Fabrication of Heat pipe 31
3.3.1 Design procedure 31
3.4 Calculation of Heat Transfer Limits 32
3.4.1 Sonic Limit 32
3.4.2 Boiling Limit 33
3.4.3 Entrainment Limit or Flooding Limit 34
3.4.4 The Dry-out Limit 34
3.5 Fabrication 36
3.6 Study of the Effectiveness of Heat Pipe 37
3.6.1 Thermal Resistance of Heat Pipe Filled with Water 38
3.6.2 Thermal Resistance of Normal Copper Pipe Filled with Air 43
3.7 Performance Study of Water and Ethanol 46
3.8 Performance Study of Heat Pipe for Different Filling Ratio 47
Chapter 4 48
Effect of Adiabatic Section on the Performance of Heat Pipe Heat Exchanger 48
4.1 Introduction 49
4.2 Calculation of heat pipe length 49
4.2.1 Heat pipe effective length 52
4.3 Previous study regarding effect of adiabatic section on heat pipe performance 53
4.4 Present Study 56
4.5 Experimental Setup 56
4.6 Data Acquisition System 60
4.7 Experimental Method 61
4.8 Data Reduction 62
4.9 Uncertainty Analysis 62
4.10 Results and Discussion 63
4.10.1 Effect of Adiabatic Section Length 63
4.10.2 Effect of Changing the Position of Adiabatic Section 65
4.10.3 Effectiveness 67
Chapter 5 HPHE Design and Performance Study 69
5.1 Mathematical Model of HPHE 70

5.1.1 Convection Resistance 70
5.1.2 Conduction Resistance 70
5.1.4 Heat Duty ($\dot{Q}$) 71
5.1.5 HPHE Design 71
5.2 Experimental Setup 74
5.2.1 Construction of Heat Pipe Heat Exchanger 74
5.2.2 Test Section 75
5.2.3 Experimental Method 76
5.3 Data Acquisition System 77
5.3.1 Measurement of Flow Rates 77
5.3.2 Measurement of Temperature 78
5.4 Data Analysis 79
5.5 Uncertainty Analysis 81
5.6 Performance of HPHE at Moderate Temperature 84
5.6.1 Heat Transfer Rate ($\dot{Q}$) 84
5.6.2 Overall Heat Transfer Coefficient (U) 85
5.6.3 Effectiveness ($\boldsymbol{\varepsilon}$) 86
5.6.4 NTU 87
5.7 Performance of HPHE at Low Temperature 89
5.7.1 Heat Transfer Rate ($\dot{Q}$) 89
5.7.2 Overall Heat Transfer Coefficient (U) 90
5.7.3 Effectiveness ($\boldsymbol{\varepsilon}$) 91
5.7.4 NTU 92
Financial Analysis 93
5.8.1 Financial Analysis for Moderate Temperature Application 93
5.8.2 Financial Analysis for Low Temperature Application 94
Chapter 6 Conclusions 95
References 98
Appendix 104
Appendix-A: Experimental data 105
Appendix-B 117
Sample Calculation 117

Measured Data for water-to-water HPHE....117
Calculated Data for water-to-water HPHE....117
Measured Data for Air-to-Air HPHE....121
Calculated Data for Air-to-Air HPHE....122
Uncertainty Analysis....124

List of Figures

Figure 1: Conventional heat pipe (CHP) [10]....7
Figure 2: (a) Two-phase closed thermosyphon, (b) Comparison between TPCT and CHP [11] 8
Figure 3: (a) Closed-loop oscillating heat pipe (CLOHP), (b) Closed-loop oscillating heat pipe with check valves (CLOHP/CV), (c) Closed-end oscillating heat pipe (CEOHP) [11] 9
Figure 4: Flat heat pipes [15]....11
Figure 5: Variable conductance heat pipe [16] 12
Figure 6: Pressure controlled heat pipe (PCHP) [17] 13
Figure 7: Diode heat pipe [18]....14
Figure 8: Rotating heat pipe (RHP) [19]....15
Figure 9: Working principle of loop heat pipe [20] 15
Figure 10: Thermal magic cooking pin [43]....23
Figure 11: Heat pipe cooling device [45]....24
Figure 12: (a) Copper Pipe processing for heat pipe; (b) Working fluid inserting 36
Figure 13: Heat pipe performance compared to the solid copper pipe....37
Figure 14: Thermal resistance of heat pipe....38
Figure 15: Thermal resistance of normal copper pipe 43
Figure 16: Heat pipe performance test....46
Figure 17: Variation of top end temperature with time....46
Figure 18: Variation of top end temperature with time for different filling ratio 47
Figure 19: Total, evaporation zone and condensation zone characteristic lengths [62] 50
Figure 20: Length of the condensation zone and total length versus the outlet air temperature, for different outlet temperatures of gases [62]....52

Figure 21: Capillary pressure, differences in liquid pressure, vapor, and maximum heat versus the adiabatic length [66].....54

Figure 22: Variation in entropy generation rate against heat load for different lengths of adiabatic section [67].....55

Figure 23: Performance at different heat input and cooling water flow rate [69].....56

Figure 24: Schematic diagram of experimental setup of HPHE.....57

Figure 25: (a) Steel Plate; (b) Acrylic Sheet.....57

Figure 26: (a) Heat pipes assembly on Steel Plate; (b) Heat pipes assembly on Acrylic Sheet.....58

Figure 27: (a) Heat pipe with separation Plate; (b) & (c) Total assembly of water-to-water HPHE without adiabatic section.....58

Figure 28: Variation of adiabatic length; (a) 32 mm adiabatic length; (b) 64 mm adiabatic length; (c) 96 mm adiabatic length.....59

Figure 29: Insulation of adiabatic section.....59

Figure 30: HPHE with different position of adiabatic section; (a) adiabatic section 32 mm upward from the center of the heat pipe; (b) adiabatic section 64 mm upward from the center of the heat pipe; (c) adiabatic section 32 mm downward from the center of the heat pipe.....60

Figure 31: Measurement of Temperature by thermocouple and selector switch.....60

Figure 32: Effect of increasing the adiabatic section length with cold water mass flow rate and heat transfer rate.....65

Figure 33: Effect of evaporation and condensation section with changing the position of adiabatic section.....67

Figure 34: Effectiveness of the heat pipe for different adiabatic section.....68

Figure 35: The designed heat exchanger.....74

Figure 36: Layout of pipes (a) Designed (top view), (b) Actual (front view).....75

Figure 37: Inlet of the hot air section.....75

Figure 38: Experimental setup for a heat pipe heat exchanger (a) Designed, (b) Actual.....76

Figure 39: Regulation of hot and cold air respectively by using (a) FD fan, (b) Bypass system.....77

Figure 40: Measurement of air flow rate at different positions.....78

Figure 41: Measurement of temperature by thermocouple and selector switch.....78

Figure 42: Flow through the heat exchanger.....79

Figure 43: Variation of heat transfer rate with air mass flow rate at moderate temperature difference.....84

Figure 44: Variation of overall heat transfer co-efficient with change of air mass flow rate at moderate temperature difference 86

Figure 45: Variation of effectiveness of HPHE with air mass flow rate at moderate temperature difference 87

Figure 46: Variation of effectiveness of HPHE with NTU at moderate temperature difference 88

Figure 47: Variation of heat transfer rate with air mass flow rate at low temperature difference 89

Figure 48: Variation of overall heat transfer co-efficient with change of air mass flow rate at low temperature difference 90

Figure 49: Variation of effectiveness of HPHE with air mass flow rate at low temperature difference 91

Figure 50: Variation of effectiveness of HPHE with NTU at low temperature difference 92

List of Tables

Table 1.1: Previous study regarding heat pipe materials 17

Table 2: Previous study regarding heat pipe working fluids 18

Table 3: Previous study regarding heat pipe working fluids filling ratio 20

Table 4: Study regarding nanofluid as the working fluid 22

Table 5: Working fluid and envelope compatibility, with practical temperature limits [56] ... 30

Table 6: Specification of wickless heat pipe 31

Table 7: Working fluid properties used in wickless heat pipe [57] 32

Table 8: Calculated heat transfer limits 36

Table 9: Uncertainty propagated into the calculated values 63

Table 10: Values of uncertainty for different parameters 83

Table 11 : Data used for the financial analysis for moderate temperature application 93

Table 12 : Financial analysis for moderate temperature application 93

Table 13 : Data used for the financial analysis for moderate temperature application 94

Table 14 : Financial analysis for moderate temperature application 94

Table 15: Description of water to water HPHE 105

Table 16: Measured data for thermal performance of HPHE without adiabatic section 105

Table 17: Measured data for thermal performance of HPHE with adiabatic section 1/9th of heat pipe 106

Table 18: Measured data for thermal performance of HPHE with adiabatic section 1/4 th of heat pipe 106

Table 19 : Measured data for thermal performance of HPHE with adiabatic section 1/3th of heat pipe 107

Table 20: Measured data for thermal performance of HPHE with adiabatic section 32 mm downward from the middle 107

Table 21: Measured data for thermal performance of HPHE with condensation section 32 mm upward from the middle 108

Table 22: Measured data for thermal performance of HPHE with condensation section 64 mm upward from the middle 108

Table 23: Description of Air to Air HPHE 109

Table 24: Measured data for waste heat recovery 109

Table 25: Calculated data for waste heat recovery 110

Table 26: Measured data for air conditioning system 111

Table 27: Calculated data for air conditioning system.....112
Table 28: Percentage uncertainty in different parameters for waste heat recovery 114
Table 29: Percentage uncertainty in different parameters for air conditioning system 115

Chapter 1

Introduction

Heat pipe heat exchanger (HPHE) is a special type of heat exchanger consisting of a desired number of heat pipes. In HPHE thermal energy is exchanged between two fluid streams by means of phase change heat transfer inside the copper tube rather than only convective heat transfer. As the latent heat of evaporation of a liquid is high, large amount of heat can be transferred efficiently by heat pipe heat exchanger with a moderate temperature gradient.

1.1 Motivation

Waste heat recovery (WHR) is essential for increasing energy efficiency. At present, about 20 to 50% of energy used in the industrial sector is rejected as waste heat [1]. Waste heat can be recovered directly (without using a heat exchanger e.g., recirculation) or indirectly (via a Heat Exchanger). Direct heat recovery is often the cheaper option but its use is restricted by location and contamination considerations. In indirect heat recovery, the two fluid streams are separated by a heat transfer surface, which can be categorized as either a passive or active heat exchanger. Passive heat exchangers require no external energy input (*e.g.* shell and tube heat exchanger, plate heat exchanger, etc.) whilst active heat exchangers require energy input (*e.g.* thermal wheel, heat pump, etc.).Waste heat can be considered as either low grade (<100°C), medium grade (100°C–400°C) or high grade (>400°C) [2]. In general, high grade waste heat is mainly limited to the iron and steel, glass, nonferrous metals, bricks and ceramics industries. Medium grade waste heat is most widely found in the chemicals, food and drink, and other process industries, as well as building utilities. Low grade waste heat can be found virtually in all areas of industry and buildings ventilation or hot water systems. With the increase of fuel price and environmental concern, waste energy recovery is becoming popular. Waste heat recovery system and technology is well established for the high quality waste energy sources whereas for the low grade energy sources, heat recovery is not popular due to technological and economical limitations. There are many WHR methods and technologies that have been employed at various stages of waste energy recovery applications. All the traditional process and the techniques are unique and are not sufficiently capable of capturing this low grade waste energy from small temperature difference. Therefore, until now this valuable energy has gone unrecovered, often vented to atmosphere. To recover this low grade waste heat from lower and moderate temperatures sources, heat pipe heat exchanger (HPHE) is an efficient way as heat pipe can extract a large amount of energy with a very limited temperature differences. Waste heat recovery by heat pipe heat exchanger (HPHE) is newer method and acts as a passive heat exchanger. HPHE design, combined with manufacturing techniques has enabled to reliably recover energy offering low

risk, low cost, easy maintenance and high value energy recovery where other heat exchangers repeatedly fail.

In a recent studies by the ADB reveals that average potential for energy savings in the industrial sector of Bangladesh is 25% and it accounts 32% for the textile, garments and leather industry [3]. A large portion of the waste energy from this industry is coming from boiler exhaust, stenter machine exhaust, dryer machine exhaust, etc. where waste heat comes at less than 100^{o}C. HPHE is not common in Bangladesh and effectiveness of this heat exchanger over this applicable low temperature ranges are yet to be investigated.

In this study, efforts have been made to evaluate the performance of the HPHE for low temperature process application and waste heat recovery from the air conditioned space.

1.2 Objectives

The objectives of this study are described below:

- To design and construct a single heat pipe that can be constructed at the ordinary workshop
- To compare heat transfer performance of a heat pipe with a normal copper pipe.
- To evaluate performance of heat pipe with different working fluid and filling ratio.
- To evaluate performance of heat pipe by varying the adiabatic section and also the evaporation and condensation section.
- To design, construct and evaluate the performance of HPHE at lower and moderate temperature application.

1.3 Scope of the Thesis

The study presented in this exposition has addressed the experimental investigation of heat pipe heat exchanger for waste heat recovery at low temperature and moderate temperature. The dissertation has been described as follows:

Chapter 1 expresses the motivation, objectives and general concepts of heat pipe.

Chapter 2 consists of a detail literature review about heat pipe and their application as HPHE by different researchers across the globe. It also presents the detail information about heat pipe history, classification and application.

Chapter 3 describes and analyses about the factors affecting heat pipe's thermal performance, *i.e.* material of the heat pipe, working fluid, filling ratio, effect of adiabatic length, and evaporation and condensation length.

Chapter 4 describes the mathematical model for design of the HPHE for air-air application. This chapter also includes construction and assembly process of the heat exchanger.

Chapter 5 presents the performance and effectiveness of heat pipe heat exchanger at the desired operating temperature range. This chapter also discusses about its application in waste heat recovery applications.

Chapter 6 represents the conclusion of the current study and also put direction about its extension towards future research.

References and appendices are added at the end of the thesis.

Chapter 2

Literature Review

2.1 Introduction

Waste heat recovery by heat pipe heat exchanger (HPHE) is an excellent way of saving energy and cost, reducing global warming and air pollution. HPHE has various applications due to its low operating cost, easy maintenance, long service life, flexibility and reliability over other traditional heat exchangers. The unique feature of HPHE provides an extremely efficient technique to transfer of energy which is 1000 times more efficient than solid pipe and 35% more efficient than other traditional heat exchanger [4]. A large number of researches have been carried out on theory, design and construction of heat pipes, especially their use in heat pipe heat exchanger.

2.2 Heat Pipe Technology

The first idea of heat pipe come out from Angier March 'AM' Perkin [5], who in 1831 took out a patent on a 'hermetic boiler tube'. He works with the idea of a working fluid for a single phase device at a high pressure. Later the descendant of Jacob Perkins [6], in 1936 was granted a patent on the Perkins Tube in which a long, twisted tube filled with water was passed over an evaporator and then a condenser. This progression utilized water functioned in two phases inside the tube where liquid turning to steam. These early design depended on gravity so that the condensed water would travel back to the evaporator; they were the precursor to the present heat pipe technology.

However, the concept of the modern heat pipe was introduced by R.S. Gaugler [7] of the General Motors Corporation in 1944. He patented a light-weight heat transfer mechanism that was originally designed for a refrigeration system. The concept of using a wick instead of gravity, inside the tube for returning the condensate fluid into evaporator was added by him. However, during that period there was no essential need for such a device, so no further development was progressed for about twenty years.

After the gaps of two decades in 1962, G.M Grover and his co-workers [8] from the Los Alamos Scientific Laboratory rediscovered the idea of heat pipe technology and newly built a prototype on the design and finally coined the name 'heat pipe'. In the first built heat pipe, water was used as the working fluid and then several tests were performed by inserting other working fluid depending on the operating temperature range. By this time the technology of heat pipe was established as useful in different industries and it became popular and very soon explored by many researchers and scientists across the world.

Throughout 1969, different organizations like NASA and other aircraft business industries showed their interest in using heat pipe. Heat pipe got application in the space program for controlling the temperature of spacecraft [9]. Starting in 1980s, Sony Corporation began incorporating heat pipes commercially in their electronic products such as receivers and amplifiers applications; afterwards use of heat pipe spread out rapidly to other high heat flux electronics components. During late 1990s, the applications for patent of heat pipe increased with increasingly high heat flux microcomputer CPUs.

At present, Heat pipe technology has been widely used for controlling and solving the critical problems that has been arising in heat transfer and temperature controlling process.

2.3 Different Types of Heat Pipes

Three types of heat pipes are widely used in commercial and industrial application: (i) conventional heat pipe (CHP), (ii) two phase closed thermosyphon (TPCT) and (iii) oscillating heat pipe (OHP). According to their uses, performance of each heat pipe is better than other.

2.3.1 Conventional Heat Pipe (CHP)

In a Conventional Heat Pipe, heat enters in the evaporator section which generates vapor at a slightly higher pressure and temperature. The increased pressure causes vapor to flow along the pipe to the condenser section, where a slightly lower temperature causes the vapor to condense and release its latent heat of vaporization. The condensed fluid returns to the evaporator section through the capillary action of the wick in the CHP.

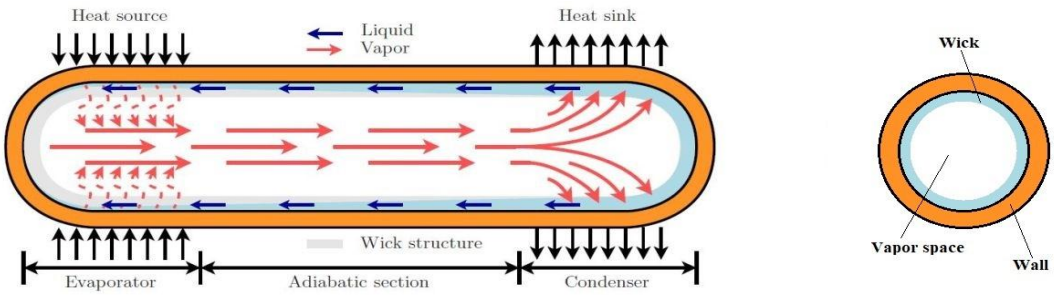

Figure 1: Conventional heat pipe (CHP) [10]

2.3.2 Two-Phase Closed Thermosyphon (TPCT)

TPCT is a high performance heat transfer device which can transfer a large amount of heat at a high temperature rate with a small temperature difference. A Two-phase Closed Thermosyphon **(**TPCT) uses gravity to transfer heat from a heat source that is located below

the cold sink. As a result, the evaporator section is situated below the condenser section. This heat pipe achieved its functionality by evaporation of the working fluid (A) in the evaporator section (B) and condensing the working fluid in the condenser section (C) and return of the condensate fluid to evaporation section (D) as presented the fig. 2 (a).

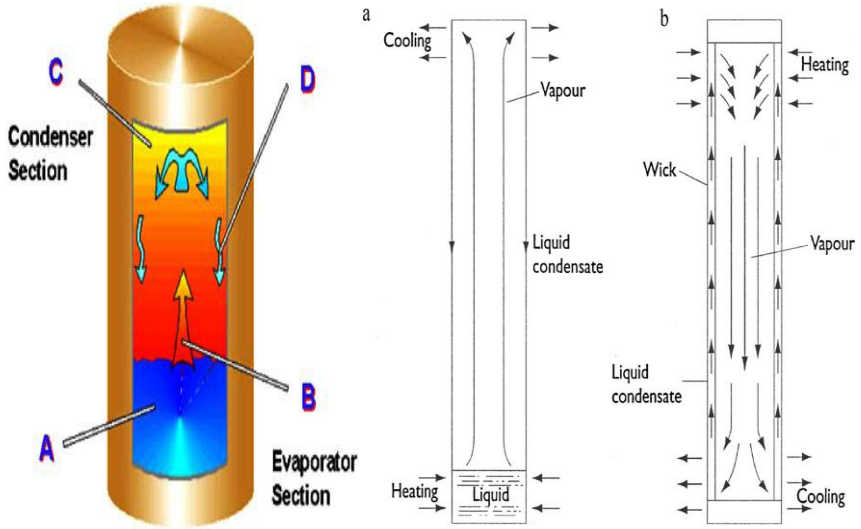

(a) **(b)**

Figure 2: (a) Two-phase closed thermosyphon, (b) Comparison between TPCT and CHP [11]

The difference between a CHP and a TPCT as shown in the fig. 2 (b) is that the TPCT uses gravity force to return the condensed fluid form the condensation section and it stands vertically where a CHP use capillary action with a wick structure inside to return the condensed fluid from condensation section and it stands both vertically and horizontally. TPCT are preferred as a better heat pipe compared to CHP because of the wicks that produces an additional resistance to the flow of condensate. MD Anwarul Hasan *et. al.* [12] investigated the performance of a gravity assisted heat pipe of diameter 12.5 mm and length 0.50 m using water as the working fluid. Experiment has been performed at various inclination angles and different heat flux input. The best performance of heat pipe is achieved at its vertical position where gravity serves to assist return of condensate from condenser to evaporator cause with the increase of inclination angle the thermal resistance increases.

2.3.3 Oscillating Heat Pipe (OHP) or Pulsating Heat Pipe (PHP)

Oscillating heat pipes (OHP), also referred to as pulsating heat pipes (PHP) is a relatively new development in the field of heat pipe technology. Originally developed and patented by Hisateru Akachi in 1990. The comparison between OHP with CHP and TPCT is that the working fluid inside the heat pipe of CHP and TPCT circulates continuously between the heat

source and the heat sink in the form of a counter current flow by capillary or gravity forces but the working fluid in an OHP oscillates in its axial direction and transfer heat with the phase change (evaporation and condensation) phenomena by oscillating movement of the fluid associated with heat pipe. The oscillating heat pipe is composed of a bundle of turns of one continuous small diameter capillary tube that allows the liquid and vapor plugs to coexist. The advantage of OHP is similar to the TPCT as here no wick structure uses to transport the liquid. The main disadvantage of OHP is that the overall resistance is typically greater, but it can be operated with larger heat fluxes.

The OHP can be formed into three main types. They are:

a) Closed-loop oscillating heat pipe (CLOHP)
b) Closed-loop oscillating heat pipe with check valves (CLOHP/CVs)
c) Closed-end oscillating heat pipe (CEOHP)

a) Closed-Loop Oscillating Heat Pipe (CLOHP)

A closed-loop oscillating heat pipe (CLOHP) has a long capillary tube with ‘n’ numbers of turn. The both ends of the tube connected together to form a closed loop. The heat is transferred by the oscillation of the working fluid in the direction of the longitudinal axis of the pipe with a super imposed bulk circulation in either direction. The CLOHP tends to have better thermal performance than other OHP devices due to the possibility of fluid circulation.

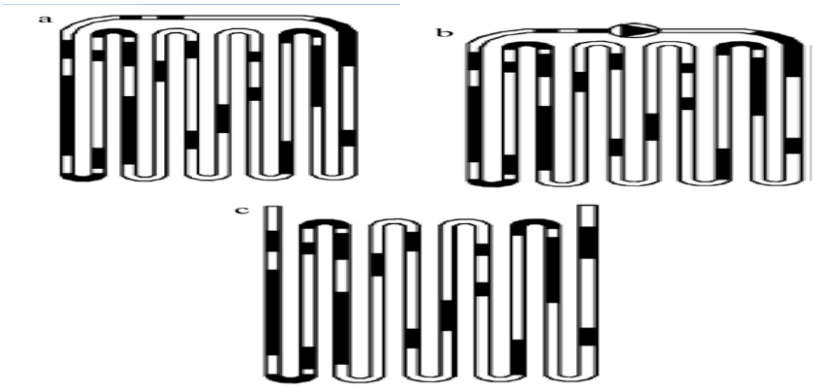

Figure 3: (a) Closed-loop oscillating heat pipe (CLOHP), (b) Closed-loop oscillating heat pipe with check valves (CLOHP/CV), (c) Closed-end oscillating heat pipe (CEOHP) [11]

b) Closed-Loop Oscillating Heat Pipe with Check Valves (CLOHP/CV)

The operating principles of CLOHP and CLOHP/CV are same rather it makes the working fluid move in a specific direction. A closed-loop oscillating heat pipe with check valves (CLOHP/CVs) is also made from a long capillary tube where a check valve is placed between the end joint of capillary tube. The check valves are a direction-control device restricting the

working fluid to circulate in one direction only. The addition of check valves increases heat transfer capability of the device, the miniaturization of the device makes it difficult and expensive to install. Md Shahidul Haque [13] analysis the thermal characteristics of an aluminum closed-loop pulsating heat pipe charged with ammonia to study the heat transfer performance of a closed loop pulsating heat pipe. The results show that, the performance of the heat pipe varies substantially for different inclinations and fill ratios and promote to further research to obtain maximum performance in practical application.

c) Closed-End Oscillating Heat Pipe (CEOHP)

In the closed-end oscillating heat pipe (CEOHP) the capillary tube is used which is closed in both ends without making any connection. The advantages of a CEOHP are its heat transfer properties in any orientation, its quick response and its internal wickless structure. Out of all types of OHP, CEOHP are the least complicated operating mechanism. The heat transfer in a CEOHP is such that, as heat is supplied at the evaporator, the vapor bubbles originate in the evaporator section through latent heat. These bubbles move to the condenser with buoyancy force producing pumping action. The Bubbles that flow into the condenser section collapse and the latent heat are released. The heat is transferred through phase change which is independent of temperature difference. The heat flux depends only on the evaporation, buoyancy force and condensation mechanism.

2.4 Some Other Types of Heat Pipes

Standard heat pipes act as thermal superconductors, transmitting heat with minimal temperature drop in both directions. By adding small amounts of Non-Condensable Gas (NCG) and modifying the heat pipe design, it is possible to create many heat pipe variations, such as:

- Vapor Chambers (planar heat pipes)
- Variable Conductance Heat Pipes (VCHPs)
- Pressure Controlled Heat Pipes (PCHPs)
- Diode Heat Pipes
- Rotating heat pipes
- Loop Heat Pipes

2.4.1 Vapor Chamber or Flat Heat Pipes

Vapor chamber is one of the highly effective thermally spread techniques used in electronics cooling. Vapor chamber heat spreaders are planar heat pipes that spread heat from concentrated heat source(s) to a large area heat sink with effective thermal conductivity greatly exceeding copper. In the most basic configuration, the vapor chamber consists of a sealed container, a wick formed inside wall of the container, and a small amount of fluid that is in equilibrium with its own vapor. As the heat is applied to one side of the vapor chamber (evaporator), the working fluid vaporizes and the vapor spreads to the entire inner volume and condenses over a much larger surface (condenser). The condensate is returned to the evaporator via capillary forces developed in the wick. Typical applications include cooling of electronic devices, both at package and system level, and cooling of power semi-conductors using heat sinks. The vapor chambers are being used in high-end gaming laptops as they are the best way to dissipate heat in high-end GPU's. As vapor chambers are slightly thicker than heat pipes, many manufacturers are avoiding it to keep the device slim and there are some vapor chambers which are just 0.4 mm thick. The vapor chamber being tested by manufacturers but till date, don't have any smart phone based on vapor chamber. Samsung introduced heat pipe in Samsung Galaxy S7 and has been used on all Samsung S and Note series devices to prevent overheating. As per Industry Insider, Samsung might adopt the vapor chamber in flagship devices which are scheduled to launch on 2019 [14].

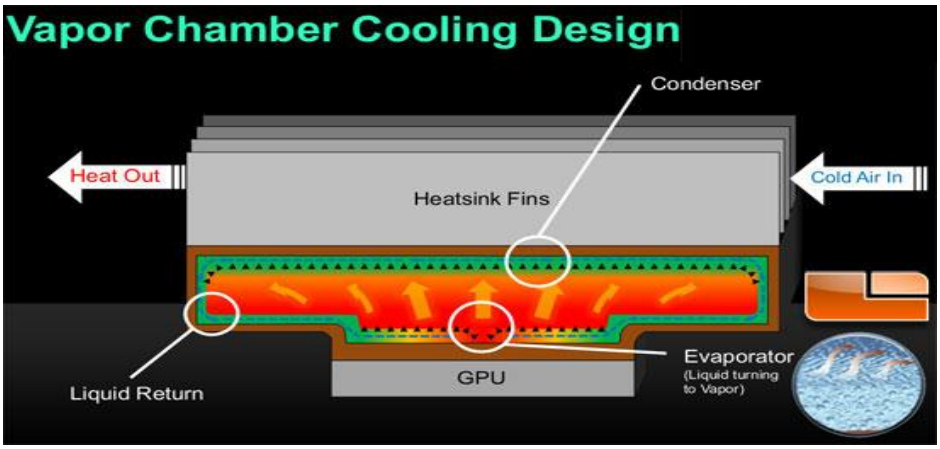

Figure 4: Flat heat pipes [15]

2.4.2 Variable Conductance Heat Pipes (VCHPs)

Variable Conductance Heat Pipes were discovered by an accident during root cause analysis (RCA) in the early 1960's. In a standard heat pipe, generally a two phase working fluid is

inserted and it consists of a wick for returning the condensate from the condenser to the evaporator. But for the variable conductance heat pipe (VCHP) a non-condensable gas inserted inside the heat pipe as well working fluid. Depending on the operating conditions, the NCG can block all, some, or none of the available condenser length. When the VCHP is operating, the NCG is swept toward the condenser end of the heat pipe by the flow of the working fluid vapor. At high powers, all of the NCG is driven into the reservoir, and the condenser is fully open as showed in fig.5. As the power is lowered, the vapor temperature drops slightly. Since the system is saturated, the vapor pressure drops at the same time. This lower pressure allows the NCG to increase in volume, blocking a portion of the condenser. At very low powers, the vapor temperature and pressure are further reduced, the NGC volume expands, and most of the condenser is blocked. This change in active condenser length minimizes the drop in evaporator and associated electronics temperatures over large changes in power and evaporator sink conditions. Variable Conductance Heat Pipes (VCHPs) are used to inertly maintain the temperature of the electronics being cooled as power and sink conditions change. Some applications, such as satellite or research balloon thermal control, where electron will be overcooled at low powers. Many of the benefits of the VCHP are the same as the standard heat pipe, while the only disadvantage over a standard heat pipe is a slight increase in design and fabrication costs.

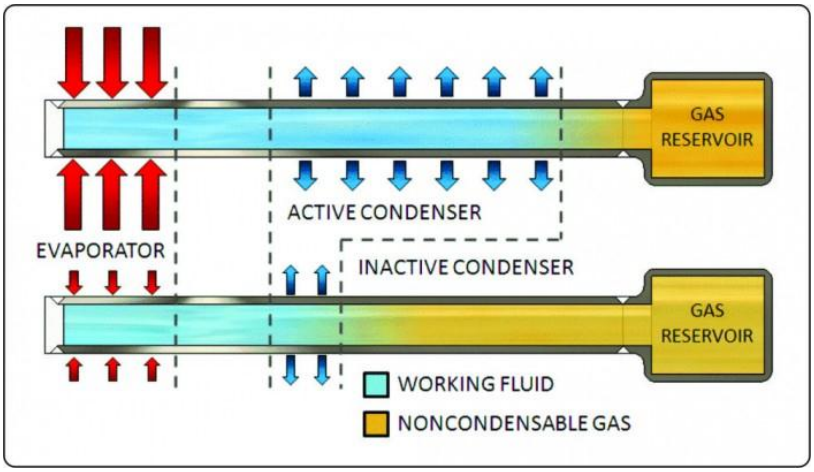

Figure 5: Variable conductance heat pipe [16]

2.4.3 Pressure Controlled Heat Pipes (PCHPs)

A Pressure Controlled Heat Pipe (PCHP) is a variation of a Variable Conductance Heat Pipe (VCHPs) where the amount of Non-Condensable Gas (NCG) or the reservoir volume is varied. Like a VCHP, the NCG is swept toward the condenser end of the heat pipe by the

flow of the working fluid vapor. The NCG then blocks the working fluid from reaching a portion of the condenser, inactivating a portion of the condenser. In a VCHP, the fraction of condenser blockage is determined by the reservoir size, the non-condensable gas charge, and the operating pressure, and cannot be adjusted once the VCHP is sealed. In difference, the condenser blockage in a PCHP is actively controlled by a bellows or piston. The operation of a bellows/piston type of PCHP is shown in fig. 6. Initially, the piston is withdrawn at higher powers, so that most of the condenser is open. When the heat load is reduced, the piston pushes additional gas into the condenser, helping to maintain the heat pipe at a constant temperature. While a VCHP passively increases the condenser blockage, PCHPs are able to react faster, and more precisely. The applications of PCHPs are for precise temperature control and high temperature power switching.

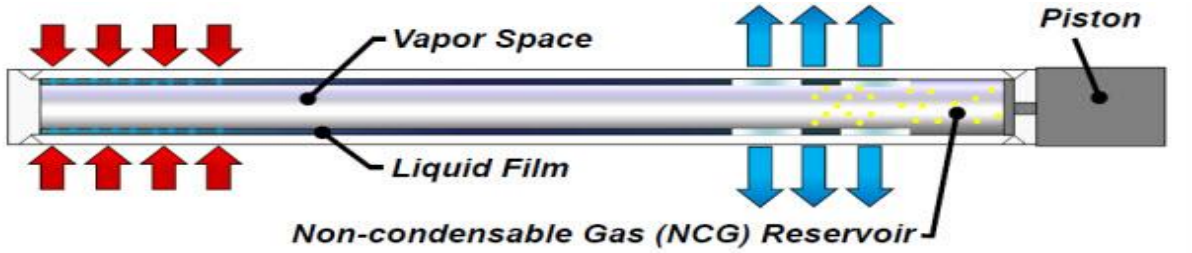

Figure 6: Pressure controlled heat pipe (PCHP) [17]

2.4.4 Diode Heat Pipes

Diode heat pipes act as a thermal diode, which transfer heat in one direction. It has a high thermal conductivity in the forward direction, and a low thermal conductivity in the reverse direction. Diode heat pipes are designed to allow the heat to flow from evaporator to condenser, while preventing flow in the reverse direction. For example, a thermosyphon act as a diode heat pipe which only transfer heat from the bottom to the top of the thermosyphon, When the thermosyphon is heated at the top, there is no liquid available to evaporate. There are two basic types of diode heat pipes (i) Liquid Trap Diodes (ii) Vapor Trap Diodes.

A Liquid Trap Diode has a wicked reservoir located at the evaporator end of the diode heat pipe. The wicks in the heat pipe and reservoir are designed so that they can't communicate with each other. During normal operation, the heat pipe behaves like a standard heat pipe. When the condenser becomes hotter than the evaporator/reservoir, the role of the evaporator and condenser are switched. Vapor evaporates from the hotter nominal condenser, and travels to the nominal evaporator and the reservoir, where it condenses. Since the reservoir wick doesn't communicate with the heat pipe wick, the reservoir quickly dries out, and becomes inactive.

A Vapor Trap Diode is fabricated in a similar fashion to a Variable Conductance Heat Pipe (VCHP). During fabrication, the heat pipe is charged with the working fluid and a controlled amount of a Non-Condensable Gas (NCG). During normal operation, the flow of the working fluid vapor from the evaporator to the condenser sweeps the NCG into the reservoir, where it doesn't interfere with the normal heat pipe operation. When the condenser becomes hotter than the evaporator, the vapor flow is from the nominal condenser to the nominal evaporator. The NCG is dragged along with the flowing vapor. In a few minutes, it completely blocks the evaporator, greatly increasing the thermal resistivity of the heat pipe.

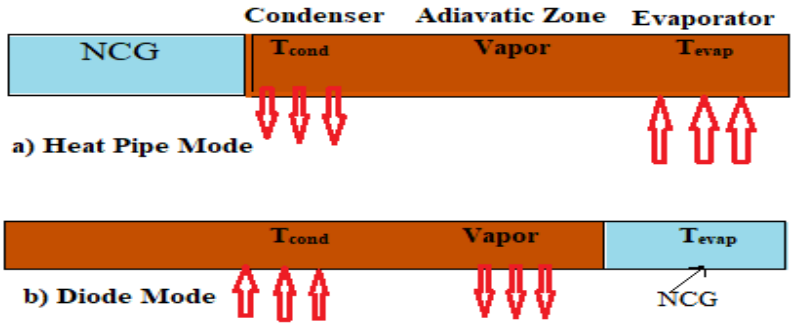

Figure 7: Diode heat pipe [18]

2.4.5 Rotating Heat Pipes

The rotating heat pipe (RHP) is a two phase heat transfer device that is designed to cool machinery by removing heat through a rotating shaft. Rotating heat pipe uses a centrifugal force where vapor travels evaporator to condenser and give up its heat by condensation then the liquid is return by a gravity force or wick. The inside diameter (I.D.) of evaporator is kept larger than the condenser inner diameter thus inside of a rotating heat pipe is a conical frustum. Heat generated in motors and other rotating machinery, e.g., electric motor/stator heat build-up, gear heat loads, bearing heat generation, etc. can be reduced by using this rotating heat pipe.

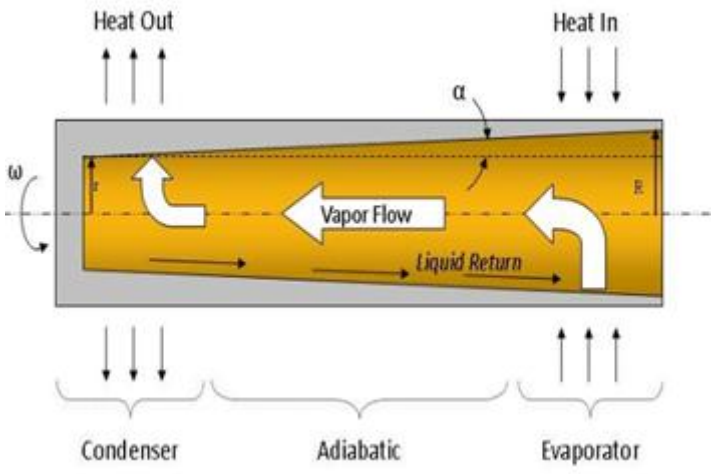

Figure 8: Rotating heat pipe (RHP) [19]

2.4.6 Loop Heat Pipe

Loop heat pipes (LHPs) are passive, two-phase heat transport devices. The technology was invented in the former Soviet Union in 1980s for spacecraft thermal control. Most current LHP uses ammonia as the working fluid and operate at temperatures between -40 and 70°C. Propylene and ethane have been used in LHPs operating at lower temperatures. Most current LHPs are fabricated with aluminum and stainless steel parts, neither of which is compatible with water. LHP is an efficient heat transfer device that could transport thermal energy over long distances, up to ten meters. It has some unique features over conventional heat pipe, e.g., gravity-unaffected and flexibility in its design and installation, which makes LHP particularly suitable for applications in solar water heating (SWH). The figures below illustrate the operating principles of a typical loop heat pipe.

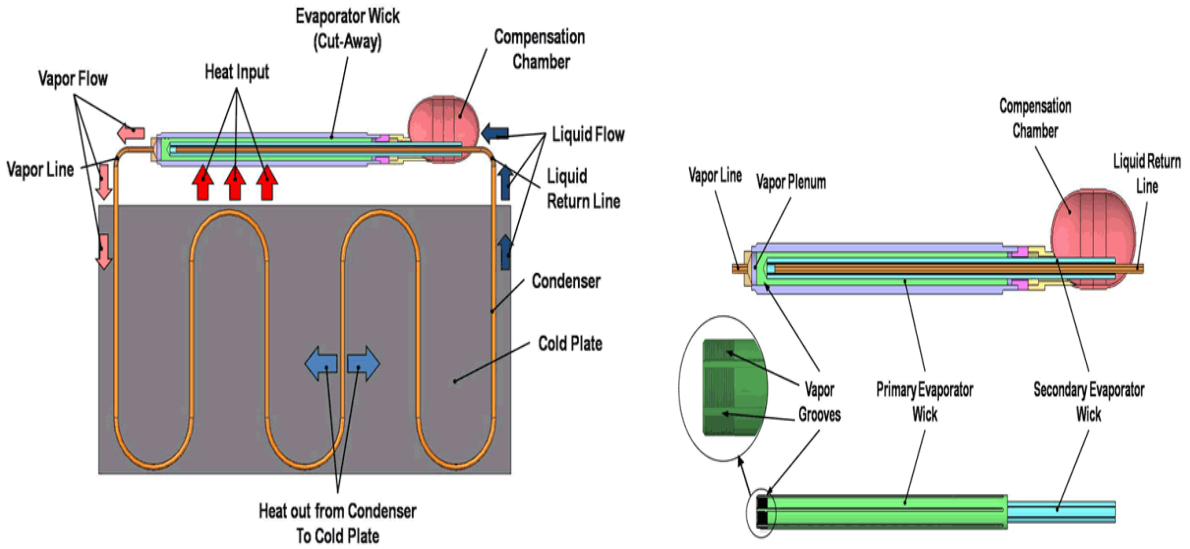

Figure 9: Working principle of loop heat pipe [20]

Heat enters the evaporator and vaporizes the working fluid at the wick outer surface. The vapor flows down a system of grooves and headers in the evaporator and the vapor line toward the condenser, where it condenses as heat is removed by the cold plate (or radiator). The two-phase reservoir (or compensation chamber) at the end of the evaporator is designed to operate at a slightly lower temperature than the evaporator (and the condenser). The lower saturation pressure in the reservoir draws the condensate through the condenser and liquid return line. The fluid then flows into a central pipe where it feeds the wick. A secondary wick hydraulically links the reservoir and the primary wick. LHPs are made self-priming by carefully controlling the volumes of the reservoir, condenser and vapor and liquid lines so that liquid is always available to the wick.

2.5 Heat Pipe Characteristics Analysis

The characteristic of heat pipe is a major topic of interest to the heat transfer researchers. Selection of material with appropriate working fluid pair, filling ratio, adiabatic length, etc. are the main characteristics which greatly influence the performance of the heat pipe. Different researchers have conducted different researchers. Major of the researches that has been conducted on this topic is listed below:

2.5.1 Study on the effect of heat pipe material

Heat pipe material has effect on the performance of the heat pipe. Different researchers have conducted research with different heat pipe materials. In the table below a list of different researches on heat pipe material has been presented.

Table 1.1: Previous study regarding heat pipe materials

Ref No:	Author and Study Year	Study Title	Material Studied	Temperature Range	Finding
[21]	Silva, Marcelino, and Riehl R (2015)	Thermal performance comparison between water-copper and water-stainless steel heat pipes designed for industrial application.	• Copper • Stainless Steel	Operating at temperature of □20 °C to □160^{o} C and heat input 25W, 50W, 75W, 100W, 125W	✓ Water-copper heat pipes performed better than water-stainless steel heat pipes ✓ Highest thermal conductivity of 20 W/^{o}C was observed for water-copper heat pipe and 8.4 W/^{o}C for water stainless heat pipe at a power of 125W.
[22]	P.Sivakumar et al. (2013)	Performance analysis of flat plate solar water heater by changing the heat pipe material.	• Copper • Stainless Steel • Aluminum	Solar heating temperature	✓ Maximum water temperature of 73.5^{o} C for copper, 69^{o} C for aluminum coated with copper oxide and 61.5^{o} C in stainless steel coated with epoxy-polyether were obtained. ✓ The collector efficiency at 9.00 hour is 39.52% for copper riser tubes, 35.79% for aluminum riser tubes and 27.79% for stainless steel riser tubes.
[23]	Jouhara H. et al. (2017)	Heat pipe based systems - advances and applications.	• Copper • Aluminum • Stainless Steel	Operating temperature between 0 °C and 200°C	✓ Copper is preferred. ✓ Aluminum is an ideal choice due to its weight advantages. ✓ Stainless steel casings cannot be used when water is chosen as the working fluid.

2.5.2 Study on the effect of working fluid

After selecting the heat pipe materials it has come to concern to select the working fluid matching with the heat pipes material which promotes better performance of heat pipe. In the table below a list different of researches on heat pipe working fluid has been tabulated.

Table 2: Previous study regarding heat pipe working fluids

Ref. No:	Author and Study Year	Study Title	Working Fluid	Heat Input	Finding
[24]	Peyghambarzadeh et al. (2013)	Thermal performance of different working fluids in a dual diameter circular heat pipe.	• Water • Methanol • Ethanol	Heat fluxes (up to 2500 W/m^2) in the evaporator and constant condenser temperature of 15°C, 25°C and 35°C.	High heat transfer coefficient of (200 W/m^2.k) are obtained at higher heat flux of 2500 W/m^2 for water and ethanol in comparison with methanol of (165 W/$m^{2.}$k).
[25]	S S Harikrishnan, Vinod Kotebavi. (2016)	Performance study of solar heat pipe with different working fluids and fill ratios.	• Methanol • Acetone • Water	The evaporator section is exposed to sunlight.	Acetone exhibited slightly more efficiency than methanol and water at optimum fill ratio of 25%.
[26]	A. K. Mozumder *et. al.* (2010)	Performance of heat pipe for different working fluids and fill ratios.	• Methanol • Acetone • Water	Different heat inputs 2W, 4W, 6W, 8W; 10W.	The overall heat transfer coefficient of heat pipe increases up to 19000 W/m2.k for acetone and 7000 W/m2.k for methanol with increase in heat input from 2W to 10W, while water filled heat pipe shows a nearly constant value of 3000 W/m2.k for 35% filling ratio.

[27]	M. Kannan and E. Natarajan (2010)	Thermal performance of a two-phase closed thermosyphon for waste heat recovery system.	• Distilled water • Ethanol • Methanol • Acetone	Operating temperature at 30 ^{o}C, 40^{o}C, 50^{o}C, 60^{o}C, 70^{o}C and input heat transfer rate of 0W to 1000W.	✓ The maximum heat transport capability was found to be high for water which increased from 425W to 650W as the operating temperature is increased from 40^{o} to 70^{o}C compared to methanol, ethanol, and acetone randomly. ✓ For the operating temperature 30^{o}C or below of 40^{o}C, methanol provide better heat transfer capability. Then water, ethanol and acetone randomly.
[28]	Ming Zhang, Zongliang Liu, Guoyuan Ma (2008)	The experimental investigation on thermal performance of a flat two-phase thermosyphon.	• Water • Ethanol	Different Heat flux	The two-phase thermosyphon with water as working fluid has a better performance than that with ethanol as working fluid.
[29]	Md. Moeenul Haque (2005)	Heat transfer characteristics of miniature heat pipes	• Ethanol • Methanol • Acetone	5W heat was input to the evaporator section of wick structure heat pipe.	Overall heat transfer coefficient of the MHP is found to be maximum for ethanol working fluid.

2.5.3 Study on the effect of filling ratio

Choosing the appropriate filling ratio is a major key for maximizing heat pipe performance. In the table below a list of different researches on heat pipe filling ratio has been tabulated.

Table 3: Previous study regarding heat pipe working fluids filling ratio

Ref. No:	Author and Study Year	Study Title	Filling Ratio	Heating Power	Finding
[30]	Yu-Hsing Lin *et. al.* (2008)	Effect of silver nano-fluid on pulsating heat pipe thermal performance.	• The working fluids include the silver nano-fluid water solution and pure water. • Filled ratio varies from 20% to 40%, 60% and 80% randomly.	Heating input in the evaporator from 5 W to 15 W, 25 W, 35 W, 45 W, 55 W, 65 W, 75 W and 85 W randomly.	40% and 60% of filled ratio shows better where filled ratio 60% was the most suitable.
[31]	Paisarn Naphon *et. al.* (2009)	Heat pipe efficiency enhancement with refrigerant nanoparticles mixtures.	The working fluid refrigerant (R11) and nanoparticles charge 25%, 37.5%, 50% and 66% of evaporator volume.	Various heat fluxes	The optimum condition is 60^{o} tilt angle and 50% charge filled.
[32]	M. Arab *et. al.* (2012)	Experimental investigation of extra-long pulsating heat pipe application in solar water heaters.	The working fluid employed is distilled water with filled ratio of 30%, 50% and 70%.	Heat flux ranges from 11 to 23 W/m^2.	The results show that PHP with filling ratio 70% has the most stable and the longest functioning duration.

[33]	E. Ibrahim *et. al.* (2012)	Heat transfer characteristics of rotating triangular thermosyphon.	R-134a refrigerant as the working fluid and three selected filling ratios of 10, 30 and 50 % of the evaporator section volume.	Heat flux of ($11 \leq q$ (W/m2) ≤ 23), and angular velocity of ($0 \leq \omega$ (rad/s) ≤ 1.36).	The maximum values of the tested heat transfer parameters of the rotational equilateral triangular thermosyphon are obtained at the filling ratio of 30 %.
[34]	Noie, S.H (2005)	Heat transfer characteristics of a two-phase closed thermosyphon	Water as a working fluid with filling ratios ($30\% \leq FR \leq 90\%$).	Input heat ($100 < Q^{\cdot} <$ 900W) under temperature range of 60□100℃	Maximum heat transfers rate occurs when filling ratio is 60%.
[35]	A. Kumar Mozumder *et. al.* (2009)	Experimental investigation of a heat pipe for different working fluids and fill ratios.	Distilled water, methanol and acetone were working fluid with filling ratio 35%, 55%, 85% and 100% of the evaporator volume.	50W heat was applied on a heat pipe evaporation section with 8 mm OD and 5 mm ID	✓ With acetone as the working fluid, 100% fill ratio of evaporator volume shows the best result. ✓ Filling ratios of working fluid greater than 55% of volume of evaporator show better results in terms of increased heat transfer coefficient, decreased thermal resistance.
[36]	T. N. Sreenivasa *et. al.* (2005)	Working fluid inventory in miniature heat pipe	35%, 55%, and 85% and100% of the evaporator volume tested for different heat input and working fluids of	50W capacity is used for providing the required heat source at the evaporator	Fill ratios of working fluid greater than 35% of volume of evaporator show better results in terms of increased heat transfer coefficient, decreased thermal resistance

2.5.4 Study of Nanofluid in heat pipe application

Further enhancement of heat pipe performance can be done by using nanofluid as the working fluid. In the table below a list of different researches on heat pipe using nanofluid as the working fluid has been presented.

Table 4: Study regarding nanofluid as the working fluid

SL No	Author and Study Year	Study Title	Nanofluid	Finding
[37]	Mashaei, P.R. and M. Shahryari (2015)	Effect of nanofluid on thermal performance of heat pipe with two evaporators; application to satellite equipment cooling.	Pure water, Al2O3–water and TiO2–water nanofluids are used as working fluids.	✓ Applying nanoparticle with smaller size and higher concentration level increases heat transfer coefficient remarkably by reducing thermal resistance of saturated porous media. ✓ It is also found that the presence of nanoparticles in water can lead to a reduction in weight of heat pipe, and thus satellite, under nearly identical condition.
[38]	H. Salehi, Saeed Zeinali Heris (2011)	Experimental study of a two-phase closed thermosyphon with nanofluid and magnetic field effect.	Nanofluid as working fluid with applying magnetic field is investigated experimentally.	✓ The thermal resistance of the thermosyphon significantly decreased with the nanoparticles concentration increasing. ✓ Nusselt number in the presence of magnetic field somewhat increased. ✓ Heat transfer rate better enhanced through nanofluid concentration increment compared to magnetic field strength enhancement.
[39]	Zeinali Heris, S., et al. (2015)	Experimental study of two phase closed thermosyphon using cuo/water nanofluid in the presence of electric field.	CuO/water nanofluid is used as the working fluid.	✓ Increase the thermal efficiency by up to 30% as compared with the case in which the working media is pure water and no electric field is applied. ✓ Utilizing an electric field is more advantageous when the input power applied to the system is lower
[40]	Noie, S.H., et al. (2009)	Heat transfer enhancement using Al2O3/water nanofluid in a two-phase closed thermosyphon	Al2O3/water nanofluid.	✓ For different input powers, the efficiency of the TPCT increases up to 14.7% when Al2O3/water nanofluid was used instead of pure water.

2.6 Applications of Heat Pipe

Heat pipe is a well-known technology. Heat pipe are popular in applications such as air conditioning, space technology, heat exchanger, cooking, CPU, laptops, processors and other electronic devices, etc.

2.6.1 Cooking

Energy conversation systems, Inc. developed the first commercial heat pipe product ‘Thermal Magic Cooking Pin’ for cooking purpose in 1966 [41].The cooking pin consisted of two layers. The outer layer or the envelope was stainless steel and the inner layer was of copper for compatibility. Water was used as working fluid in the cooking pins. The main purpose was to make grilled meat. During operation, one end of the heat pipe poked through the roast and the other end extends into the oven where it draws heat to the middle of the roast. It generally reduces the cooking time for large pieces of meat as its high effective thermal conductivity [42].

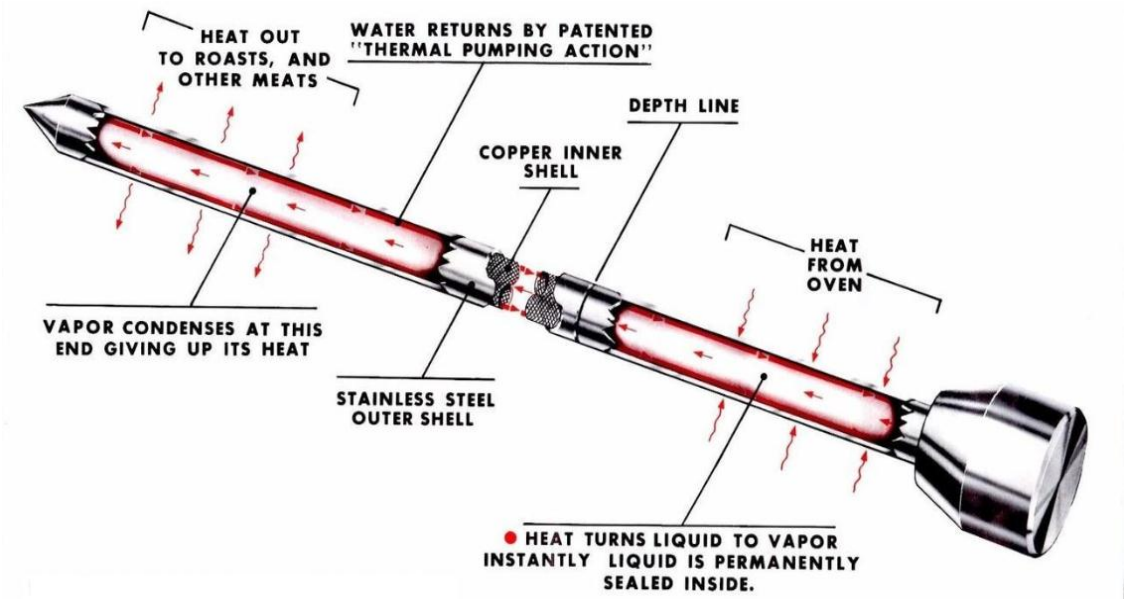

Figure 10: Thermal magic cooking pin [43]

2.6.2 Spacecraft

Spacecraft satellites are used for communications, global positioning systems and also for defense purpose. The function of a heat exchanger in a spacecraft system is to control the temperature and keep the overall systems operating at a constant range. Spacecrafts are very complicated systems. Among their complicacies are: heat is removed from the spacecraft by

thermal radiation only, limited electrical power available, favoring passive solutions and long life times, with no possibility of maintenance. This all complicated problems were managed by using heat pipe technology from the idea R. S. Gaugler [7]. A heat pipe is a simple passive heat transfer device that can efficiently transfer heat from hot space to cold space without using any electrical or mechanical power. Thus, Heat pipes and loop heat pipes are used extensively in spacecraft.

2.6.3 Computer and Electronic Device

The use of heat pipes in computer systems began in the late 1990s, when increased power requirements and subsequent increases in heat emission resulted in great demands on cooling systems. Heat pipes are a well-known thermal technology used in computing applications for cooling the electronic device. The research has been going on heat pipe for effectively removing heat from heat generating components like the CPU, GPU and laptop or computers. The heat pipes used in the electronic device are reducing vibration, noise as it acts as a passive heat transfer device. Critical design of heat pipes reducing the electronic component weight. Tanvir Reza Tanim *et. al.* [44] conducted a study on cooling of desktop computer using heat pipes to observe the effect of cooling fan in the condenser section along with the large heat sink. Heat pipe gives better performance compared to use of fan only.

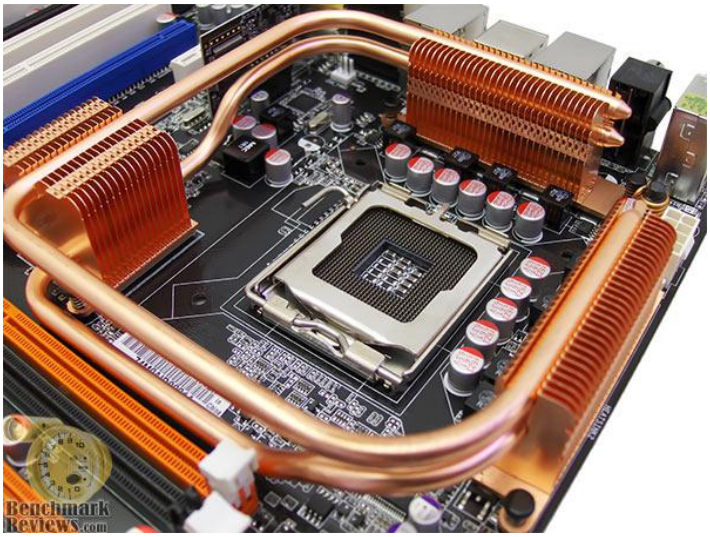

Figure 11: Heat pipe cooling device [45]

2.6.4 Solar Thermal

Heat pipes are also extensively used in solar thermal water heating applications. The most efficient solar hot water heaters in the market are evacuated tubes with heat pipes. In these applications, a heat pipe that is made from copper tube with distilled waters as working fluid

which is located within an evacuated glass tube and slanting towards the sun. Comparing to conventional "flat plate" solar water collectors, an individual absorber tube of an evacuated tube collector is up to 40% more efficient. Sarvenaz Sobhansarbandi [46] study on evacuated tube solar collector integrated with multifunctional absorption-storage materials. This work presents a novel method of integrating phase change materials within the evacuated tube solar collectors for solar water heaters. The operation of solar water heater with the proposed solar collector is investigated during both normal and on-demand (stagnation) operation. Beyond the improved functionality for solar water heater systems, the results from this study show efficiency improvement of 26% for the normal operation and 66% for the stagnation mode, compared with standard solar water heaters that lack phase change materials.

2.6.5 Heat Pipes in Air-Conditioning and Waste Heat Recovery Systems

The use of heat exchangers incorporating heat pipes in building and air-conditioning sectors have been emphasized in literature to decrease the operational costs of the system in order to reach energy saving capacity. S.H Noie-Baghban and Majideian [47] research on waste heat recovery using heat pipe heat exchanger (HPHE) for surgery rooms in hospitals. The characteristic design and heat transfer limitations of single heat pipes for three types of wick and three working fluids have been investigated. Construction of heat pipes, including washing, inserting the wick, creating the vacuum, injecting the fluid and installation have also been carried out. After obtaining the appropriate heat flux, the air-to-air heat pipe heat exchanger was designed, constructed and tested under low temperature ($15\pm55^{o}C$) operating conditions, using methanol as the working fluid. Experimental results for absorbed heat by the evaporator section are very close to the heat transfer rate obtained from computer simulation. Considering the fact that this is one of the first practical applications of heat pipe heat exchangers, it has given informative results and paved the way for further research.

Huang Wei and You Hongjun [48] study an application of the separated and gravity types of heat pipeline exchanger for recovery energy in the electrical factory and the air-conditioning system. Result shows heat pipeline exchanger’s utilization not only effectively decreased energy loss and reduced equipment corrosion and environmental pollution, but also improved the factory’s competition, with great benefits reached by the industry.

Mathur [49] investigated the impact on overall energy consumption of treating ventilation air by retrofitting a heat pipe heat exchanger unit. Using the climatic conditions of St. Louis, Missouri, an in-depth performance investigation was carried out for the year round operation

of the HVAC system equipped with the heat exchanger. The heat exchanger comprised of six rows of heat pipes in a horizontal orientation with an effectiveness of 60%. The findings of the study revealed that a heat pipe heat exchanger may be effectively used for increasing the efficiency of the existing HVAC systems.

Gan and Riffat [50] studied the effectiveness of using heat pipe heat recovery units for naturally ventilated buildings. Experimental work was carried out inside a testing chamber which was divided into two zones with a horizontal partition. Supply air entered through the lower zone and return air was extracted from the upper zone. A heat pipe heat recovery unit was housed in the supply and exhausts duct for exchange of heat between the supply and exhaust air streams. The results displayed that external air velocities have a significant effect on the performance of the heat pipe heat recovery unit wherein the effectiveness decreases with increasing air speeds. The work concluded that the effectiveness of the unit was 17% superior using two banks of heat pipes compared to a single bank.

M. Ahmad Zadeh [51] investigated the impact of Heat Pipe Based Heat Exchangers (HPHE) on the performance of an air-conditioning system in a library building. According to the results, the system behavior in terms of provided air conditions is appropriate and marginally inside the comfort area with the added eight-row HPHE. In addition, it was shown that by adding HPHE to the system, a significant amount of energy recovery could be achieved.

Nikhil S. Chougule *et. al.* [52] made a review on heat pipe for air conditioning applications. This paper focused on the dehumidification enhancement and sensible heat recovery aspects of heat pipe heat exchanger for an air conditioning application. This review concluded that, the use of heat pipe heat exchanger for heat recovery and dehumidification enhancement application makes significant changes in indoor air quality and energy consumption. So the use of HPHX is strongly recommended for Air Conditioning applications.

Hongting Ma *et. al.* [53] study on heat pipe assisted exchanger used for industrial waste heat recovery using the on-line cleaning device. The performance characteristics of a HPHE have been investigated experimentally by analyzing heat transfer rate, heat transfer coefficient, effectiveness, exergy efficiency and number of heat transfer units (NTU). A specially designed on-line cleaning device was used to clean the heat exchange tubes and enhance heat transfer. The results indicate that the heat transfer ratio and heat transfer coefficient increase with waste water mass flow rates increasing at constant cold water mass flow rate. It also

concluded that the heat transfer performance has been significantly improved after using the on-line cleaning device.

Hussam Jouhara *et. al.* [54] performed an experimental and theoretical investigation of a flat pipe heat exchanger for waste heat recovery in the steel industry. In this paper, the design, manufacture and testing of an innovative heat recovery system based on a Flat Heat Pipe heat exchanger (FHP) consists of stainless steel heat pipes is described. The thermal performance of the FHP was investigated both in the laboratory and on an industrial plant and the energy. It is concluded from the results that the FHP is an innovative high efficiency technology for waste heat recovery from such industrial applications.

Tian and W.Q.Tao [55] research on a new type waste recovery gravity heat pipe exchanger. In this study a heat pipe exchanger has been designed and applied to recover thermal energy in high temperature exhaust gas emitted from setting machine in the dyeing and printing industry. Three-month continuous operation of recovering dirty exhaust gas waste heat shows that the new type heat pipe exchanger can save 15% natural gas without any blockage of the gas side channel.

2.7 Present Work

HPHE is not common in Bangladesh. Performance of the HPHE varied significantly with the operating temperature. In this study, efforts have been made to evaluate the performance of the thermosyphon based HPHE which can be manufactured at an ordinary lab for low temperature waste heat application and waste heat recovery from the air conditioned space. The result of the thesis intended to have application in the industrial appliances and commercial building energy efficiency program.

Chapter 3

Performance Assessment of Heat Pipe (Thermosyphon)

The performance of heat pipe is one of the most important research areas in the field of thermal engineering. Due to its capability to transfer large amount of heat at a low temperature difference, heat pipe has a great importance in low grade energy transfer application. Researchers observed that geometrical, operational and environmental factors have significant influence on the performance of heat pipe.

3.1 Factors Affecting the Thermal Performance of Heat Pipe (Thermosyphon)

From different literature survey, it was observed that following factors affect thermal performance of the thermosyphon type heat pipe:

a. Properties of working fluid
b. Filling ratio
c. Coolant flow rate
d. Coolant temperature
e. Heat load
f. Inside pressure of thermosyphon
g. Thermosyphon material properties
h. Length of various sections (evaporator section, adiabatic section and condenser section)

Among these parameters, four parameters- heat pipe material, working fluid, filling ratio and length of various sections (evaporator section, adiabatic section and condenser section) are more dominating on the performance of the heat pipe. In this study, performance of heat pipe has been analyzed experimentally for these parameters.

3.2 Selection of Heat Pipe Material and Working Fluid

The heat pipe material is selected based on a trade-off: thermal conductivity, compatibility with working fluid, strength/mass and cost. A heat pipe material system includes the envelope material, the wick material, the working fluid, and any braze, solder or weld filler materials used in sealing the heat pipe. In the thermosyphon type heat pipe wick is not used, among other materials, working fluid is selected based on the application temperature range and envelop material is selected based on the compatibility with the working fluid. Copper, Stainless steel, Steel, Monel, Hayne, Inconel, Nickel, Titanium, and Aluminum are commonly used as the envelop material of heat pipe.

Since heat pipes were rediscovered by George Grover in 1963 [7], extensive tests had been conducted to determine compatibility of heat pipe envelope material with working fluid pairs. Proper selection of heat pipe envelope material compatible with working fluids allows a system to operate for 15-20 years or more without maintenance. If incompatible fluids/material pairs are chosen, corrosion and non-condensable gas (NCG) is formed. Corrosion causes leaks that stop heat pipe operation. NCG blocks a portion of the condenser and reduces maximum heat pipe power at a given temperature. Fluid/material compatibility is very important. The most common envelope and working fluid combinations are presented in the table below.

Table 5: Working fluid and envelope compatibility, with practical temperature limits [56]

Operating Min Temp., °C	Operating Max Temp., °C	Working Fluid	Envelope Materials
-271	-269	Helium	Stainless Steel, Titanium
-258	-243	Hydrogen	Stainless Steel
-24	-234	Neon	Stainless Steel
-214	-160	Oxygen	Aluminum, Stainless Steel
-203	-170	Nitrogen	Aluminum, Stainless Steel
-170	0	Ethane	Aluminum, Stainless Steel
-150	40	Propylene	Aluminum, Stainless Steel, Nickel
-80	50	R134a	Stainless Steel
-65	100	Ammonia	Aluminum, Steel, Stainless Steel, Nickel
-60	~ 25 to 100	Methanol	Copper, Stainless Steel
-112	78 (useful range 0 to 130)	Ethanol	Copper, Stainless Steel
-50	~ 100	Acetone	Aluminum, Stainless Steel
20	280, short term to 300	Water	Copper, Monel, Nickel, Titanium
100	350	Naphthalene	Al, Steel, Stainless Steel, Titanium, Cu-Ni
200	300, short term to 350	Dowtherm A /Therminol VP	Al, Steel, Stainless Steel, Titanium
200	400	AlBr3	Hastelloys
400	600	Cesium	Stainless Steel, Inconel, Haynes, Titanium
500	700	Potassium	Stainless Steel, Inconel, Haynes

Once the operating temperature range of the heat pipe is known, the working fluid is chosen. The heat pipe envelope materials are chosen compatible with the working fluid. The operating temperature range of this study is □20℃ to □80℃ and at this temperature limit ethanol, methanol, acetone and distillated water are preferable as the working fluid. Among these working fluids, water is more available, easy to handle in an ordinary workshop, cheaper and good compatibility with copper. As copper has superior thermal conductivity compared to other available materials water/copper pair are chosen for construction of the wickless heat pipe.

3.3 Design and Fabrication of Heat pipe

3.3.1 Design procedure

Copper was selected for construction of heat pipe. Heat pipes can be of different diameter. The standard diameter used for the construction of heat pipes are: 3, 4, 5, 6, 8 and 13, 25.4 mm. The diameter and length of a heat pipe can be obtained by design procedures which vary with condensation, evaporation and adiabatic length of heat pipe. Appropriate designs of heat pipe ensure safety, reliability and better performance. In this study, a wickless heat pipe capable of transferring heat of 1000 W at a vapor temperature between 20^0C and 80^0C over a distance of 280 mm was selected for experimentation. The mass flow rates at evaporator and condenser section was considered to be constant. Therefore the length of evaporator, adiabatic and condenser section was taken as 124 mm, 32 mm and124 mm respectively. The specifications of heat pipe geometry and working fluid properties are given in Table 6 and 7.

Table 6: Specification of wickless heat pipe

Working Fluid	Water
Container Material	Copper
Circular Section Geometry	OD=13 mm and ID=11.5 mm
Total Length of Pipe (L)	280 mm
Length of Evaporator Section (L_e)	124 mm
Length of Adiabatic Section (L_a)	32 mm
Length of Condenser Section (L_c)	124 mm

Table 7: Working fluid properties used in wickless heat pipe [57]

Working Fluid	T Temp (^{0}C)	p_v Saturation pressure (10^5 Pa)	h_{fg} Latent heat (kJ/Kg)	ρ_l Liquid density (kg/m^3)	ρ_v Vapor density (kg/m^3)	μ_l Liquid viscosity (10^{-3} N.s/m2)	μ_v Vapor viscosity (10-7 N.s/m^2)	k_l Liquid thermal conduct-ivity (W/m.K)	k_v Vapor thermal conduct -vity (W/m.K	Σ Liquid surface tension (10^{-3} N/m)
Water	80	0.4735	2308.9	971.82	0.2932	0.3510	113.0	0.669	0.0231	62.69
Methanol	80	2.2	1084.4	735.5	2.084	0.2710	115.0	0.200	0.0199	17.5
Ethanol	80	1.086	960.0	757.0	1.430	0.4320	103.0	0.169	0.0199	17.3

3.4 Calculation of Heat Transfer Limits

There are various parameters that put limitations and constraints on the steady and transient operation of wickless heat pipe. Physical phenomenon that might limit heat transport in heat pipes is due to sonic, boiling, entrainment or flooding limit and dry out limit. The heat transfer limitation can be any of the above limitation depending on the size and shape of the pipe, working fluid and operating temperature. The lowest limit among the constraints defines the maximum heat transport limitation of wickless heat pipe at given temperature. The heat transfer limits for the present wickless heat pipe were calculated as follows:

3.4.1 Sonic Limit

The evaporator and condenser section of a heat pipe represent a vapor flow channel with mass addition and extraction due to evaporation and condensation, respectively. The vapor velocity increases along the evaporator and reaches the maximum at the end of the evaporator section. The limitation of such a flow system is similar to that of converging-diverging nozzle with a constant mass flow rate, where the evaporator exit corresponds to the throat of nozzle. Sonic limit was computed using expressions reported by Dunn and Reay [58]:

$$Q = \rho_v h_{fg} A_v \sqrt{\frac{\gamma R_v T_v}{2(\gamma + 1)}}$$

The water properties from the property Table 3 are as follows:

h_{fg}= 2308.9 kJ/kg, ρ_v= 0.2932 kg/m^3, R_v= 0.461 kJ/kgK, T_v= 80^{0}C=80+273=353 K, γ = 1.3, D_i = 0.0115 m.

$A_v = \frac{\pi}{4} D_i^{\,2} = \frac{\pi}{4} \times 0.0115^2 = 2.3387 \times 10^{-4}$ m^2

$$Q = 0.2932 \times\ 2308.9\ \times 2.0387\ \times 10^{-4} \sqrt{\frac{1.3\ \times\ 0.461\ \times\ 353}{2(1.3\ +\ 1)}}$$

$$Q = 1.0734\ \text{kW} =\ 1073.42\ \text{W}$$

3.4.2 Boiling Limit

The boiling limitation is due to large fill charges and high radial heat fluxes in the evaporator section. As the heat flux is increased, nucleate boiling becomes more intense in the evaporator section. Further increase in heat flux results in more vigorous boiling. At the critical heat flux, the vapor bubbles coalesce near the pipe wall. At this point, the wall temperature increases rapidly. The boiling limit was evaluated based on a correlation proposed by Gorbis and Savchenkov [59]:

$$Q = k_u[h_{fg}\rho_v{}^{0.5}[\sigma g(\rho_l - \rho_v)]^{0.25}]$$

$$k_u =\ 0.0093(\text{AR})^{-0.18}\left(\frac{\text{Di}}{L_c}\right)^{-0.88} (FR)^{-0.74}(1 + 0.03\ \text{Bo}\ )^2 2\ <\ \text{Bo} <\ 60$$

The water properties from the property Table 3 are as follows:

h_{fg}= 2308.9 kJ/kg, ρ_v= 0.2932 kg/m^3, ρ_l= 971.82 kg/m^3, g = 9.981 m/s^2, σ = 62.69x10^{-3}

, Di = 0.0115m, Le = 0.124 m, La = 0.032 m, Lc= 0.124 m

$$AR = Aspect\ Ratio = \left(\frac{L_e}{\text{Di}}\right) = \frac{0.124}{0.0115} =\ 10.78$$

$$FR = Filling\ Ratio = \frac{\text{Volume of the liquid (m}^3\text{)}}{\text{Volume of the evaporator (m}^3\text{)}} = \frac{6.43\ \times 10^{-6}}{12.8\ \times 10^{-6}} = 0.502$$

$$Bo = \text{Di}\left[\frac{g(\rho_l - \rho_v)}{\sigma}\right]^{0.5}$$

$$Bo = 0.0115\left[\frac{9.81(971.82\ -\ 0.2932)}{62.69\ \times\ 10^{-3}}\right]^{0.5}$$

$$Bo = 4.483$$

$$k_u =\ 0.0093(10.782)^{-0.18}\left(\frac{0.0115}{.124}\right)^{-0.88} (0.502)^{-0.74}(1 + 0.03 \times\ 4.483)^2$$

$$k_u = 0.105$$

$$Q = 0.105[2308.9\ \times\ 0.2932^{0.5}[62.69\ \times\ 10^{-3} \times\ 9.81\ \times (971.82\ -\ 0.2932)]^{0.25}]$$

$Q = 0.11014\text{kW} = 1101.47\ W$

3.4.3 Entrainment Limit or Flooding Limit

This limit occurs for large fill charges, high axial heat flows, but small radial evaporator heat fluxes. The high axial heat flow causes a high relative velocity between the counter-current vapor and liquid flows, and consequently an increase in the shear stresses at the vapor/liquid interface. Thereby, large surface waves are induced at the vapor/liquid interface. Thus instability of the liquid flow is created, which leads to an entrainment of liquid. The flooding limit was evaluated based on a correlation proposed by Faghri [60]:

$$Q = Kh_{fg}A_{cross}[\sigma g(\rho_l - \rho_v)^{0.25}][\rho_v{}^{-.25} + \rho_l{}^{-.25}]^{-2}$$

$$K = \left(\frac{\rho_l}{\rho_v}\right)^{.14} t\text{an}^2(\text{Bo})^{0.25}$$

$$Bo = \text{Di}\left[\frac{g(\rho_l - \rho_v)}{\sigma}\right]^{0.5}$$

The water properties from the property Table 3 are as follows:

h_{fg}= 2308.9 kJ/kg,ρ_v= 0.2932 kg/m^3, ρ_l= 971.82 kg/m^3, g = 9.981 m/s^2,σ = 62.69x10^{-3}, Di = 0.0115 m, Le = 0.124 m, La = 0.032 m, Lc= 0.124 m

$$Bo = 0.0115\left[\frac{9.81(971.82 - 0.2932)}{62.69 \times 10^{-3}}\right]^{0.5}$$

$$Bo = 4.483$$

$$K = \left(\frac{971.82}{0.2932}\right)^{.14} t\text{anh}^2(4.483)^{0.25}$$

$$K = 2.007$$

$$Q = 2.007 \times 2308.9 \times 1.0387 \times 10^{-4}\,[9.81 \times 62.69 \times 10^{-3}(971.8 - 0.2932)^{0.25}] \times [0.293^{-.25} + 971.82^{-.25}]^{-2}$$

$$Q = .1125\text{KW} = 1125\ \text{W}$$

3.4.4 The Dry-out Limit

The dry-out limit is established when the friction losses of the condensate flow and the shear forces at the vapor/liquid interface are exceeding the pumping force, viz. gravity force. The liquid, which is lacking in the evaporator, is held at the condenser end due to the vapor flow force. When dry-out starts a substantial amount of liquid is held at the condenser end and the vapor flow force is decreasing due to the reduced evaporation rate. Thus the weight of the

liquid plug in the condenser can overcome the vapor force and liquid flows downward to rewet the evaporator surface. The continuous rise of the evaporator wall temperature is, therefore, superimposed by temperature fluctuations. The dry-out limit occurs at the bottom of the evaporator in the liquid falling film mode. The dry-out limit was computed based on an improved Cohen and Baylay model [61].

The water properties from the property Table 3 are as follows:
h_{fg}= 2308.9 kJ/kg,ρ_v= 0.2932 kg/m^3, ρ_l= 971.82 kg/m^3, g = 9.981 m/s^2, σ = 62.69x10^{-3},
D_i=D_e=D_c= 0.0224 m, L_e = 0.124 m, L_a = 0.032 m, L_c= 0.124 m

$$\left(\frac{Q}{\rho_v h_{fg}}\right)\left[\frac{\sigma g(\rho_l-\rho_v)}{{\rho_v}^2}\right]^{-.25} = A_{cross}\left[\frac{g{\rho_l}^2\left(\frac{D_c}{D_e}\right)}{3\mu_l L_e\sqrt[4]{\sigma g{\rho_v}^2(\rho_l-\rho_v)}}\right]^{-0.25}$$

$$\times\left[\frac{\frac{V_t}{\pi D_c}}{\left[\left(\frac{4}{5}\ \mathrm{Lc}\right)+\mathrm{La}\right]+\left(\frac{D_e}{D_c}\right)^{0.67}\left(\mathrm{La}+\frac{3}{4}\ \mathrm{Le}\right)}\right]^3\times\left[\frac{\left(\frac{V_e}{V_t}\right)\left(\frac{V_l}{V_e}\right)-\left(\frac{\rho_v}{\rho_l}\right)}{1-\left(\frac{\rho_v}{\rho_l}\right)}\right]^3$$

$$\left(\frac{Q}{0.2932\ \times\ 2308.9}\right)\left[\frac{62.69\ \times\ 10^{-3}(971.82-\ 0.2932)}{0.2932^2}\right]^{-0.25} = 1.0387\ \times 10^{-4}$$

$$\times\left[\frac{9.81\ \times\ 971.82^2\left(\frac{0.0115}{0.0115}\right)}{3\ \times\ 3510\ \times\ 10^{-3}\ \times.263\ \sqrt[4]{62.69\ \times\ 10^{-3}\times\ 9.81\ \times\ 0.2932^2(971.82-\ 0.2932)}}\right]^{-0.25}$$

$$\times\left[\frac{\frac{2.90\times\ 10^{-5}}{3.1416\times.0115}}{\left[\left(\frac{4}{5}\times 0.124\right)+.032\right]+\left(\frac{.0115}{.0115}\right)^{0.67}\left(0.124+\frac{3}{4}\times 0.124\right)}\right]^3$$

$$\times\left[\frac{\left(\frac{1.288\times 10^{-5}}{2.90\times 10^{-5}}\right)\left(\frac{1.288\times 10^{-5}}{1.288\times 10^{-5}}\right)-\left(\frac{0.2932}{971.82}\right)}{1-\left(\frac{0.2932}{971.82}\right)}\right]^3$$

$$Q = .1050KW = 1050W$$

Table 8: Calculated heat transfer limits

Type of limit	Heat transfer rate
Sonic limit	1110W
Boiling limit	1101.47W
Flooding limit	1125W
Dry-out limit	1050W

The lowest limit among the four constraints defines the maximum heat transport limitation of the wickless heat pipe as shown in Table 8. The lowest limit is dry-out limit having maximum heat transfer rate of 1050 W. Therefore it was decided to apply the heat input of 1000 W at evaporator section because the input heat (1000 W) is lower than all of the heat transfer limits, the wickless heat pipe operates without any problem.

3.5 Fabrication

Heat pipe was fabricated from1/2 inch diameter copper pipe with a length of 11 inch. The two ends of copper pipe were sealed with 1.3 inch copper sheet of 2 mm thickness. A small hole was drilled on the sealed copper sheet for injection of working fluid. Working fluid was injected into the pipe through the hole and being heated. When the working fluid was being boiled and steam is coming out, the hole was sealed by soldering (silver). Time was given to cool down. Vacuum was created after the working fluid getting cooled; thus heat pipe was fabricated at the easiest way with low cost.

(a) **(b)**

Figure 12: (a) Copper Pipe processing for heat pipe; (b) Working fluid inserting

3.6 Study of the Effectiveness of Heat Pipe

The performance of the fabricated heat pipe was analyzed at two constant temperatures of □45℃ and □60℃ by comparing with a normal copper pipe. The experiment was conducted by placing one end of the heat pipe and copper pipe in a constant temperature water bath and other end in the atmosphere as shown in the fig.13. Heat is transferred from the water and temperature of the pipes top end was increased with time and it was measured with a thermocouple. To reduce the heat loss from the heat pipe, proper insulation was applied. Temperature readings of the thermocouple were recorded at regular time interval of 1 minute. Temperature response of the thermocouple with time is presented in fig.13 for the heat pipe and normal copper pipe.

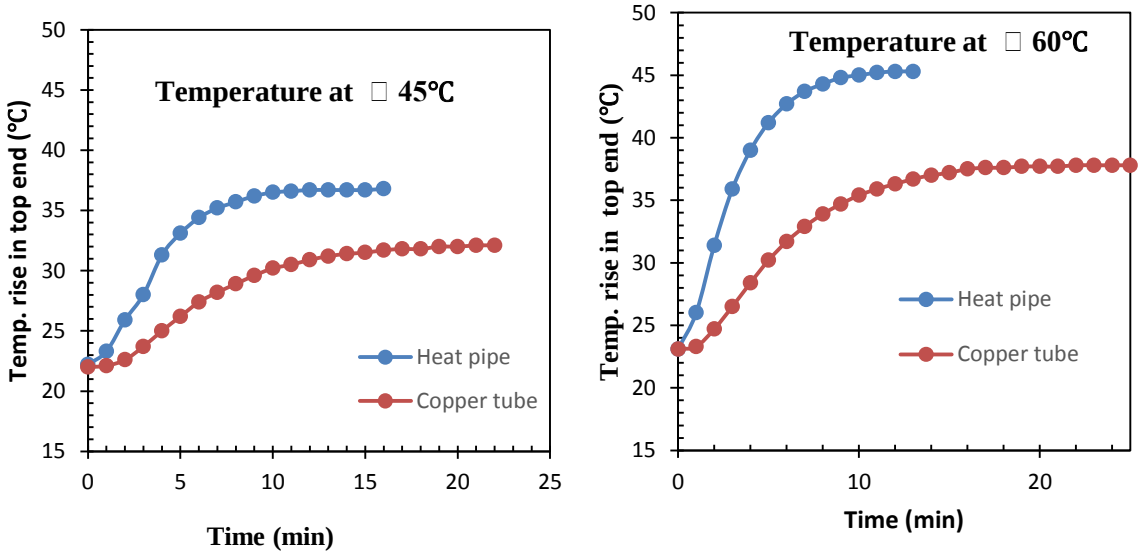

Figure 13: Heat pipe performance compared to the solid copper pipe

The result shows that for both temperatures condition heat pipe provides better performance compared to that of the normal or solid copper pipe. When the bath temperature was □45℃, heat pipe reaches 35℃ from 22℃ at 8 minutes whereas copper pipe reaches 30℃ from 22℃ at 22 minutes. For bath temperature of □60℃, heat pipe reaches 45℃ from 23℃ at 9 minutes whereas copper pipe reaches 36℃ from 23℃ at 18 minutes. So, it can be predicted that the constructed heat pipe provides better thermal performance at both low temperature and high temperature compared to that of the normal copper pipe.

3.6.1 Thermal Resistance of Heat Pipe Filled with Water

Experiments conducted with the heat pipe show clear superiority in thermal performance compared to that of the copper tube. To enhance better understanding, thermal resistance analysis of the heat pipe was performed.

$R_{c,w}$	Radial conduction through condenser wall
$R_{c,in}$	Internal condensation resistance in condenser
$R_{e,w}$	Radial conduction through evaporator wall
$R_{e,in}$	Internal evaporation resistance in evaporator
$R_{a,w}$	Axial conduction resistance between evaporator and condenser section wall
$R_{a,in}$	Axial conduction resistance of liquid film between evaporator and condenser section
$R_{e,int}$	Interfacial condensation thermal resistance
$R_{e,int}$	Interfacial evaporation thermal resistance
R_v	Thermal resistance due to vapor pressure drop

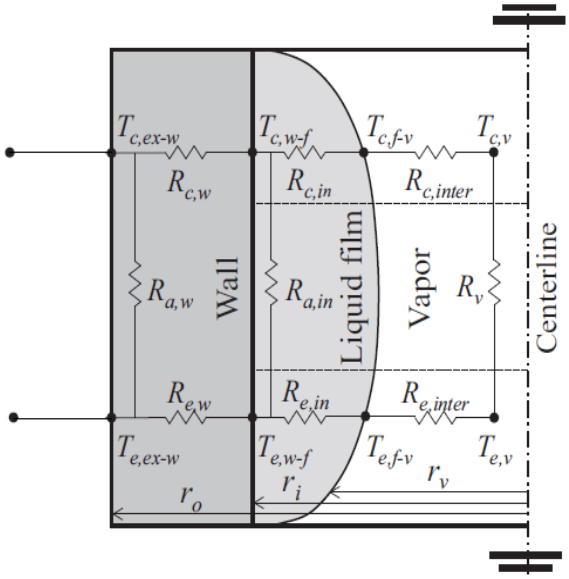

Figure 14: Thermal resistance of heat pipe

The major thermal resistances of cylindrical TS are shown in Fig.14. In this figure, $R_{c,w}$, $R_{c,in}$, $R_{e,w}$, $R_{e,in}$, $R_{a,w}$, $R_{a,in}$, $R_{c,inter}$, $R_{e,inter}$, R_v and denote the resistances associated with the evaporator wall, the internal resistance of the evaporator section, interfacial evaporation, conduction through the wall and liquid film between evaporator and condenser, the vapor pressure drop along the TS length, conduction through the condenser wall, the internal resistance of the condenser section, and interfacial condensation, respectively. The individual resistances are as follows:

- Radial conduction through the condenser section wall ($R_{c,w}$)

$$R_{c,w} = \frac{ln\frac{r_o}{r_i}}{2\,\pi\,k_w\,L_e}$$

$$R_{c,w} = \frac{ln\frac{0.0065}{0.0115}}{2 \times 3.1416 \times 38 \times 0.277}$$

$$R_{c,w} = 0.000182969\ \frac{K}{W}$$

- Internal condensation in the condenser section ($R_{c,in}$)

In general, the thermal resistance due to condensation in the condenser section of the TS is represented by:

$$R_{c,in} = \frac{1}{h_{c,in}\, A_{c,in}}$$

Where, $h_{c,in}$ is the heat transfer coefficient associated with conduction through the liquid film inside a TS in the condenser, and $A_{c,in}$ is the inner surface area of the liquid film in the condenser section that is taken to be equal to the inner surface area of the condenser wall considering the relative thinness of the liquid film. Nusselt analysis for condensation on a vertical flat plate is commonly used to evaluate the internal heat transfer coefficient,

$$\mathrm{h}_{c,in} = 1.71\left[\frac{\mathrm{g}\,\rho_\mathrm{l}\,(\rho_\mathrm{l}-\rho_\mathrm{v})\mathrm{k_l}^3\,\mathrm{h_{fg}}\,\mathrm{r_i}}{\mu_\mathrm{l} q_\mathrm{TS}}\right]^{1/3}$$

$$\mathrm{h}_{c,in} = 1.71\left[\frac{9.81 \times 988 \times (988-0.0831) \times 2.38\ \times 10^6\ \times 0.00575}{0.00055 \times 26.11}\right]^{1/3}$$

$$\mathrm{h}_{c,in} = 14635.732\ W/m^2.K$$

$$\therefore R_{c,in} = \frac{1}{h_{c,in}\, A_{c,in}}$$

$$R_{c,in} = \frac{1}{14635.732 \times 0.013\ \times 0.277}$$

$$R_{c,in} = 0.0214\ \frac{K}{W}$$

- Radial conduction through the evaporator section wall ($R_{e,w}$)

$$R_{e,w} = \frac{ln\frac{r_o}{r_i}}{2\,\pi\, k_w\, L_e}$$

$$R_{e,w} = \frac{ln\frac{0.0065}{0.0115}}{2 \times 3.1416 \times 38 \times 0.277}$$

$$R_{e,w} = 0.000182969\ \frac{K}{W}$$

- Internal evaporation in the evaporator section ($R_{e,in}$)

In general, internal evaporation occurs simultaneously in (i) an underlying liquid pool and (ii) a liquid film in a region above the pool and on the interior walls of the TS. A widely-used correlation associated with the nucleate boiling regime has been proposed by Shiraishi *et. al.* [62] and takes the following form:

$$□_p = 0.32\ {q''_p}^{0.4} \left(\frac{P_v}{P_{atm}}\right)^{0.23} \left(\frac{g^{0.2}{\rho_l}^{0.65}{C_{p,l}}^{0.7}{k_l}^{0.3}}{{\rho_v}^{0.25}□_{fg}{}^{0.4}{\mu_l}^{0.1}}\right)$$

$$□_p = 0.32 \times 5217.105^{0.4} \times \left(\frac{12350}{101325}\right)^{0.23} \times \left(\frac{9.81^{0.2} \times 988^{0.65} \times 4175^{0.7} \times 0.645^{0.3}}{0.0831^{0.25} \times 2382700^{0.4} \times 0.00055^{0.1}}\right)$$

$$□_p = 2814.358\ W/m^2.K$$

The heat transfer coefficient related to the liquid film in the upper region of the evaporator section, $□_f$ is also dependent on the heat transfer regime. For a relatively small heat flux, Nusselt theory for film wise evaporation takes the following form, albeit for evaporation [63],

$$\mathrm{h_f} = 1.71\left[\frac{\mathrm{g\ \rho_l\ (\rho_l - \rho_v){k_l}^3\ h_{fg}\ r_i}}{\mu_l q_{TS}}\right]^{1/3}$$

$$\mathrm{h_f} = 14635.732\ W/m^2.K$$

The combined internal thermal resistance of the evaporator section is calculated using the heat transfer coefficients associated with the liquid pool and annular liquid film,

$$R_{e,in} = \frac{1}{\mathrm{h_p A_p + h_f\ (A_{e,in} - A_p)}}$$

$$R_{e,in} = \frac{1}{2814.358 \times 0.005 + 2814.258\ (0.01 - 0.005)}$$

$$R_{e,in} = 0.01145\ \frac{K}{W}$$

- Axial conduction between evaporator and condenser section wall $R_{a,w}$ in Fig.14 is accounted for by the expression-

$$R_{a,w} = \frac{\mathrm{L_a}}{\pi(\mathrm{{r_o}^2 - {r_i}^2})\ \mathrm{K_w}}$$

$$R_{a,w} = \frac{0.003}{\pi(0.0065^2 - 0.00575^2) \times 385}$$

$$R_{a,w} = 0.270\ \frac{K}{W}$$

- Similarly, axial conduction evaporator and condenser section $R_{a,in}$ in Fig.14 could be approximated by-

$$R_{a,in} = \frac{\mathrm{L_a}}{\pi(\mathrm{r_i}^2 - \mathrm{r_v}^2)\,\mathrm{K_{lf}}}$$

$$R_{a,in} = \frac{0.003}{\pi(0.00575^2 - 0.00475^2) \times 0.6224}$$

$$R_{a,in} = 146.120\ \frac{K}{W}$$

- Evaporation at the evaporator liquid–vapor interface ($R_{e,inter}$)

$$R_{e,inter} = \frac{1}{\mathrm{h_{e,inter}}\ \mathrm{A_{e,i}}}$$

Where, $\mathrm{h_{e,inter}}$ is the interfacial evaporation heat transfer coefficient [64] and obtain from:

$$\mathrm{h_{e,inter}} = \left(\frac{2\alpha}{2-\alpha}\right)\left(\frac{\mathrm{h_{fg}}^2}{\mathrm{T_v} v_{\mathrm{fg}}}\right)\sqrt{\frac{1}{2\pi \mathrm{R_g T_v}}}\left(1 - \frac{\mathrm{P_v} v_{\mathrm{fg}}}{2\mathrm{h_{fg}}}\right)$$

$$\mathrm{h_{e,inter}} = \left(\frac{2 \times 0.4}{2-0.4}\right)\left(\frac{2382700^2}{323\ \times 12.045}\right)\sqrt{\frac{1}{2\pi \times 461.5}}\left(1 - \frac{12350 \times\ 12.045}{2 \times 238270}\right)$$

$$\mathrm{h_{e,inter}} = 730380.048\ W/m^2.K$$

$$\therefore R_{e,inter} = \frac{1}{\mathrm{h_{e,inter}}\ \mathrm{A_{e,i}}}$$

$$R_{e,inter} = \frac{1}{7.30 \times 10^5 \times 3.1416 \times 0.0115 \times 0.277}$$

$$R_{e,inter} = 1.374 \times 10^{-4}\ \frac{K}{W}$$

- Condensation at the condenser liquid–vapor interface ($R_{c,inter}$)

$$R_{c,inter} = \frac{1}{\mathrm{h_{c,inter}}\ \mathrm{A_{c,i}}}$$

Where, $h_{c,inter}$ is the internal condensation heat transfer coefficient that is also determined using Eq.

$$\mathrm{h_{c,inter}} = \left(\frac{2\alpha}{2-\alpha}\right)\left(\frac{\mathrm{h_{fg}}^2}{\mathrm{T_v} v_{\mathrm{fg}}}\right)\sqrt{\frac{1}{2\pi \mathrm{R_g T_v}}}\left(1 - \frac{\mathrm{P_v} v_{\mathrm{fg}}}{2\mathrm{h_{fg}}}\right)$$

$$\mathrm{h_{c,inter}} = 7.30 \times 10^5\ W/m^2.K$$

$$\therefore R_{c,inter} = \frac{1}{\mathrm{h_{c,inter}}\ \mathrm{A_{c,i}}}$$

$$R_{c,inter} = \frac{1}{7.30 \times 10^5 \times 3.1416 \times 0.0115 \times 0.277}$$

$$R_{c,inter} = 1.374 \times 10^{-4}\ \frac{K}{W}$$

- Thermal resistance due to vapor pressure drop (R_v)

A thermal resistance can be associated with these effects and takes the following form for cylindrical TS with laminar vapor flow:

$$R_v = \frac{8R_g\mu_v T^2{}_v}{\Pi^2{}_{fg} P_v \rho_v}\left[\frac{\frac{L_e+L_c}{2}+L_a}{r_i{}^4}\right]$$

$$R_v = \frac{8 \times 461.5 \times 1.06 \times 10^{-5} \times 323^2}{\Pi^2{}_{fg} P_v \rho_v}\left[\frac{\frac{0.277+0.277}{2}+0.003}{0.00575^4}\right]$$

$$R_v = 5.7102 \times 10^{-5}\ \frac{K}{W}$$

- Total Thermal Resistance of a Heat Pipe (R_{TS})

$$R_{TS} = \frac{\left[R_{e,w} + R_{c,w} + \frac{(R_{e,in}+R_{e,inter}+R_v+R_{c,inter}+R_{c,in})(R_{a,in})}{(R_{e,in}+R_{e,inter}+R_v+R_{c,inter}+R_{c,in})+(R_{a,in})}\right](R_{a,w})}{\left[R_{e,w} + R_{c,w} + \frac{(R_{e,in}+R_{e,inter}+R_v+R_{c,inter}+R_{c,in})(R_{a,in})}{(R_{e,in}+R_{e,inter}+R_v+R_{c,inter}+R_{c,in})+(R_{a,in})}\right] + (R_{a,w})}$$

$$R_{TS} = \frac{[0.000183 + 0.000183 + \frac{(0.01145+1.374\times10^{-4}+5.71\times10^{-5}+1.374\times10^{-4}+0.0215)(146.120)}{(0.01145+1.374\times10^{-4}+5.71\times10^{-5}+1.374\times10^{-4}+0.0215)+(146.120)}](0.267)}{[0.000183 + 0.000183 + \frac{(0.01145+1.374\times10^{-4}+5.71\times10^{-5}+1.374\times10^{-4}+0.0215)(146.120)}{(0.01145+1.374\times10^{-4}+5.71\times10^{-5}+1.374\times10^{-4}+0.0215)+(146.120)}] + (0.267)}$$

$$\therefore R_{TS} = 0.02694\ \frac{K}{W}$$

3.6.2 Thermal Resistance of Normal Copper Pipe Filled with Air

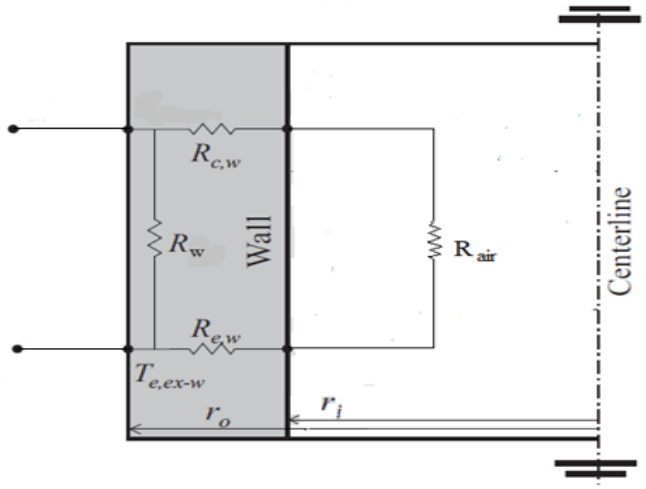

$R_{e,w}$	Radial conduction through evaporator wall
$R_{c,w}$	Radial conduction through condenser wall
R_{air}	Internal natural convection resistance of air
R_w	Axial conduction resistance between evaporator and condenser section wall

Figure 15: Thermal resistance of normal copper pipe

- Radial conduction through the evaporator section wall ($R_{e,w}$)

$$R_{e,w} = \frac{ln\frac{r_o}{r_i}}{2\,\pi\,k_w\,L_e}$$

$$R_{e,w} = \frac{ln\frac{0.0065}{0.0115}}{2 \times 3.1416 \times 38 \times 0.277}$$

$$R_{e,w} = 0.000182969\ \frac{K}{W}$$

- Radial conduction through the condenser section wall ($R_{c,w}$)

$$R_{c,w} = \frac{ln\frac{r_o}{r_i}}{2\,\pi\,k_w\,L_e}$$

$$R_{c,w} = \frac{ln\frac{0.0065}{0.0115}}{2 \times 3.1416 \times 38 \times 0.277}$$

$$R_{c,w} = 0.000182969\ \frac{K}{W}$$

- Internal natural convection resistance of air

$$R_{air} = \frac{1}{\mathrm{h_{air}\,A}}$$

The characteristic length and the Rayleigh number in this case are,

$$L_c = \frac{\mathrm{A_s}}{\mathrm{P}} = \frac{2\pi \mathrm{rH}}{2\pi \mathrm{r}} = \mathrm{H} = 0.558\ \mathrm{m}$$

$$R_{a_L} = \frac{\mathrm{g}\beta(\mathrm{T_s} - \mathrm{T_\infty})\mathrm{L_c}^3}{\vartheta^2}\ \mathrm{Pr}$$

$$R_{a_L} = \frac{9.81 \times \frac{1}{323} \times (70 - 30) \times 0.558^3}{(1.798 \times 10^{-5})^2} \times .7228$$

$$R_{a_L} = 472036808.1$$

The natural convection Nusselt number can be determined from the following Eq.

$$Nu = 0.54\ {R_{a_L}}^{1/4}$$

$$Nu = 0.54\ (472036808.1)^{\frac{1}{4}}$$

$$Nu = 79.60$$

Heat transfer co-efficient,

$$\square = \frac{K}{L_c} Nu$$

$$\square = \frac{0.02735}{0.558} \times 79.60$$

$$\square_{air} = 3.90\ W/m^2.K$$

Internal convection resistance of air,

$$R_{air} = \frac{1}{\mathrm{h_{air}\ A}}$$

$$R_{air} = \frac{1}{3.91 \times 3.1416 \times 0.0115 \times 0.558}$$

$$R_{air} = 12.70\ \frac{K}{W}$$

- Axial conduction between evaporator and condenser section wall $R_{a,w}$ in Fig.15 is accounted by the expression-

$$R_w = \frac{\mathrm{L_a}}{\pi(\mathrm{r_o}^2 - \mathrm{r_i}^2)\ \mathrm{K_w}}$$

$$R_w = \frac{0.003}{\pi(0.0065^2 - 0.00575^2) \times 385}$$

$$R_w = 0.270\ \frac{K}{W}$$

∴ Total thermal Resistance of Copper Tube Filled with Air,

$$R_T = \frac{(R_{e,w} + R_{air} + R_{c,w})(R_{a,w})}{(R_{e,w} + R_{air} + R_{c,w}) + (R_{a,w})}$$

$$R_T = \frac{(0.000183 + 12.7 + 0.000183)(0.270)}{(0.000183 + 12.7 + 0.000183) + (0.270)}$$

$$\therefore R_T = 0.264 \frac{K}{W}$$

3.7 Performance Study of Water and Ethanol

The performance of water/copper compatibility was checked by constructing two heat pipes with two different fluids: distilled water and ethanol. Both fluids are inserted at a certain level, then same experiment was performed for both heat pipes as presented in the fig.16.

Figure 16: Heat pipe performance test

One end of the heat pipes are placed into a hot water reservoir and other end were attached with thermocouple. The whole setup was placed in an insulated container. The top end temperatures were measured and recorded for both heat pipes. To compare the performance of heat pipes filled with water and ethanol, the top end temperatures of the two pipes were plotted against time.

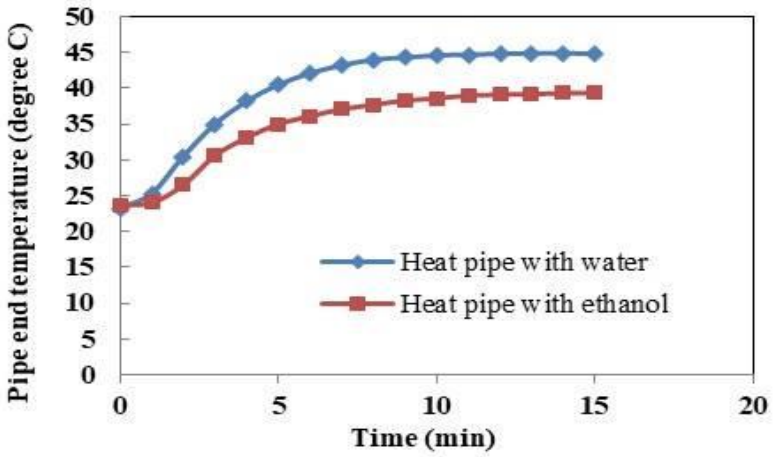

Figure 17: Variation of top end temperature with time

The result presented in the fig.17 shows that the temperature curve of heat pipe with water is steeper than ethanol indicating that heat transfer rate of water filled heat pipes is more compared to that of the ethanol filled heat pipe. Due to higher density and thermal properties, water inside the heat pipe can carry more heat compared to that of the ethanol.

3.8 Performance Study of Heat Pipe for Different Filling Ratio

Working fluid is considered as the heart of heat pipe as it contributes the major share in transferring heat from the hot end to the cold end. Working fluid inside the heat pipe should be filled at proper limit; if working fluid is filled more or less than the proper limit, performance of the heat pipe will be reduced. So, a certain level of heat pipe volume must be filled by working fluid for ensuring maximum performance. Different researcher have conducted researches on filling ratio [28-32] and concluded that water gives better performance at 50% to 70% filling ratio. In this study, water was selected as the working fluid. For studying the performance of heat pipe at different filling ratio; five heat pipes (thermosyphon) were constructed with filling ratio of 35%, 45%, 50%, 60% and 75% of heat pipe's evaporation volume. The experiment was conducted following the procedure as described in the previous section.

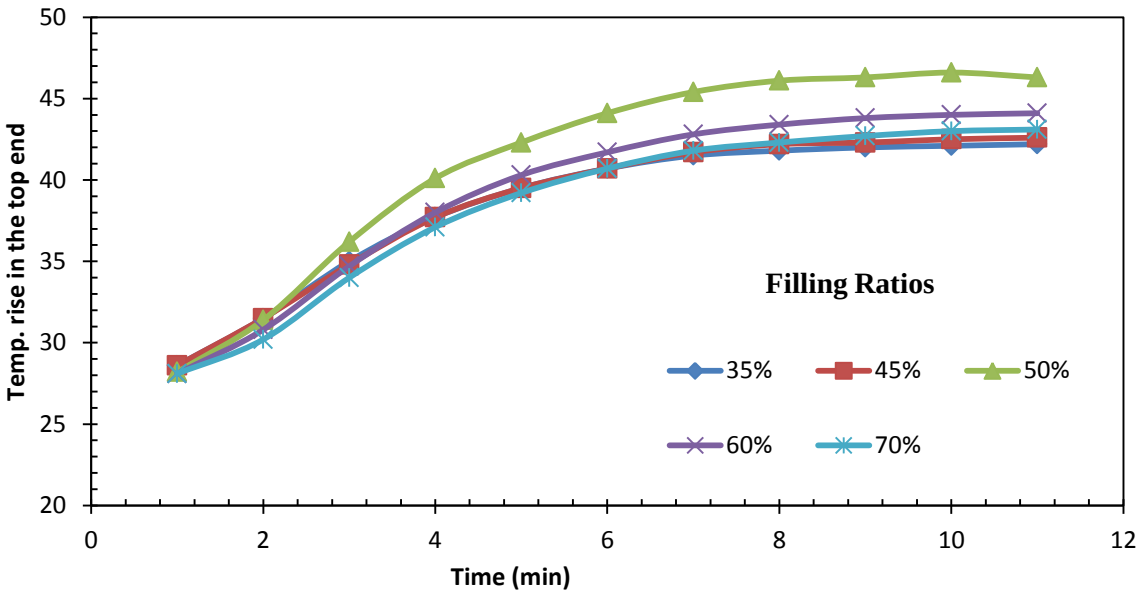

Figure 18: Variation of top end temperature with time for different filling ratio

As can be seen from figure 18, temperature in the condensation section is increasing with time for different filling ratio and heat pipe with 50% filling ratio responses faster than others and reaches maximum temperature of 47^{o}C. As, heat pipe with 50% filling ratio provides better performance than heat pipes with other filling ratio, heat pipe with 50% filling ratio was used for construction of the heat pipe heat exchanger.

Chapter 4

Effect of Adiabatic Section on the Performance of Heat Pipe Heat Exchanger

4.1 Introduction

A heat pipe heat exchanger (HPHE) is generally consists of three sections: (i) evaporation, (ii) condensation and (iii) adiabatic section. Adiabatic section separates the evaporator and the condenser sections by an appropriate distance. During operation of heat pipe, heat is applied on the evaporator section and is conducted through the container wall to the wick structure or direct into the working fluid in thermosyphon which causes vaporization of the working fluid. The resulting vapor, due to the pressure difference, moves through the adiabatic section to the condenser section where the vapor gets condensed releasing the latent heat of vaporization to the heat sink. The condensed liquid is forced back to the evaporator section due to capillary action of the wick material or by gravity force in thermosyphon. Thus heat pipe works continuously transporting latent heat from the evaporator to the condenser as along as sufficient capillary pressure or gravity force works on the working fluid.

Heat pipe can be design with adiabatic section or without adiabatic section. In both cases, heat pipe performs better compared to the pure material. However, most of the heat pipe is designed with the adiabatic section as it provides flexibility, stability and reliability during operation; although it has some limitations as adiabatic section's length and position plays a vital role on the heat transfer performance.

4.2 Calculation of heat pipe length

Heat recovery equipment based on two phase thermosyphon consists of an outer envelope with thermosyphon grooved inside. According to the operating principle of thermosyphon, heat is transferred from the evaporator, located at the bottom where hot gases flow, to the condenser, located at the top, where the fluid to be heated circulates.

It can be considered that the efficiency of the thermosyphon is 95% [65]. The energy balance for steady state conditions for heat transfer application may be expressed as:

$$\dot{m}_a\, c_{pa}\left(T_{a,out} - T_{a,in}\right) = \dot{m}_g\, c_{pg}\left(T_{g,in} - T_{g,out}\right) \quad \ldots\ldots\ldots\ldots\ldots\ldots\ldots\ldots\ldots\ldots \quad (1)$$

Applying the continuity equation gives the following expression

$$\rho_a A_a v_a c_{pa}\left(T_{a,out} - T_{a,in}\right) = \rho_g A_g v_g c_{pg}\left(T_{g,in} - T_{g,out}\right) \quad \ldots\ldots\ldots\ldots\ldots\ldots\ldots\ldots \quad (2)$$

In addition, the area for the passage of air A_a is defined as the product of the length of the thermosyphon condensation zone, l_c, by the width of the passage of air, a:

$$A_a = l_c a \quad \ldots\ldots\ldots\

these considerations into account and substituting equations (3) and (4) in equation (2) gives the expression (6)

$$\rho_a l_c c_{pa}(T_{a,out} - T_{a,in}) = 0.95\, \rho_g l_e c_{pg}(T_{g,in} - T_{g,out}) \quad \ldots\ldots\ldots\ldots\ldots\ldots\ldots\ldots \quad (6)$$

To determine one of the design parameters sought, which is the ratio between the length of the condensation zone and the total length of the thermosyphon, equations (5) and (6) are resolved simultaneously and following equation (7) is obtained.

$$\frac{l_c}{l_t} = \frac{0.95\, \rho_g c_{pg}(T_{g,in} - T_{g,out})}{0.95\, \rho_g c_{pg}(T_{g,in} - T_{g,out}) + \rho_a c_{pa}(T_{a,out} - T_{a,in})} \quad \ldots\ldots\ldots\ldots\ldots\ldots\ldots \quad (7)$$

From equation (5) and equation (7), the relation between the length of the evaporation zone and the total length of the thermosyphon (8) is obtained as follows:

$$\frac{l_e}{l_t} = 1 - \frac{l_c}{l_t} \quad \ldots\ldots\ldots\ldots\ldots\ldots\ldots\ldots\ldots\ldots\ldots\ldots \quad (8)$$

However, the equations developed above, consider only energy and mass balances, this analysis could lead to violations of the second law of thermodynamics. To be sure that the results do not violate this law, the mathematical models to calculate the entropy production in the system are used. Just for recalling that the total entropy change must be greater than or equal to zero.

If the air is considered as an ideal gas and the isobaric heating process is reversible, then the entropy change of air is expressed as follows:

$$\Delta \dot{s}_a = \dot{m}_a\, c_{pa} \ln\left(\frac{T_{a,out}}{T_{a,in}}\right) \quad \ldots\ldots\ldots\ldots\ldots\ldots\ldots\ldots\ldots\ldots\ldots\ldots \quad (9)$$

Similarly, for combustion gases the entropy change is expressed as follows:

$$\Delta \dot{s}_g = \dot{m}_g\, c_{pg} \ln\left(\frac{T_{g,out}}{T_{g,in}}\right) \quad \ldots\ldots\ldots\ldots\ldots\ldots\ldots\ldots\ldots\ldots\ldots\ldots \quad (10)$$

The expression to calculate the total entropy change of the system is as follows:

$$\Delta \dot{s}_{sys} = \Delta \dot{s}_a + \Delta \dot{s}_g \quad \ldots\ldots\ldots\ldots\ldots\ldots\ldots\ldots\ldots\ldots\ldots\ldots \quad (11)$$

As an example, a parametric analysis to study the relationship of the lengths of the zones of evaporation and condensation with respect to the total length of the thermosyphon was

carried out. The outlet temperatures of both air and combustion gases were varied. The air inlet temperature is assumed to be 25°C and the combustion gases of 250°C. The investigated interval of the air outlet temperature is 35ºC to 105°C. If temperature difference between the entrance and outlet of both air and gas are equal to 70 ºC,

$$T_{g,in} - T_{g,out} = T_{a,out} - T_{a,in} = 70\ ºC \quad \ldots\ldots\ldots\ldots\ldots\ldots\ldots\ldots\ldots\ldots\ldots\ldots \quad (12)$$

So, at the exit of the air preheater, outlet temperatures of air and hot gases are equal to $T_{a,out}$= 95 °C and $T_{g,out}$= 180 °C. This requires that the ratios of the lengths of the zones must be 42% of total length l_t as shown in fig.18, and le must be 58% of the total length of the thermosyphon according to the equations (7) and (8).

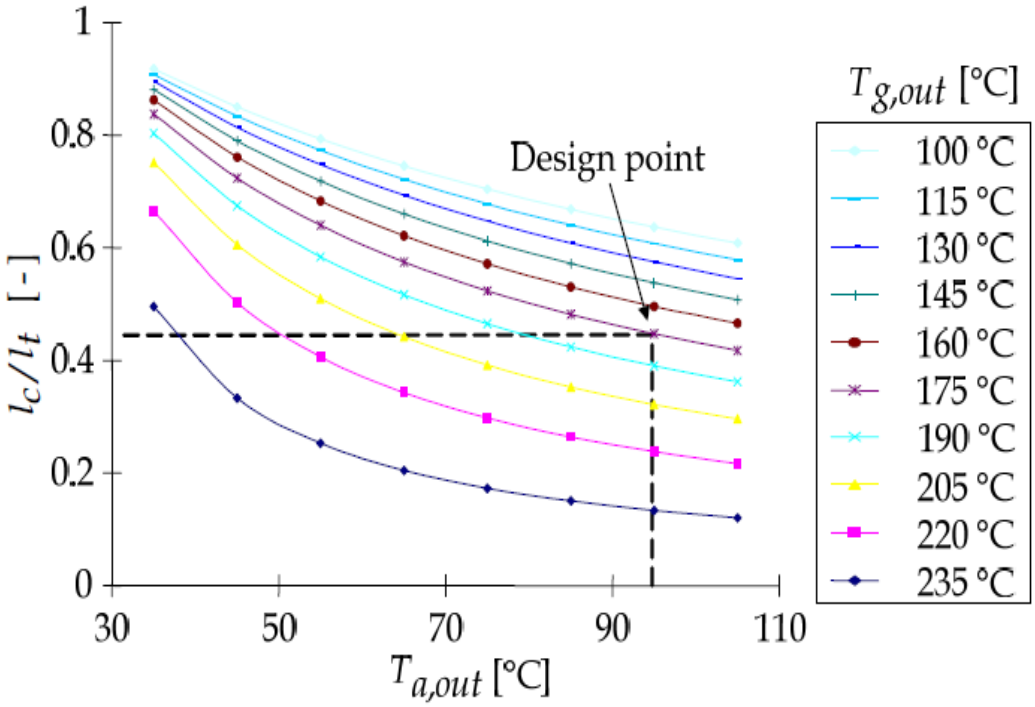

Figure 20: Length of the condensation zone and total length versus the outlet air temperature, for different outlet temperatures of gases [65]

4.2.1 Heat pipe effective length

The effective length is used to characterize the heat pipe zone of fluid circulation with a constant heat flux. It is defined by the following expression [66]:

$$L_{eff} = \int_0^{L_t} \int_0^{W_v} f_n \ (x,z)dxdz \quad \ldots\ldots\ldots\ldots\ldots\ldots\ldots\ldots\ldots\ldots\ldots\ldots \quad (13)$$

Where, L_t is the total heat pipe length and W_v is the heat pipe vapor width. The function $f_n(x, z)$ is piecewise defined for each zone of the heat pipe, assuming that local heat flux is dissipated following a linear evolution.

For the evaporation zone ($0 \leq z \leq L_e$):

$$f_n(z) = \frac{z}{w_v L_e} \quad \ldots\ldots\ldots\ldots\ldots\ldots\ldots\ldots\ldots\ldots \quad (14)$$

For the adiabatic zone ($L_e \leq z \leq L_e + L_a$):

$$f_n(z) = \frac{1}{w_v} \quad \ldots\ldots\ldots\ldots\ldots\ldots\ldots\ldots\ldots\ldots \quad (15)$$

For the condensation zone ($L_e + L_a \leq z \leq L_t$):

$$f_n(z) = \frac{L_t - z}{w_v L_e} \quad \ldots\ldots\ldots\ldots\ldots\ldots\ldots\ldots\ldots\ldots \quad (16)$$

Where L_c is the condenser heat pipe length and L_a is the adiabatic length of the heat pipe.

The effective length is given as the following:

$$L_{eff} = \frac{L_e}{2} + L_a + \frac{L_c}{2} \quad \ldots\ldots\ldots\ldots\ldots\ldots\ldots\ldots\ldots\ldots \quad (17)$$

4.3 Previous study regarding effect of adiabatic section on heat pipe performance

Different researchers have conducted experimental study to find the appropriate length of adiabatic section. It has been reported by several researchers that, shorter adiabatic section length has a great impact for increasing thermal performance of HPHE. Faghri and Buchko [67] showed that decreasing the adiabatic section length can significantly increase the capillary limit, which increase the thermal performance by increasing heat transfer rate. Sukchana, Jaiboonma [68] presented that shorter in adiabatic section length increase thermal efficiency of the heat pipe and favorable heat fluxes are found to for shorter adiabatic length. François *et. al.* investigated [69] the influence of the heat pipe's adiabatic length for a fixed length of evaporator of 1.3 cm where adiabatic lengths L_a varies between 0 to 5 cm. The performance of their study is presented in fig.21; the liquid and vapor pressure difference increases with increasing adiabatic length whereas they are decreasing with heat transfer rate.

The maximum heat transfer rate observed when the adiabatic length is short. Indeed, the effective length, defined by $L_{eff} = 0.5(L_e + L_c) + La$, increases when the adiabatic length 'La' increases. The increase of the effective length increases the area of the vapor–liquid heat transfer.

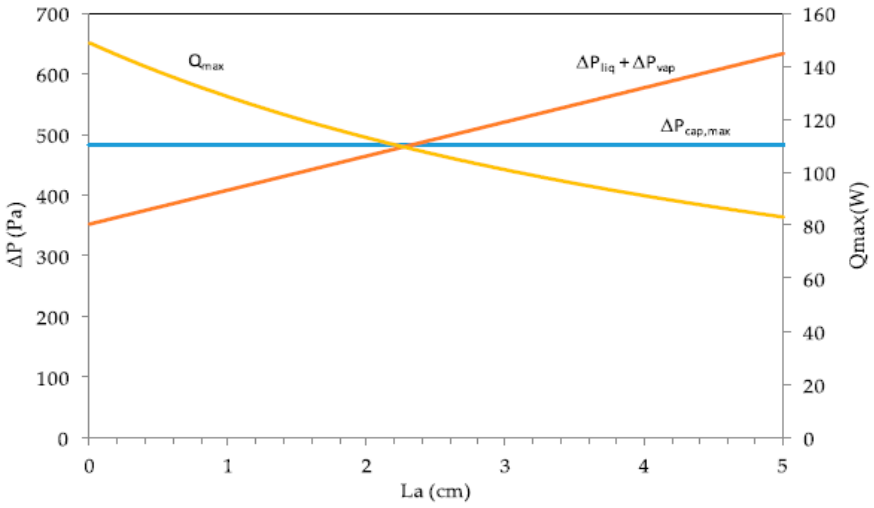

Figure 21: Capillary pressure, differences in liquid pressure, vapor, and maximum heat versus the adiabatic length [69]

Rakesh and Chandrasekharan [70] showed variation of entropy generation against heat load for different lengths of adiabatic section with a constant sink temperature of 303 K. Entropy generation rate is found to increase with heat load, and the rate of increase is more when heat load increases. This is due to the fact that, with the increase in heat load, temperature difference between the walls of evaporator and condenser increases and pressure drop also increases results in entropy generation. For same operating conditions, entropy generation rate is found to increase with the length of adiabatic section. As the length of the adiabatic section increases, effective length of the heat pipe also increases; this in-turn increases pressure drop in the liquid wick and vapor core along the heat pipe which results in increase of entropy generation. The rate of increase is found to be more at higher heat flux. Entropy generation rate is found to increase from 1.09×10^{-3} to 3.88×10^{-2} W/m^3·K for the heat input range of 100 to 600 W without the adiabatic section. The entropy rate is found to be almost doubled when the length of adiabatic section is varied from 0 to 0.5 m, for the corresponding heat flux.

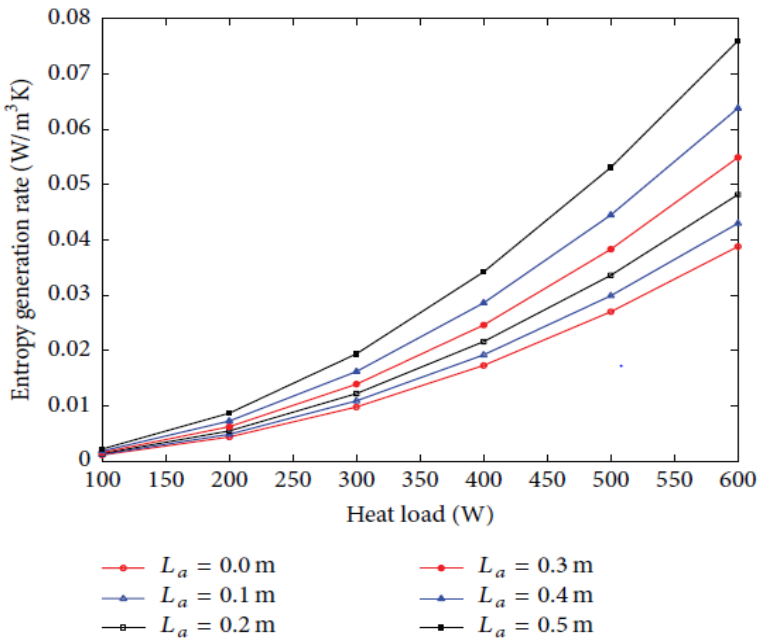

Figure 22: Variation in entropy generation rate against heat load for different lengths of adiabatic section [70]

Wang *et. al.* [71] have carried out a series of experiments to investigate the effect of evaporation and condensation length on the thermal performance of a flat plate heat pipes (FPHP). In the experiment, FPHPs has the heat transfer length (L) of 255 mm and the width of 25 mm. The evaporation section length was 20, 30, 40, 50 and 70 mm, respectively. The condensation section length was 20, 40, 50, 60, 80 and 100, respectively. Moreover, the FPHP achieved the maximum heat transport capability of 132.2 W (the heat transport efficiency reached 94.4%) at heating power of 140W, when the length of evaporation section and condensation section both were 50 mm. which conclude that condenser length and evaporation length should be equal.

Anjankar and Yarasu [72] have carried out experiment on a vertical two phase closed thermosyphon. The tests were conducted at different heat inputs, condenser length of working fluid and constant evaporator length of 300 mm. A closed copper tube with a length of 1000 mm and inner and outer diameters of 26 and 32 mm was used as the thermosyphon. Three lengths of condenser 450, 400, and 350 have been studied. The performance at 450 mm condensers length is maximum than that of 400 and 350 mm condenser lengths for all the flow rate. They concluded that condenser section length should be 1.5 times to that of evaporator length to get good thermal performance.

It can be seen from fig.23 that at 500 W input heat and 10 liter per hour flow rate of water at 450 mm condenser length with 300 mm constant evaporation length and 250 mm adiabatic length thermosyphon efficiency is highest.

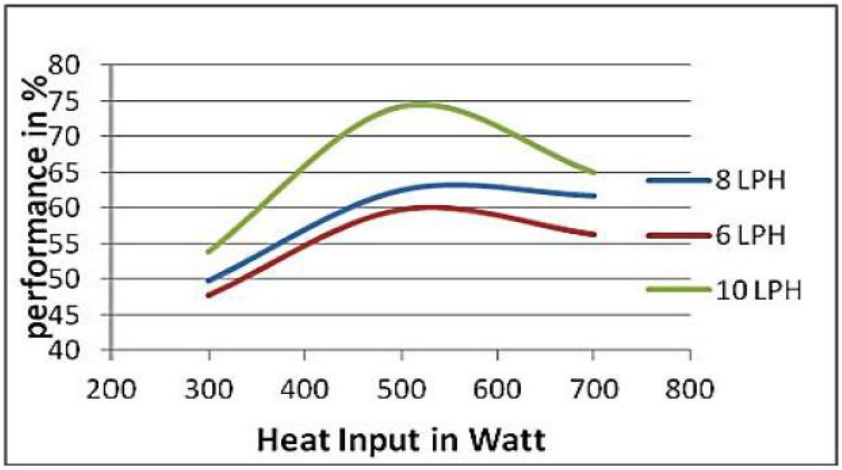

Figure 23: Performance at different heat input and cooling water flow rate [72]

4.4 Present Study

In this study, thermal performance of heat pipe heat exchanger (HPHE) was investigated for different length and position of the adiabatic section.

4.5 Experimental Setup

Four experimental setup for heat pipe heat exchanger were constructed:

i. HPHE without adiabatic section
ii. HPHE with 32 mm adiabatic section
iii. HPHE with 64 mm adiabatic section
iv. HPHE with 96 mm adiabatic section

Position of the adiabatic section was also varied. The experimental setup was consisted of a water-water HPHE, a data collection system, a water heater of 1000 W, four k-type thermocouples, cold water chamber, valves for controlling the water mass flow rate as presented in the fig. 24. The water in the evaporation section was heated by heater which was connected with a voltage variac to control temperature. A provision for cold water flow was available in case water temperature rise too much; the line is opened to allow the cold water flowing through the chamber carrying the excess heat.

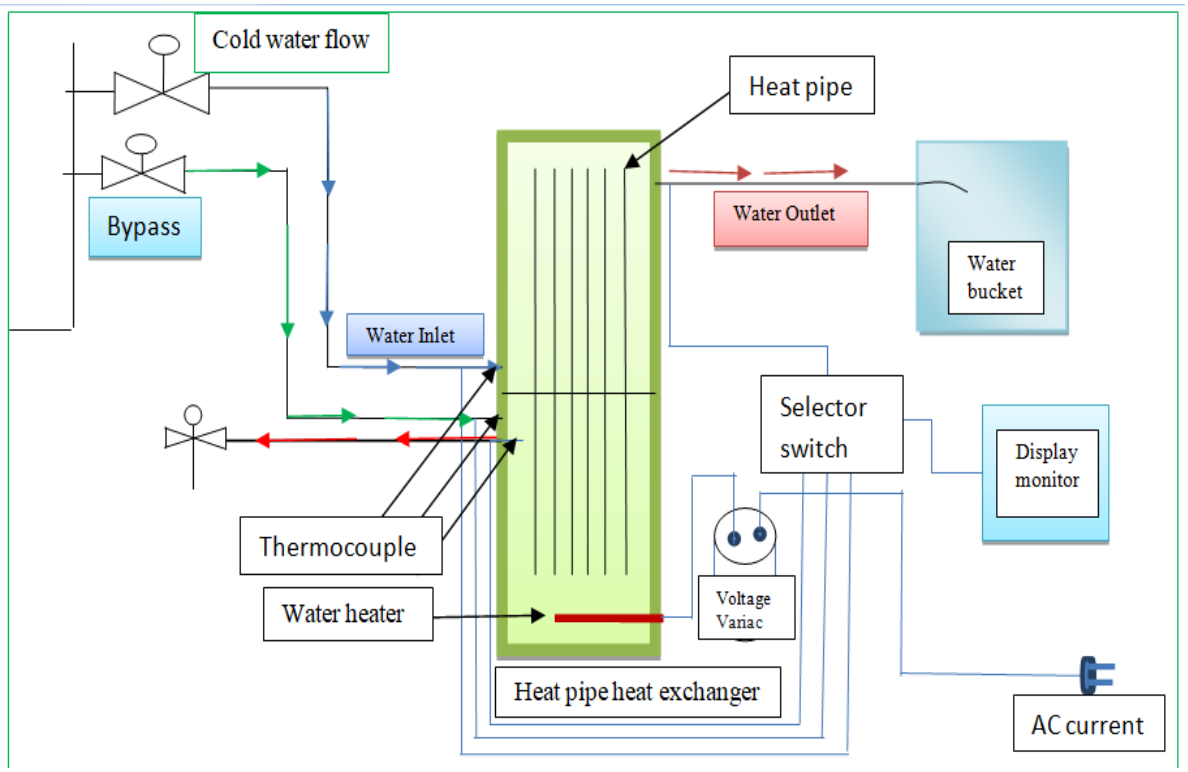

Figure 24: Schematic diagram of experimental setup of HPHE

HPHE consisted of a number of heat pipes. For this study, twenty four heat pipes were used for constructing four heat pipe heat exchangers (HPHE), where each consists of six heat pipes. For the HPHE without adiabatic section, a steel plate of 5 mm thickness was used as a separation between the evaporation and condensation section. For HPHE with adiabatic section was prepared by separating the middle portion of the heat pipe with acrylic plate and insulating the region between the acrylic plates as presented in the fig.26.

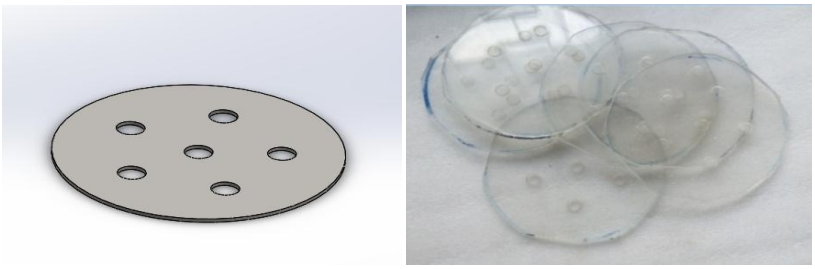

(a) (b)

Figure 25: (a) Steel Plate; (b) Acrylic Sheet

The heat pipes were assembled between two water reservoirs placed vertically; bottom one acts as an evaporator and top one acts as a condenser. Thus water-water HPHE was prepared for the experiment.

(a) (b)

Figure 26: (a) Heat pipes assembly on Steel Plate; (b) Heat pipes assembly on Acrylic Sheet

In the evaporation section of the HPHE, an electric heater of 1000 W was placed for heating up the water at a constant temperature of □70°C. The condenser was connected with two hose pipes to carry out the transferred heat from the condenser. All the external surfaces of the HPHE were insulated using glass wool and PVC pipe. The length of the evaporator and condensation section in HPHE was 8 inch and 10 inch, respectively.

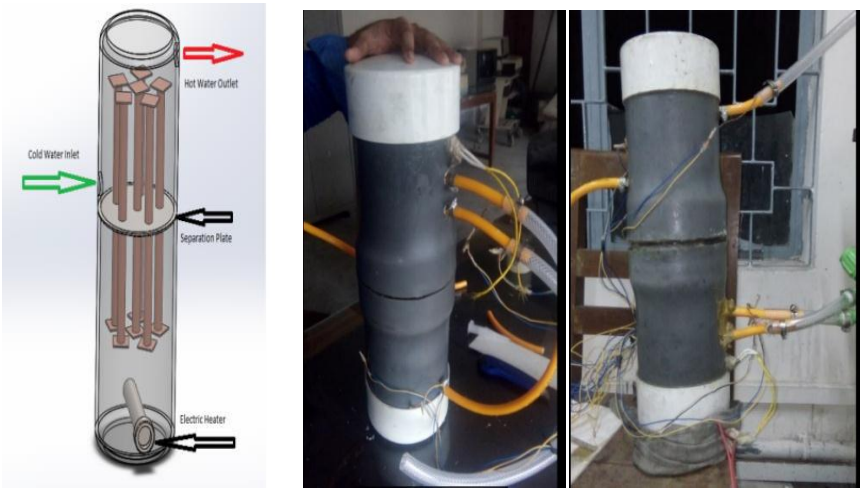

Figure 27: (a) Heat pipe with separation Plate; (b) & (c) Total assembly of water-to-water HPHE without adiabatic section

Three HPHE was constructed with adiabatic section. The length of the adiabatic section was varied at 32 mm, 64 mm and 96 mm from the center of heat pipes with a constant 10 inch evaporation section length as shown in fig.28.

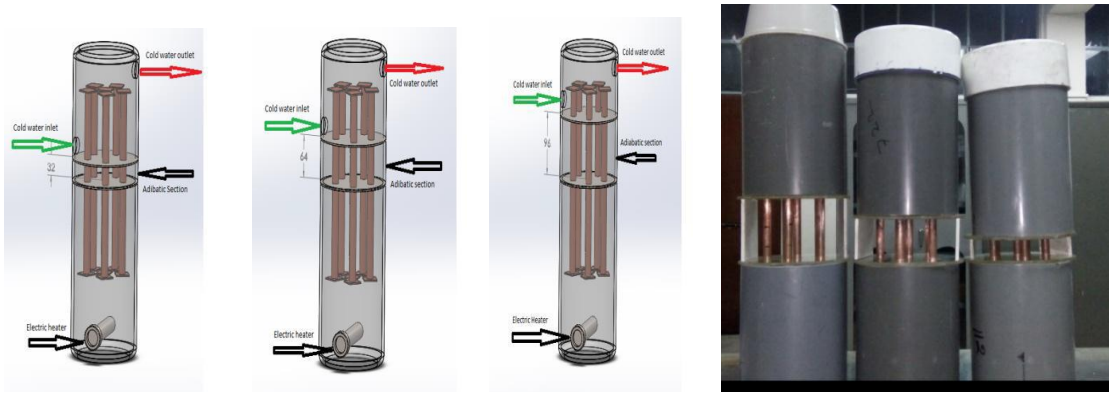

(a) (b) (c) (d)

Figure 28: Variation of adiabatic length; (a) 32 mm adiabatic length; (b) 64 mm adiabatic length; (c) 96 mm adiabatic length

The adiabatic section was properly insulated with glass wool and warped by a heat reflective insulation foil. So, heat is transferred by the heat pipes from the condensation section to the evaporation section without any loss in adiabatic section.

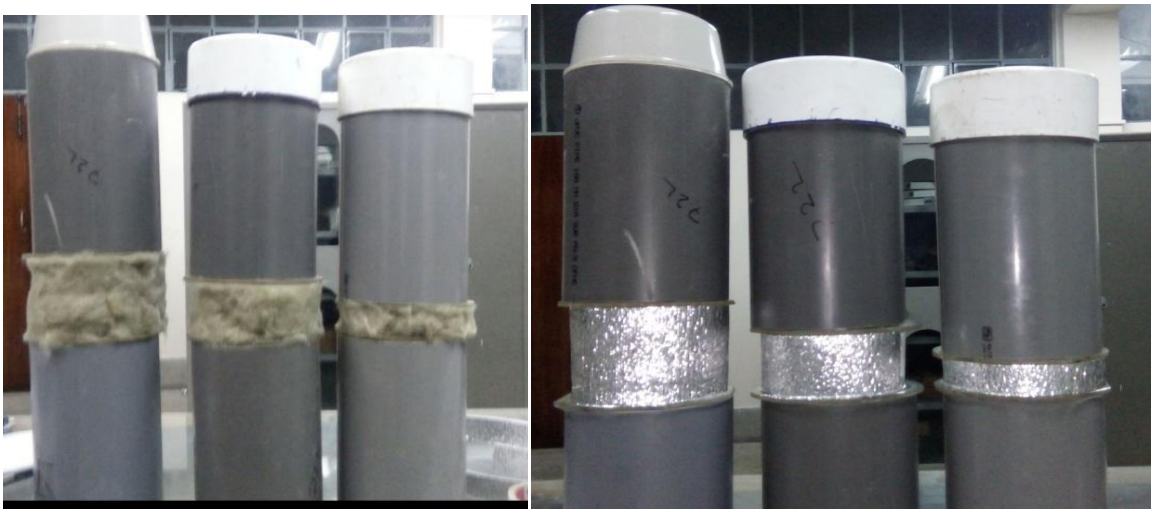

(a) (b)

Figure 29: Insulation of adiabatic section

To study the effect of the position of the adiabatic section, the adiabatic section was varied from the center of the heat pipes to upward at 32 mm and 64 mm, and downward at 32 mm as presented in the fig.30.

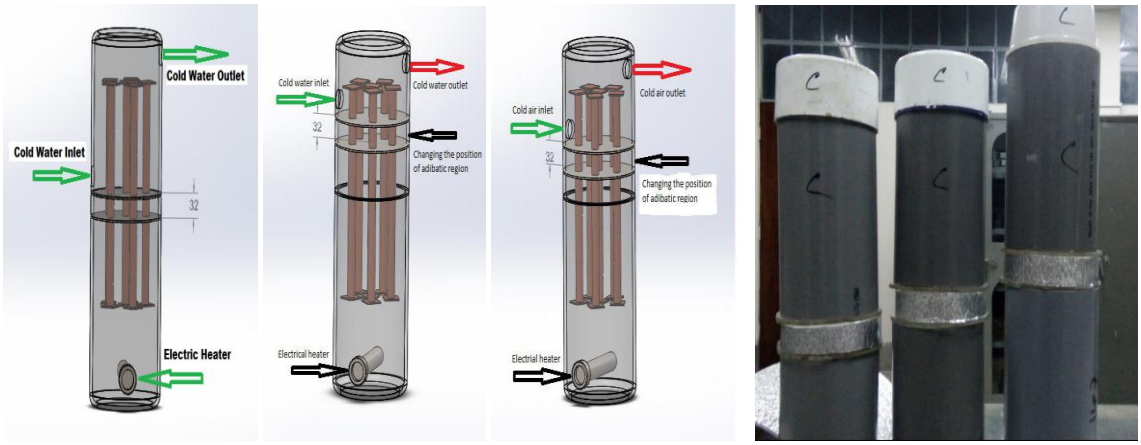

(a) (b) (c) (d)

Figure 30: HPHE with different position of adiabatic section; (a) adiabatic section 32 mm upward from the center of the heat pipe; (b) adiabatic section 64 mm upward from the center of the heat pipe; (c) adiabatic section 32 mm downward from the center of the heat pipe

4.6 Data Acquisition System

Cold water was flowed into the condensation section through a hose pipe. Flow rate of the water was varied by the connected valve for individual set of data. Mass flow rate of water was measured by bucket and stop watch method [73]

Temperature of the water entering and exiting the condensation and evaporation section of the heat pipe heat exchanger was measured by four k-type thermocouples. The thermocouples were connected with a display unit through a selector switch.

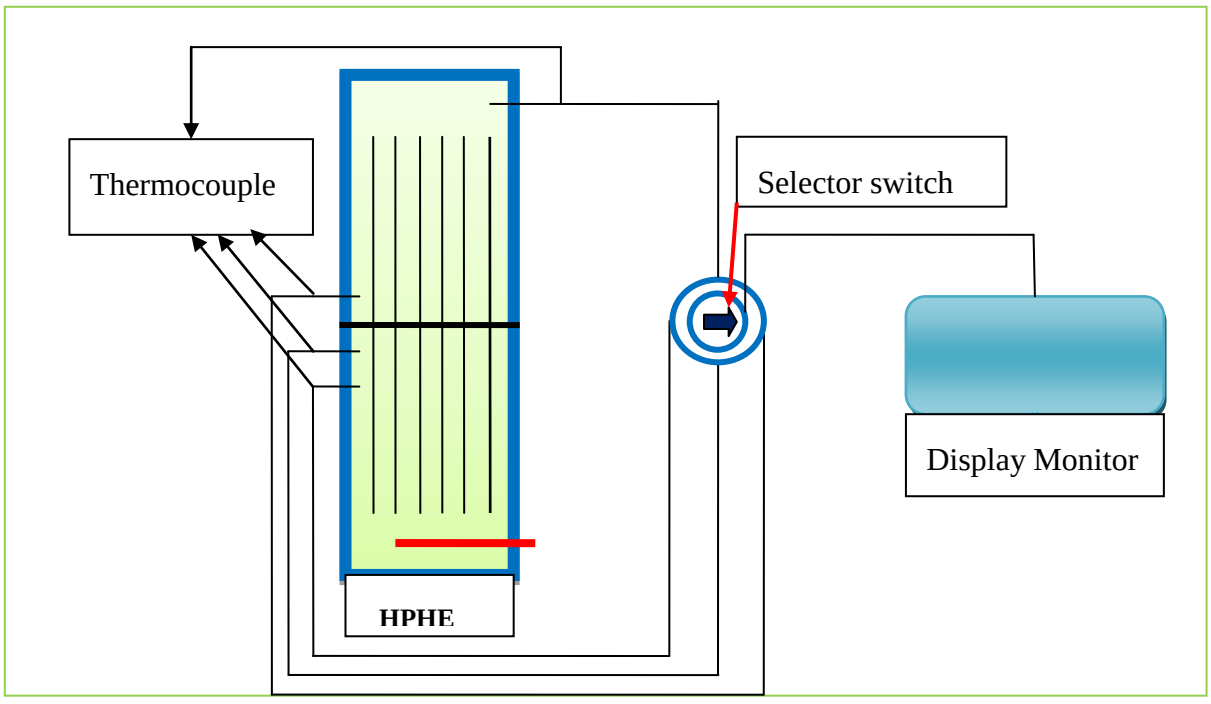

Figure 31: Measurement of Temperature by thermocouple and selector switch

4.7 Experimental Method

Water was heated at a constant temperature of □70℃ by a water heater placed in the evaporation section. The cold water at atmospheric temperature was passed through the upper chamber (condensation section). The two chambers were separated by a separation plate (without adiabatic section) or adiabatic section. After switching on the experimental setup, about one hour time was given to achieve steady state condition. Steady state condition was monitored by measuring the temperature at regular interval. Once the steady state condition was achieved, data was measured. The approach was repeated by varying the water flow rate.

4.8 Data Reduction

The heat transfer rate ($\dot{Q}$) for the HPHE was calculated from the cold water mass flow rate by following equation:

$$\dot{\mathbf{Q}} = \dot{\mathbf{m}}_{\mathbf{cw}}\mathbf{Cp}_{\mathbf{cw}}(\mathbf{T}_{\mathbf{cw,in}} - \mathbf{T}_{\mathbf{cw,out}}) \quad \ldots\ldots\ldots\ldots\ldots\ldots\ldots\ldots\ldots\ldots \quad (18)$$

Where, ṁ is the mass flow rate, Cp is the specific heat capacity, and *T* is the temperature. The subscript **cw** refers to the cold water, "**cw, in** and **cw, out**" refer to the inlet and outlet of cold water, respectively.

The overall heat transfer coefficient *U* of the HPHE is defined as follows, W/ (m^2 .K):

$$\mathbf{U} = \dot{\mathbf{Q}} / \mathbf{A}\,\Delta\mathbf{T} \quad \ldots\ldots\ldots\ldots\ldots\ldots\ldots\ldots\ldots\ldots \quad (19)$$

Where, *A* is the overall heat transfer area of the HPHE, (m^2) and temperature difference ΔT, *(K).*

The effectiveness of HPHE is defined as the ratio of the actual heat transfer rate *Q* in a given heat exchanger to the maximum possible heat transfer rate $\mathbf{Q}_{\mathbf{max}}$:

$$\boldsymbol{\varepsilon} = \dot{\mathbf{Q}} / \dot{\mathbf{Q}}_{\mathbf{max}} \quad \ldots\ldots\ldots\ldots\ldots\ldots\ldots\ldots\ldots\ldots \quad (20)$$

Where ($\dot{Q}$) is the actual heat transfer rate and ($\dot{\mathbf{Q}}_{\mathbf{max}}$) is the maximum possible heat transfer rate in the given heat exchanger.

4.9 Uncertainty Analysis

In each measurement, there exist some uncertainties. These uncertainties come into account mainly due to limitations of measuring instruments. Uncertainty of the instruments was estimated as below:

- Lengths and diameters: ± 0.5 mm.
- Temperatures : ± 0.5□
- Mass flow rate of water: ± 0.0005 kg/s

The uncertainty propagated into the calculated value was estimated following the Klin and Mcclintoc's method relation below.

If $R = R(x_1, x_2, \ldots\ldots, x_n)$is a given function of independentvariables$x_1, x_2, \ldots\ldots, x_n$; and $w_1, w_2, \ldots\ldots, w_n$are the associateduncertainties, then uncertainty of the result $(w_R)$is given by:

$$w_R = \sqrt{(\frac{\partial R}{\partial x_1} w_1)^2 + (\frac{\partial R}{\partial x_2} w_2)^2 + \ldots\ldots\ldots + (\frac{\partial R}{\partial x_n} w_n)^2} \quad \ldots\ldots\ldots\ldots\ldots\ldots \quad (21)$$

The best estimate of the true mean value, R_t, would be stated as:

$$R_t = \bar{R} \pm w_R \ (P\%) \quad \ldots\ldots\ldots\ldots\ldots\ldots\ldots\ldots\ldots\ldots\ldots\ldots\ldots\ldots\ldots\ldots\ldots\ldots \quad (22)$$

Where, the sample mean, $\bar{R}$is found from:

$$\bar{R} = R(\bar{x}_1, \bar{x}_2, \ldots\ldots, \bar{x}_n) \quad \ldots\ldots\ldots\ldots\ldots\ldots\ldots\ldots\ldots\ldots\ldots\ldots\ldots\ldots\ldots\ldots\ldots\ldots \quad (23)$$

Uncertainties associated with the calculated values were estimated as listed in the table below:

Table 9: Uncertainty propagated into the calculated values

Sl. No.	Parameters	Uncertainties (%)
1.	Pipe diameter	0.33
2.	Plate area	0.77
3.	Fin area	5.48
4.	Mass flow rate	2 % ~ 10 %
5.	Heat input	3 % ~ 5 %
6.	Cold water temperature rise	5.89 % □ 23.57 %
7.	Heat transfer rate	11.60 % □ 25.29 %
8.	Effectiveness (ε)	11.68 % □ 25.34 %

4.10 Results and Discussion

4.10.1 Effect of Adiabatic Section Length

For analyzing performance of HPHE, the experiment was conducted without adiabatic section Fig. 27 (a), where a steel plate was used as a separation plate at the middle of the heat pipe heat exchanger (HPHE) that equally divided the heat pipe in the evaporation and condensation section. The experiment was again conducted with adiabatic section for observing the effect of adiabatic section on heat pipe. Experiments were carried out by increasing the length of adiabatic section from the middle at 32 mm, 64 mm and 96 mm as

shown in the fig.28 (a),-& (c).The performance of HPHE was evaluated for each adiabatic length. The results are presented in fig.32; with increasing of mass flow rate of cold water, heat transfer rate increases. As the length of the adiabatic section increases, effective length of the heat pipe also increases; this in turn increases pressure drop in the liquid and vapor core along the heat pipe which results in increase of entropy generation and decrease of heat transfer rate. The maximum 680W heat transfer rate was observed in the experiment without adiabatic section. In this case, heat transfer occurred from the evaporation section to the condensation section by both heat pipes and separation plate thus increases the heat transfer surface area which promotes heat transfer rate. Performances of the HPHE with shorter adiabatic length of 32 mm provides better than the longer adiabatic length of 64 and 96 mm, where heat transfer rate was varied from 554 W, 443 W and 388 W respectively for 32 mm, 64 mm and 64 mm length of adiabatic section. In the higher adiabatic length, inside the heat pipe the liquid film of working fluid from the condenser section to evaporator section remaining in the higher vapor space and also take longer time to return the condensate fluid by gravity flow. Thus shorter adiabatic length is preferred for HPHE.

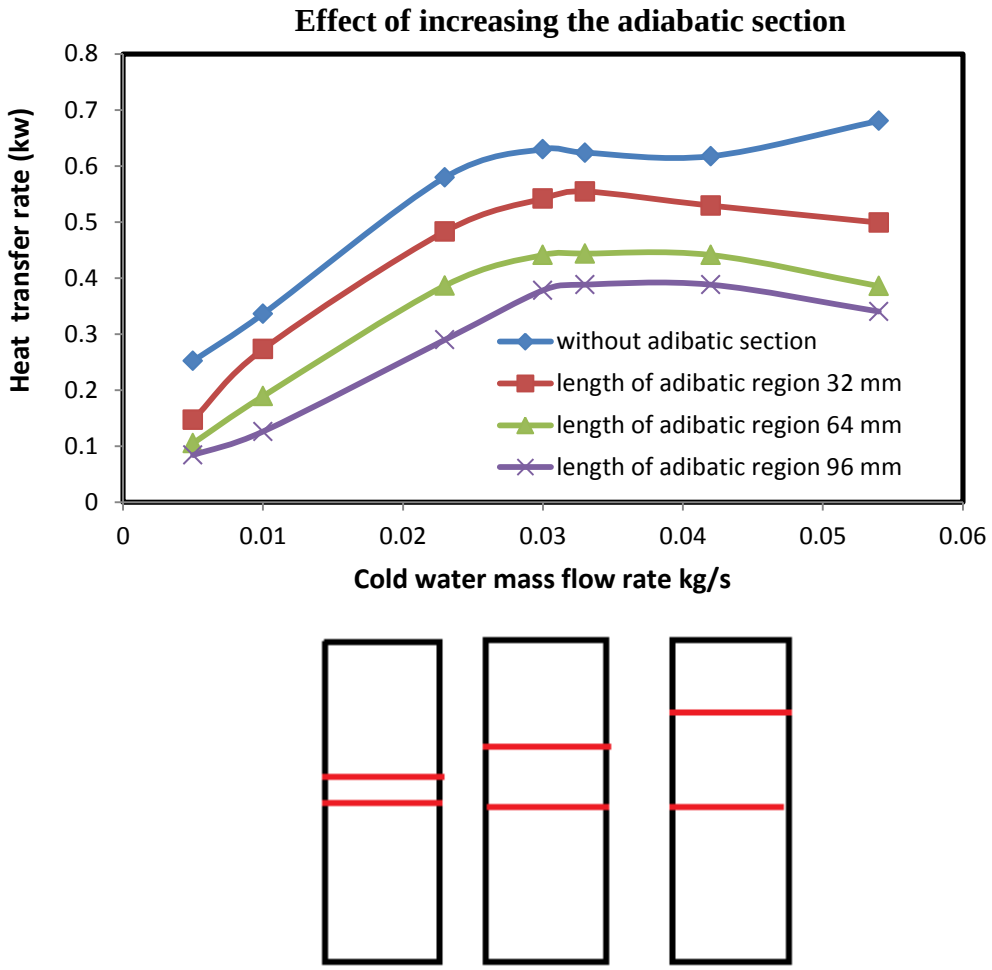

Figure 32: Effect of increasing the adiabatic section length on heat transfer rate

4.10.2 Effect of Changing the Position of Adiabatic Section

Appropriate position of the adiabatic section between evaporation and condensation section also increase the thermal performance of HPHE. For investigating thermal performance of HPHE, the positions of adiabatic section was changed from center of the heat pipe to upward at 32 mm, 64 mm and downward at 32 mm with a constant 32 mm adiabatic length as presented in the fig.30 (a) - (c). The performance of HPHE was evaluated for each position of adiabatic section. The highest performance was obtained when condensation length was bigger as adiabatic section was 32 mm downward from the center of heat pipe. The result is showed in fig.33, larger condensation length provides better performance than larger evaporation length where heat transfer rate varies from 570W for larger condensation length (as adiabatic section at 32 mm downward from center position of heat pipe) to 550W, 470W for longer evaporation length (as adiabatic section at 32, 64 mm upward from the center of heat pipe).

At higher heating power, condensation section length keeps bigger than the evaporation section length. So, film of working fluid that gets condensed properly in the condensation section and give up all of its latent heat and return to the evaporation section. For this reason, the position of adiabatic section at 32 mm and 64 mm upward from the center of heat pipe, thermal performance of heat pipe decreases as condensation length decreases. In other words, increasing condensation section length would make the heat pipe (thermosyphon) dry out at a lower heating power, which indicated that the heat transfer limit is decreased. It was related to the capillary limit. The heat pipe with a bigger condensation section length (at high heating power) allows vapor from evaporator to condense more rapidly. But due to the capillary limit, the condensed liquid could not flow rapidly back to the evaporator and then there was less working liquid at the evaporator, which could make the heat pipe dry out. So that the heat pipe with bigger condensation section length would dry out at a lower heating power. Thus in HPHE, an appropriate position of adiabatic section is needed between evaporation and condensation section. Larger condensation length is needed for higher heating power and lower condensation length is needed for lower heating power.

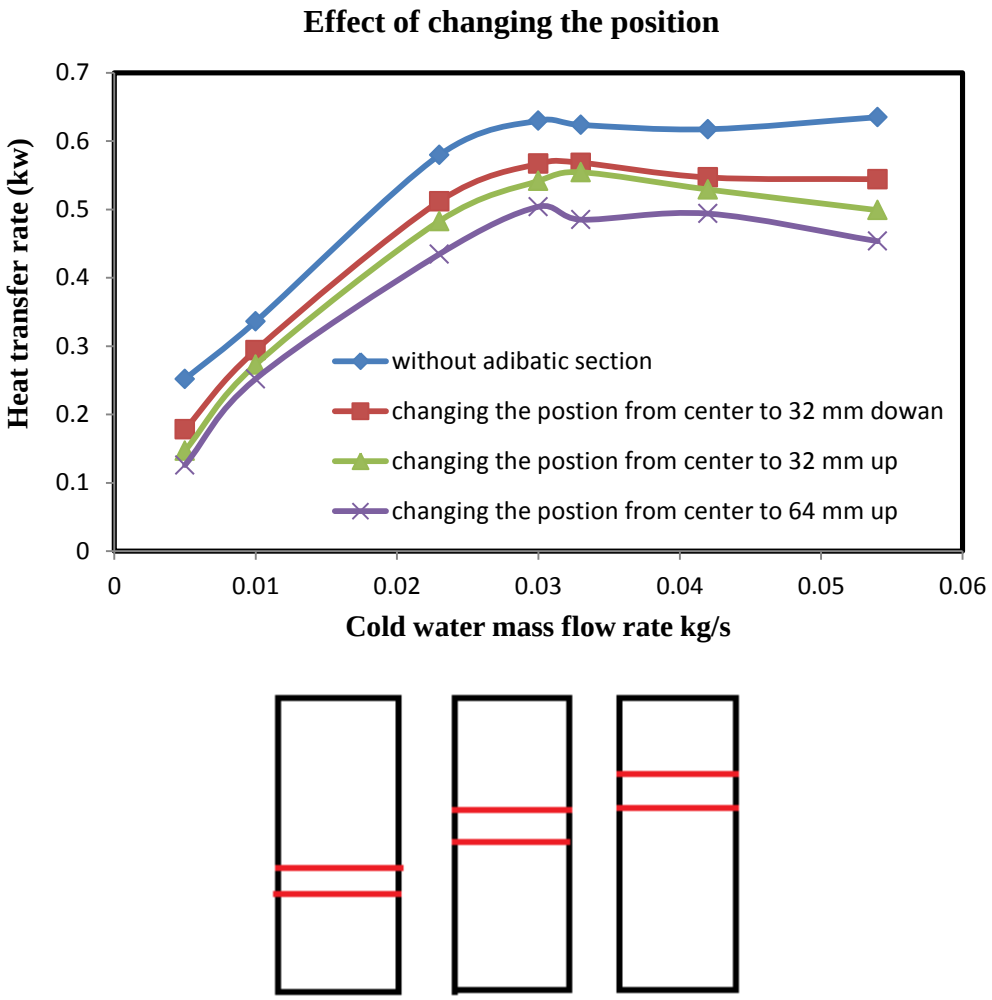

Figure 33: Effect of position of adiabatic section on HPHE performance

4.10.3 Effectiveness

The main purpose of this study was to investigate the effect of adiabatic region on HPHE, where the experiments have done without adiabatic section, increasing the adiabatic section and changing the adiabatic section position. Effectiveness of the heat pipe for different condition of adiabatic section was calculated by comparing the actual heat transfer rate to that of the maximum heat transfer rate. The result presented in fig.34 shows that the maximum effectiveness of 68% was observed for the heat pipe without adiabatic section followed by 55.4%, 44.3% and 38.8% for heat pipe with adiabatic section length of 32 mm, 64 mm and 96 mm. 57%, 53% and 47% effectiveness was calculated for the heat pipe with adiabatic length of 32 mm downward and 32 mm and 64 mm upward from center of heat pipe.

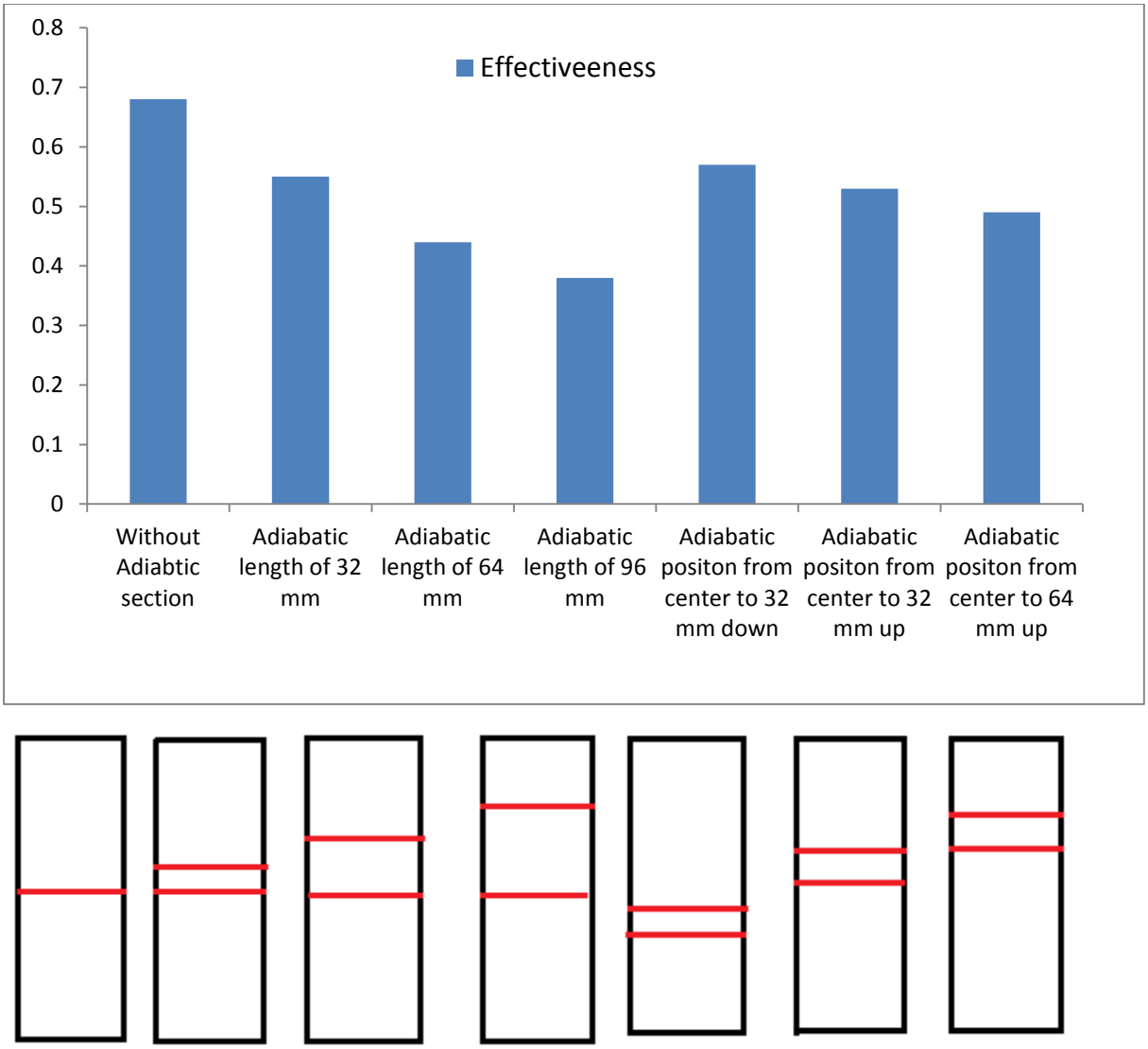

Figure 34: Effectiveness of the heat pipe for different adiabatic section

Chapter 5

HPHE Design and Performance Study

5.1 Mathematical Model of HPHE

The mathematical model of HPHE was developed with the concept of thermal resistance. It was mainly dependent on the geometry of heat pipe, fin and the thermal properties of medium (air, working fluid). The whole system of heat transfer was divided by three stages for the purpose of design simplicity; heat entered the heat pipe from hot air through its evaporator surface area by convection, then it was transferred from hot side to cold side through heat pipes by conduction and phase change heat transfer process and finally it was released to the cold side by convection through the heat pipes condenser surface area.

5.1.1 Convection Resistance

Calculation of convection resistance of HPHE was based on the Newton's law of cooling for convection heat transfer rate

$$\dot{Q}_{conv} = hA_s(T_1 - T_2) \quad \text{.....} \quad (24)$$

It can be re-arranged as:

$$\dot{Q}_{conv} = \frac{(T_1 - T_2)}{R_{conv}} \quad \text{.....} \quad (25)$$

Where,

$$R_{conv} = \frac{1}{hA_s} \quad \text{.....} \quad (26)$$

A_s Was total surface area of heat pipes including fin area.

5.1.2 Conduction Resistance

Calculation of conduction resistance was based on Fourier's law of heat conduction.

$$\dot{Q}_{cond} = \frac{kA(T_1 - T_2)}{L} \quad \text{.....} \quad (27)$$

It can be re-arranged as:

$$\dot{Q}_{cond} = \frac{(T_1 - T_2)}{R_{cond}} \quad \text{.....} \quad (28)$$

Where,

$$R_{cond} = \frac{L}{kA} \quad \ldots\ldots\ldots\

Heat pipe:

Outer diameter: 12.7 mm

Inner diameter: 11.2 mm

Fin Dimension: 38 mm × 38 mm

Number of fin per tube: 7

Length at condenser: 558.8 mm

Area of fin: [For single tube at one side (condenser or evaporator) only]

$$A_t = 2 \times 3.5 \times \left(0.0382 - \frac{\pi}{4} \times 0.0132\right) + \pi \times 0.013 \times 0.56 + \frac{\pi}{4} \times 0.0132 \text{ m}^2$$

$$= 0.032 \text{ m}^2$$

$$A_b = \pi \times 0.013 \times 0.56 + \frac{\pi}{4} \times 0.0132 \text{ m}^2$$

$$= 0.023 \text{ m}^2$$

Reynold's number: [Using bare heat pipe diameter]

$$Re = \frac{\rho v D}{\mu} \quad \ldots\ldots\ldots\ldots\ldots\ldots\ldots\ldots\ldots\ldots\ldots\ldots\ldots\ldots\ldots\ldots\ldots\ldots\ldots\ldots\ldots\ldots \quad (31)$$

$$= \frac{1.17 \times 2 \times 0.013}{1.84 \times 10^{-5}} = 1.65 \times 10^3$$

Heat transfer Coefficient: [Using empirical relation]

$$h = C_1 \left(\frac{K_{ex}}{2r_o}\right)\left(\frac{A_t}{A_b}\right)^{-\frac{3}{8}} Re^{\frac{5}{8}} Pr^{\frac{1}{3}} \quad \ldots\ldots\ldots\ldots\ldots\ldots\ldots\ldots\ldots\ldots\ldots\ldots\ldots\ldots\ldots\ldots\ldots\ldots\ldots\ldots\ldots\ldots\ldots\ldots \quad (32)$$

$$= 26.42 \text{ W/m}^2\text{K}.$$

Equation:

$$\Delta T = \frac{Q}{n}\left(\frac{1}{hA} + \frac{L}{kA} + \frac{1}{hA}\right) \quad \ldots\ldots\ldots\

5.2 Experimental Setup

An experimental setup was designed and constructed to investigate heat transfer performance of the HPHE at low temperature operation.

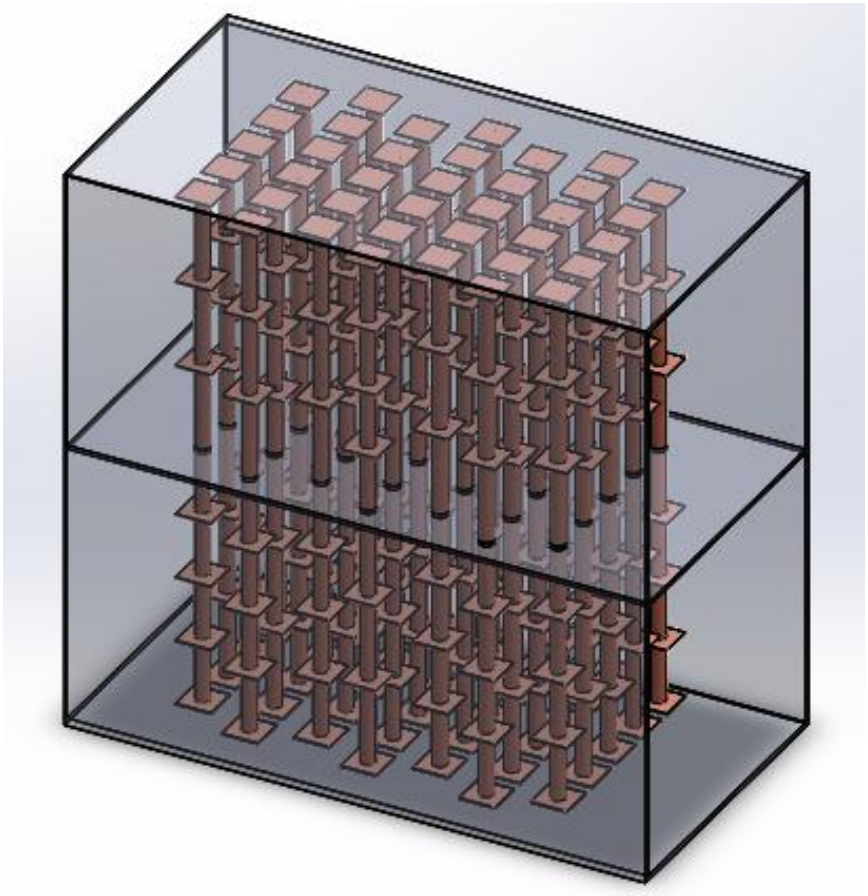

Figure 35: The designed heat exchanger

5.2.1 Construction of Heat Pipe Heat Exchanger

In this study, the designed HPHE was consisting of thirty eight heat pipes that were arranged vertically on the separation plate in seven rows; each row consisting of five or six heat pipes. The arrangement of heat pipes on the separation plate is shown in fig.36. Tubes were arranged in triangular formation for creating turbulence flow in both condensation and evaporation sections. Each heat pipe consisted of seven square fins with dimension 38mm × 38mm (~1.5 inch ×1.5 inch) made of copper sheet. Fins were arranged in the heat pipes in such way that made the flow zigzag and created more turbulence and thus increased the heat transfer rate.

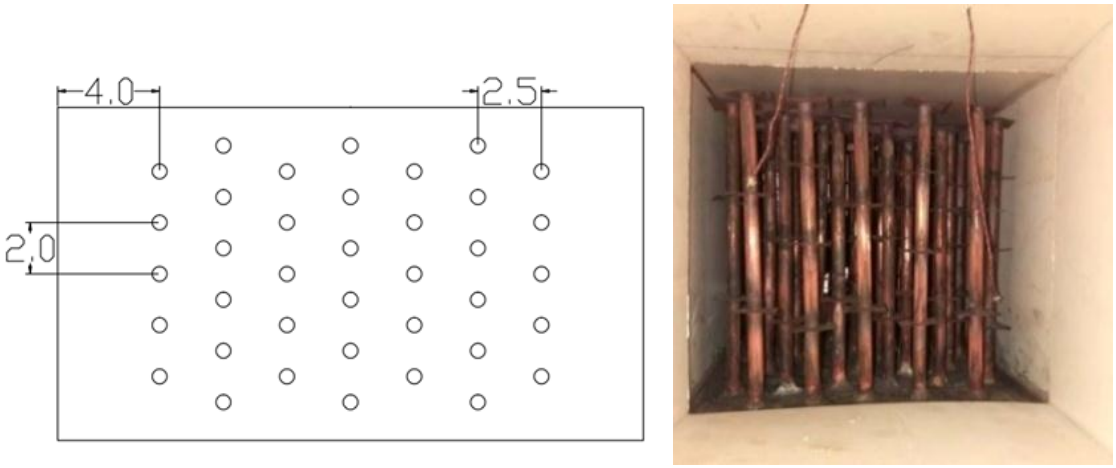

(a) **(b)**

Figure 36: Layout of pipes (a) Designed (top view), (b) Actual (front view)

5.2.2 Test Section

The test section consisted of a HPHE, cold and hot air ducts, a data collection system, two fans for cold and hot air passing, an air pre-heater, eight k-type thermocouples, etc. as shown in figure 37. To get more uniform temperature of hot air, a metal wire mesh was attached at downstream of the heater. The constructed HPHE was placed between the two ducts for hot and cold air flow in such a way that its evaporation section remained inside the hot air stream and condensation section remained inside the cold air stream. Two fans were placed at the two ends of the ducts to produce air flow. An air–preheated of 4.5 kW was placed inside the lower duct for heating the air. The temperature of air is controlled between 40°C and 75°C. The cold air in the condensation section is taken either from the atmosphere or air conditioning system. For measuring the temperature of hot and cold air in condensation and evaporation inlets and outlets, there were eight k-type thermocouples.

(a) **(b)**

Figure 37: Inlet of the hot air section

The overall setup is shown in following fig.38.

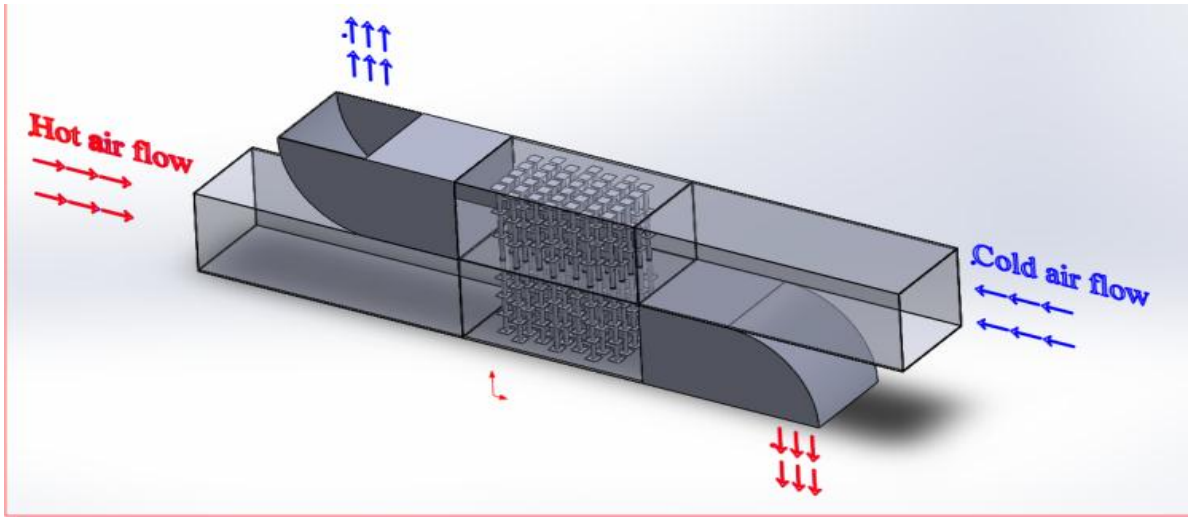

(a)

(b)

Figure 38: Experimental setup for a heat pipe heat exchanger (a) Designed, (b) Actual

5.2.3 Experimental Method

Data have been collected after the system reached steady state. Air was heated by flowing it over a resistance heater. The hot air was passed through the lower duct. The cold air was taken either from atmosphere or from an air conditioning system. Then it was passed through the upper duct. After starting the experiment, a significant time (about an hour) was given to achieve steady state. The parameters that indicated steady state were steady temperatures and steady flow velocities. After starting the setup, temperatures and velocities were measured at regular time interval. When two or three consecutive readings showed the same value, the setup was assumed to be at steady state. After reaching the system at steady state, data were recorded. The procedure was repeated for different flow. Between every two consecutive

recordings, at least thirty minutes time interval was given to ensure the system is at steady state.

5.3 Data Acquisition System

The two fluids (hot and cold air) were passed through the two sections. Hot air was passed through the lower duct and cold air was passed through the upper duct and heat was transferred from the lower duct to the upper duct by means of the heat pipe. A significant portion of heat is also by transferred by conduction through the separation plate.

5.3.1 Measurement of Flow Rates

The hot air flow rate was maintained by regulating a FD fan located at the inlet of the lower duct and the cold air flow rate was regulated by using bypass system.

Figure 39: Regulation of hot and cold air respectively by using (a) FD fan, (b) Bypass system

Both of the flow rates were measured using anemometer, which was kept at right angle to the direction of flow. To reduce error, velocities were measured at nine positions at the inlet and outlet of each duct and average values were taken for calculation. The positions and measurement procedure is shown in fig.40.

Figure 40: Measurement of air flow rate at different positions

5.3.2 Measurement of Temperature

Reduction of the hot air temperature occurred at the heat exchanger portion of the experimental setup. Inlet and outlet temperatures of both hot and cold air streams were measured by thermocouples. Two thermocouples were placed at each position by drilling tiny holes on the wall of the ducts. After inserting the thermocouple wire, the hole is sealed by the silicon glue to prevent any air leak.

Figure 41: Measurement of temperature by thermocouple and selector switch

To get better accuracy of temperature readings, the vertical position of the tips of the thermocouples were changed. Thus temperatures at various positions inside the duct were measured and arithmetic average was taken for calculation of heat transfer rate, thermal conductivity, heat transfer coefficient, etc.

5.4 Data Analysis

The heat transfer rate ($\dot{Q}$) or the HPHE from the hot flow air can be calculated by the following equation:

$$\dot{Q} = \dot{m}_{HA} \times C_{p,HA}(T_{HA,in} - T_{HA,out}) \quad \text{.....} \quad (34)$$

Where, $\dot{m}_{HA}$is the mass flow rate of hot air,

$C_{p,HA}$ is the specific heat capacity of the hot air,

$T_{HA,in}$ and $T_{HA,out}$ refer to the inlet and outlet temperatures of hot air respectively.

Similarly, $\dot{Q}$ can be also obtained by the cold air from the following formula,

$$\dot{Q} = \dot{m}_{\mathrm{CA}} \times C_{p,CA}(T_{CA,in} - T_{CA,out}) \quad \text{.....} \quad (35)$$

Where, $\dot{m}_{CA}$is the mass flow rate of cold air,

$C_{p,CA}$ is the specific heat capacity of the cold air,

$T_{CA,in}$ and $T_{CA,out}$ refer to the inlet and outlet temperatures of cold air respectively.

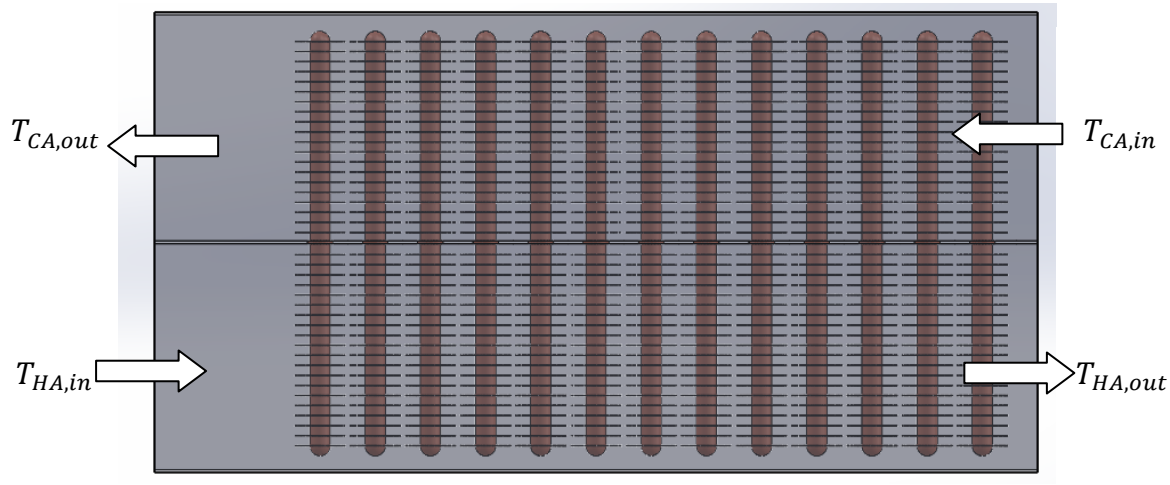

Figure 42: Flow through the heat exchanger

The cold side heat transfer rate calculated was not exactly equal to that of the hot side as there was a significant heat loss. Cold side was considered for calculating the rate of heat transfer, thermal conductivity etc.

The overall heat transfer coefficient, *U* of the HPHE is defined as follows, W/ (m^2 K):

$$U = \frac{\dot{Q}}{A \times \Delta T_{lm}} \quad \ldots\ldots (36)$$

Where, A (m^2) is the overall heat transfer area of the HPHE.

ΔT_{lm}(K) is the Logarithmic mean temperature difference, which is calculated for a counter-flow arrangement as follows:

$$\Delta T_{lm} = \frac{(T_{HA,in} - T_{CA,out}) - (T_{HA,out} - T_{CA,in})}{ln[\frac{(T_{HA,in} - T_{CA,out})}{(T_{HA,out} - T_{CA,in})}]} \quad \ldots\ldots (37)$$

The effectiveness of HPHE is defined as the ratio of the actual heat transfer rate ($\dot{Q}$) in a given heat exchanger to the maximum possible heat transfer rate ($\dot{Q}_{max}$):

$$\varepsilon = \frac{\dot{Q}}{\dot{Q}_{max}} \quad \ldots\ldots (38)$$

The following equation can be used to calculate the maximum theoretical heat transfer rate:

$$\dot{Q}_{max} = C_{min}(T_{HA,in} - T_{CA,in}) \quad \ldots\ldots (39)$$

Where, $C_{min}$is the smaller one of the heat capacities of hot air (C_{HA}) and cold fresh air (C_{CA}), kJ/K. C_{HA} and C_{CA} are calculated by following relations:

$$C_{HA} = m_{HA} C_{p,HA} \quad \ldots\ldots (40)$$

$$C_{CA} = m_{CA} C_{p,CA} \quad \ldots\ldots (41)$$

C_{max} is the larger one of the hot (C_{HA}) and cold air (C_{CA}) specific heat capacities.

R is the ratio of the minimum and maximum heat capacity of the two fluid streams:

$$R = \frac{C_{min}}{C_{max}} \quad \ldots\ldots (42)$$

The number of heat transfer units (*NTU*), an important parameter for the heat exchanger, is expressed as follows:

$$NTU = \frac{U \times A}{C_{min}} \quad \ldots\ldots\ldots\

$$w_R = \sqrt{(\frac{\partial R}{\partial x_1} w_1)^2 + (\frac{\partial R}{\partial x_2} w_2)^2 + \ \ldots\ldots\ldots + (\frac{\partial R}{\partial x_n} w_n)^2} \qquad \ldots\ldots\ldots\ldots\ldots\ldots\ldots \quad (45)$$

The best estimate of the true mean value R_t would be stated as:

$$R_t = \bar{R} \pm w_R \ (P\%) \qquad \ldots\ldots\ldots\ldots\ldots\ldots\ldots\ldots\ldots\ldots\ldots\ldots\ldots\ldots\ldots\ldots\ldots\ldots \quad (46)$$

Where the sample mean, $\bar{R}$ is found from:

$$\bar{R} = R(\bar{x}_1, \bar{x}_2, \ldots\ldots, \bar{x}_n) \qquad \ldots\ldots\ldots\ldots\ldots\ldots\ldots\ldots\ldots\ldots\ldots\ldots\ldots\ldots\ldots\ldots\ldots\ldots \quad (47)$$

The values of different areas such as flow area, heat transfer area, fin area etc. were calculated from the measured lengths and diameters. They were found to be 0.25% to 2.5% uncertain.

The equation for mass flow rates of air included the parameters flow area and air velocity. As these values contained uncertainties, the calculated mass flow rates are also subjected to uncertainty. The values of uncertainty for mass flow rate varied between 2% and 15%.

The heat loss rate of hot air or heat gain rate of cold air are simple functions of mass flow rates and temperature difference between inlet and outlet. The uncertainty in total heat transfer rate or heat duty was found to vary between 6% and 14% for moderate temperature applications. For low temperature applications, the uncertainty values varied between 11% and 28%.

The next steps of calculations included determination of logarithmic mean temperature difference (LMTD), the overall heat transfer coefficient, effectiveness, number of heat transfer units (NTU), etc. In each step of calculation, uncertainty increases. Thus the final results carry the maximum values of uncertainty.

The typical values of uncertainty for different parameters are summarized in the following table:

Table 10: Values of uncertainty for different parameters

Parameter	**Uncertainty (±)**	
	At Moderate Temperature	**At Low Temperature**
Flow area	0.33%	0.33%
Heat transfer area	2.48%	2.48%
Mass flow rate of air	2~15%	2~15%
Heat transfer rate	6~14%	11~28%
Logarithmic mean temperature difference (LMTD)	0.18~0.33%	0.51~0.63%
Overall heat transfer coefficient	6~14%	12~20%
$\dot{Q}_{max}$	0.26~0.42%	0.67~0.83%
Effectiveness (ε)	6~14%	11~20%
NTU	7~15%	12~20%

5.6 Performance of HPHE at Moderate Temperature

The performance of the HPHE was evaluated by calculating the parameters such as heat transfer rate (W), overall heat transfer co-efficient (U), effectiveness (ε) and NTU. Several graphs were plotted to evaluate the performance clearly. All this parameters were calculated with the data obtained from the experimental observation. This experiment was performed in case of moderate temperature heat recovery system. In this system, the hot air inlet temperature was kept between 60□ and 80□ and the cold air temperature was kept at nearly atmospheric temperature.

5.6.1 Heat Transfer Rate (Q̇)

Heat transfer rates were calculated from the temperature difference of hot air inlet and outlet and were plotted with the variation of hot air mass flow rates. Hot air mass flow rate was varied keeping the cold air mass flow rate at a constant value. Then the same experiment was repeated for different constant cold air mass flow rates.

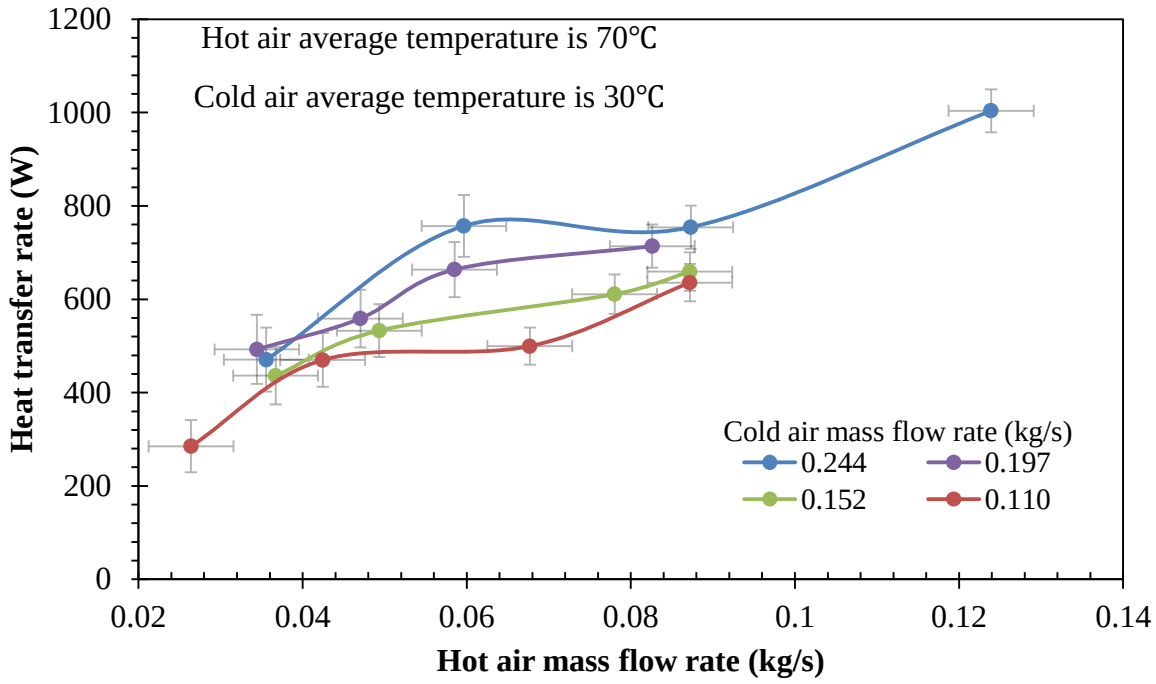

Figure 43: Variation of heat transfer rate with air mass flow rate at moderate temperature difference

From the graph, it can be observed that heat transfer rate is increased with increasing hot air mass flow rate for a constant cold air mass flow rate. At high hot and cold air mass flow rates, the heat transfer rate becomes maximum. In this experiment, for a constant cold air mass flow

rate of 0.244 kg/s, heat transfer rate is minimum 470.42 W at hot air mass flow rate of 0.04 kg/s and maximum 1003.4 W at hot air mass flow rate of 0.124kg/s. It was also found nearly similar result for different experiments at different constant cold air mass flow rates with varying hot air mass flow rate; heat transfer rate varied from 476 W to 703 W for cold air mass flow rate 0.197 kg/s and varied from 430 W to 637 W for 0.152 kg/s. The increase of heat transfer rate with increase of mass flow rate is clear from these experimental results. As the hot air flow rate grows up, the heating power is increased, and the liquid film changes into nuclear boiling with a large number of bubbles, which enhances heat transfer rate which increases the heat exchange coefficient as presented in fig.43. This indicates that the heat transfer efficiency can be improved by increasing the flow rate of hot air in practice.

5.6.2 Overall Heat Transfer Coefficient (U)

One of the most important performance parameters of a heat exchanger is its overall heat transfer co-efficient. It was measured for each experiment of HPHE using the heat transfer rate (W) from the temperature difference of cold air inlet and outlet. Theoretically heat transfer rate at hot side and cold side would be same but due to conductive heat losses through set-up and convection heat losses to air, some significant differences observed in the experiment. The reason for using cold side heat transfer rate was for remaining at safe side because it was lower than hot side heat transfer rate. Using smaller value of heat transfer rate for calculating U gave more practical and valid result. Graphs were plotted by same procedure as described earlier in case of plotting curves of heat transfer rate.

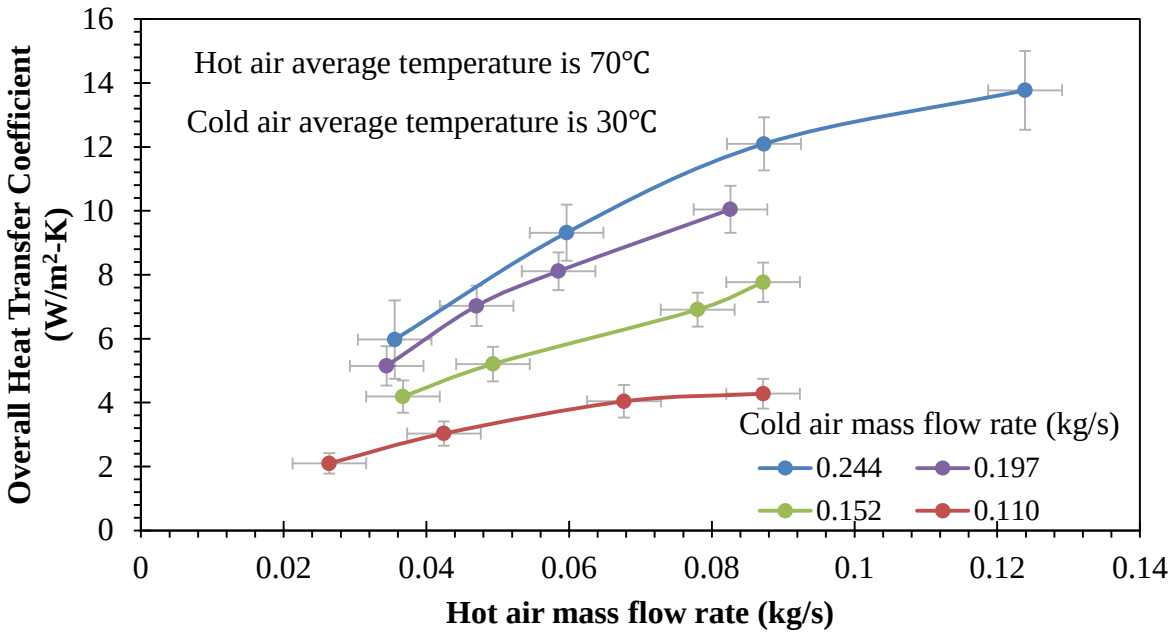

Figure 44: Variation of overall heat transfer co-efficient with change of air mass flow rate at moderate temperature difference

From the graph, it has been found that the relationship between overall heat transfer coefficient (U) and mass flow rates were also similar as described previously in section 5.6.1. It was summarized from an experiment that for a constant cold air mass flow rate of 0.244 kg/s, overall heat transfer co-efficient was increased from a minimum value of 6 W/m^2-K to a maximum value of 13.9 W/m^2-K when hot air mass flow rate was increased from 0.04 kg/s to 0.124 kg/s. If it compared for cold air mass flow rate, it was summarized from experimental data that heat transfer co-efficient also increase with increasing the cold air mass flow rate that varied from 4.2 to 7.8 W/m^2-K at cold air mass flow rate 0.152 kg/s and varied from 5 W/m^2-K to 10 W/m^2-K for cold air mass flow rate of 0.197 kg/s.

5.6.3 Effectiveness (ε)

It is also an important performance parameter for a heat exchanger. It was calculated from experimental data and plotted against mass flow rate following the procedure as described in the earlier sections.

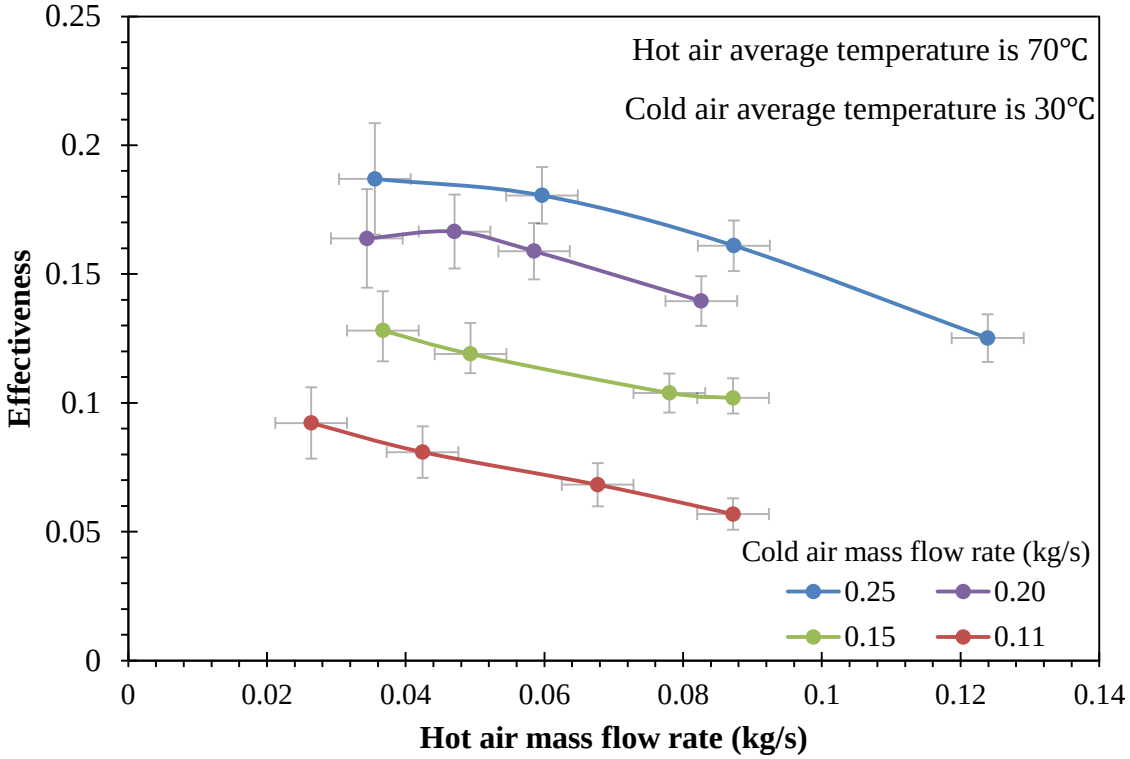

Figure 45: Variation of effectiveness of HPHE with air mass flow rate at moderate temperature difference

From this graph, it is clear that the relationship between effectiveness and mass flow rate is different from previous sections. Effectiveness decreases with increasing of hot air mass flow rates at a constant cold air mass flow rate. It was summarized from analyzing data of an experiment that for cold air mass flow rate 0.244 kg/s, effectiveness was decreased from 0.19 to 0.13 when hot air mass flow rate increased from 0.04 to 0.124 kg/s. HPHE was found more effective for lower mass flow rate.

5.6.4 NTU

Number of Transfer Units (NTU) is a function of the effectiveness and also an important performance parameter. NTU was calculated and a graph was plotted indicating the variation of effectiveness with NTU.

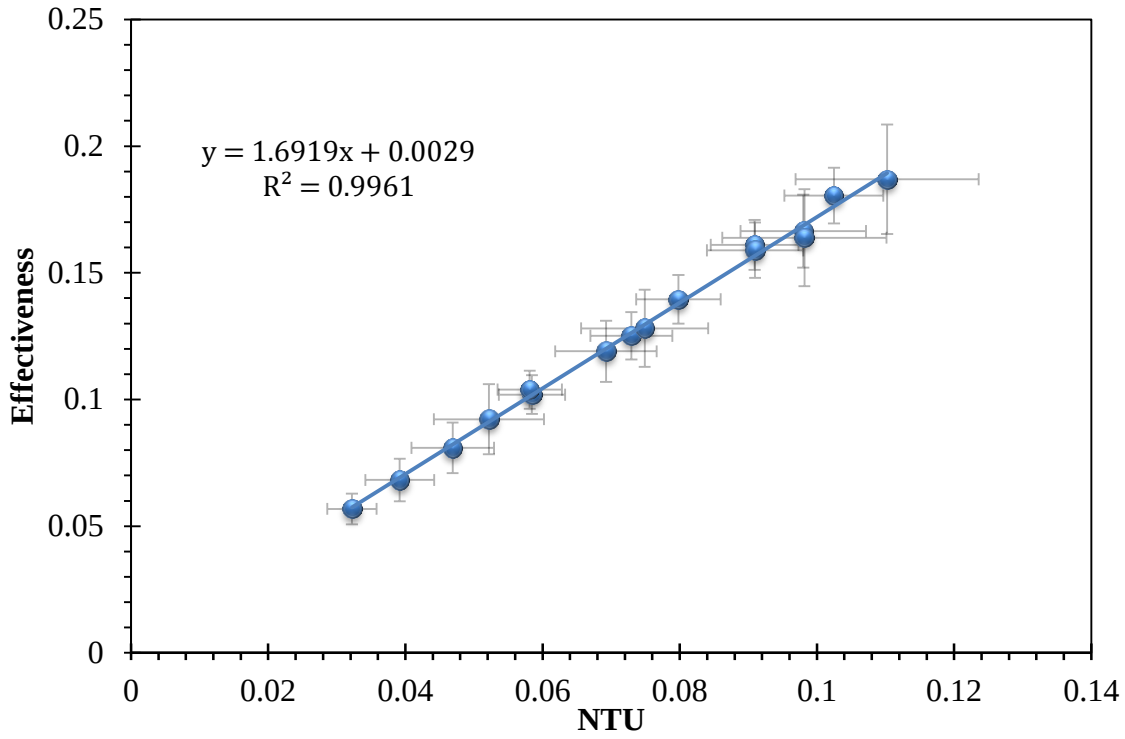

Figure 46: Variation of effectiveness of HPHE with NTU at moderate temperature difference

From the graph, a linear relationship was found between effectiveness and NTU. It was because NTU is directly proportional with heat transfer coefficient and as heat transfer co-efficient increased with increasing air mass flow rates, NTU was also increased and when NTU is increased effectiveness of HPHE also increased as the nature of their relationship described in theory [66]. The effectiveness varying from 0.052 to 0.182, and the relationship could be expressed from the best fit straight line as $\varepsilon = 1.691\ \mathrm{NTU} + 0.002$

5.7 Performance of HPHE at Low Temperature

The performance of the HPHE at low temperature heat recovery application (such as HVAC) was evaluated by calculating the same parameters described in section 5.3 such as heat transfer rate (W), overall heat transfer co-efficient (U), effectiveness (ε) and NTU. Several graphs were plotted to evaluate the performance clearly. All these parameters were calculated with data obtained from the experimental observation. These experiments were tried to perform at same condition as in a HVAC system. In this system, the hot air inlet temperature was tried to keep around 40□ and the cold air temperature was tried to keep at 20□.

5.7.1 Heat Transfer Rate ($\dot{Q}$)

Heat transfer rates were calculated from the temperature difference of cold air inlet and outlet temperature and were plotted with the variations of cold air mass flow rates. Cold air mass flow rate was varied keeping the hot air mass flow rate at constant. The experiment was repeated for different hot air mass flow rates.

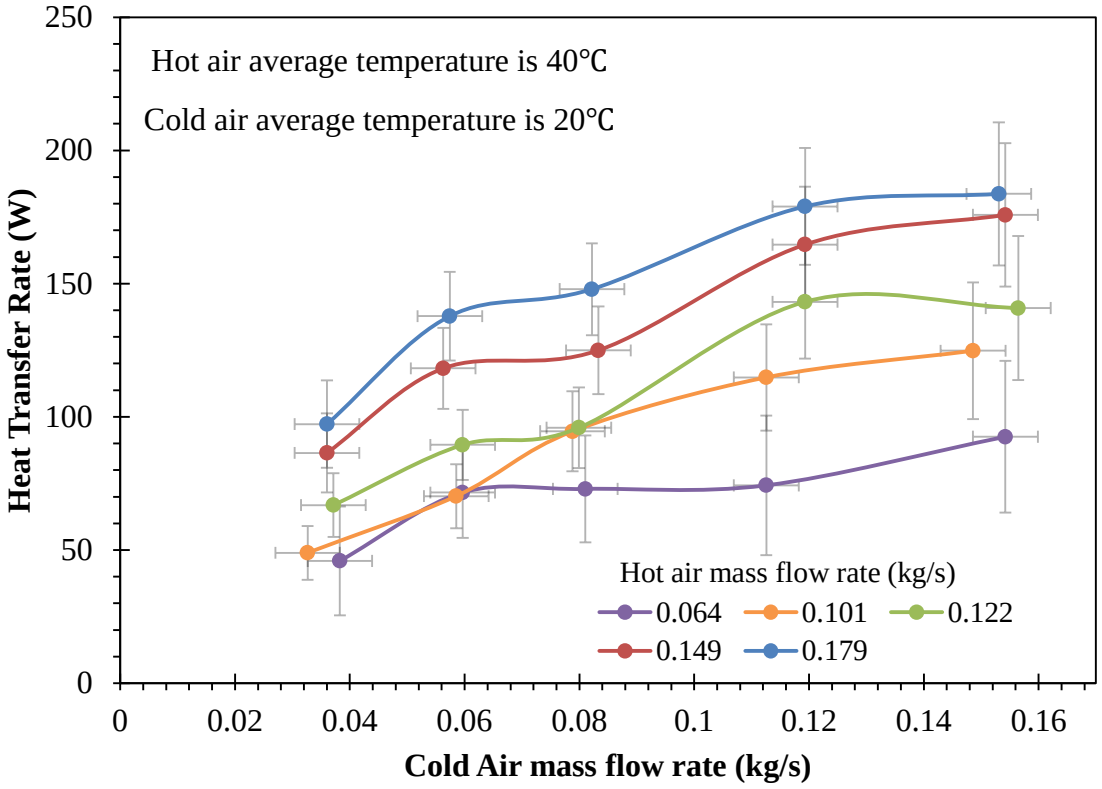

Figure 47: Variation of heat transfer rate with air mass flow rate at low temperature difference

From the graph, it could be observed that, heat transfer rate increases with increasing of cold air mass flow rate for a constant hot air mass flow rate. For a constant hot air mass flow rate of 0.1 kg/s, heat transfer rate was minimum 97.23 W at cold air mass flow rate of 0.04 kg/s

and maximum 183.65 W at cold air mass flow rate of 0.16 kg/s. It was also found nearly similar result from comparison of different experiments at different constant hot air mass flow rate. Such as heat transfer rate varies from 66.84 W to 140 W for hot air mass flow rate of 0.122 kg/s and varies from 86.42 W to 185 W for hot air mass flow rate 0.149 kg/s. Increase of heat transfer rate with increase of mass flow rate was clear from these experimental results.

5.7.2 Overall Heat Transfer Coefficient (U)

Overall heat transfer coefficient was measured for the experiment of HPHE using heat transfer rate (W) from the temperature difference of cold air inlet and outlet. Theoretically heat transfer rate at hot side and cold side would be same but due to conductive heat losses through set-up and convection heat losses to air, there were differences between those two heat transfer rates and the difference was up to 15%. Heat transfer rate calculated from the cold side was used for all the calculations as the calculated U is confirmed by both the hot side and cold side. Graphs were plotted by same procedure as described earlier.

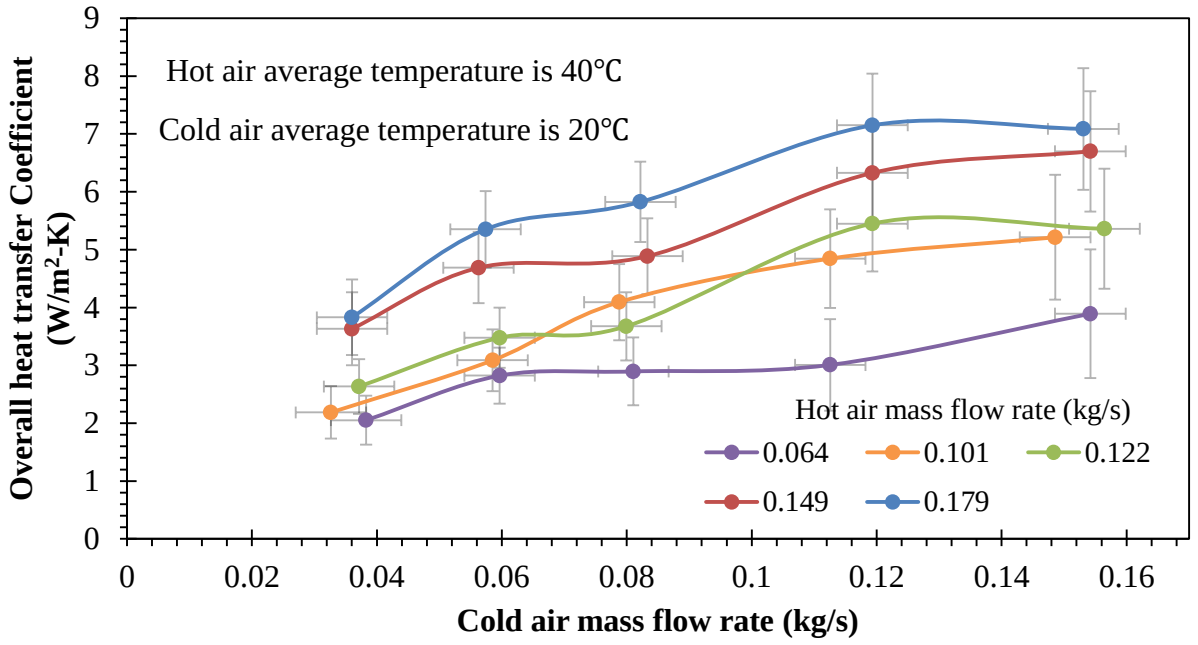

Figure 48: Variation of overall heat transfer co-efficient with change of air mass flow rate at low temperature difference

From the graph, it was found that the relationship between overall heat transfer coefficient (U) and mass flow rates were similar as described in the previous section. It was summarized from an experiment that for hot air mass flow rate 0.1 kg/s, overall heat transfer co-efficient was increased from minimum 3.8 w /m^2.k to maximum 7.14w/m^2.k when cold air mass flow

rate was increased from 0.04 kg/s to 0.179 kg/s. It can be summarized from different experimental data that U was varied from 2.65 to 5.49 w/m^2.k at cold air mass flow rate 0.12 kg/s and varied from 3.65 to 6.79 w/m^2.k at cold air mass flow rate 0.149 kg/s.

5.7.3 Effectiveness (ε)

Effectiveness of the heat exchanger was calculated from experimental data and plotted against mass flow rate following the same procedure as described in the earlier sections.

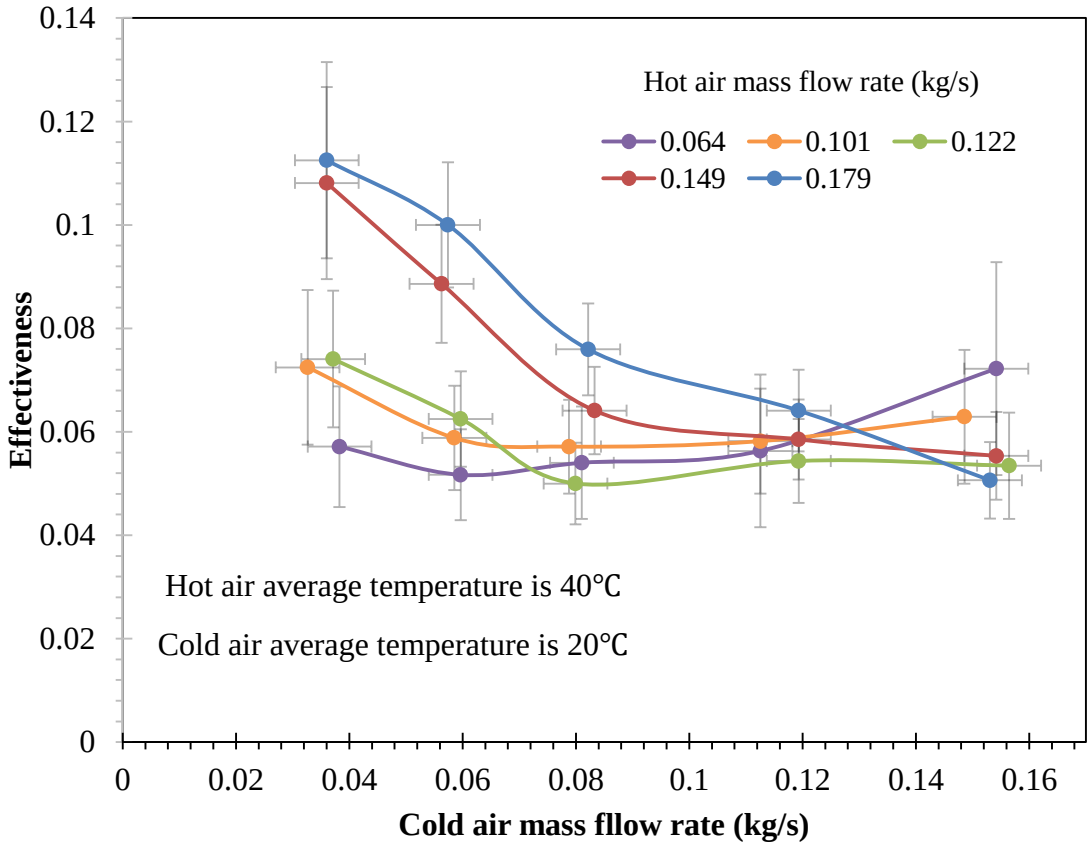

Figure 49: Variation of effectiveness of HPHE with air mass flow rate at low temperature difference

From this graph it can been seen that the relationship between effectiveness and mass flow rate was different than heat transfer rate and heat transfer co-efficient. Here effectiveness decreases with increasing hot air mass flow rates for a constant cold air mass flow rate. It was summarized from analyzing data of an experiment that for hot air mass flow rate 0.14 kg/s, effectiveness was decreased from 0.11 to 0.06 when cold air mass flow rate increased from 0.04 to 0.15 kg/s and same observation was observed for other experimental data. It could be concluded that this HPHE is more effective at lower mass flow rate.

5.7.4 NTU

Number of Transfer Units (NTU) is a function of the effectiveness and also an important performance parameter. Here, NTU was calculated and a graph was plotted indicating the variation of effectiveness with NTU.

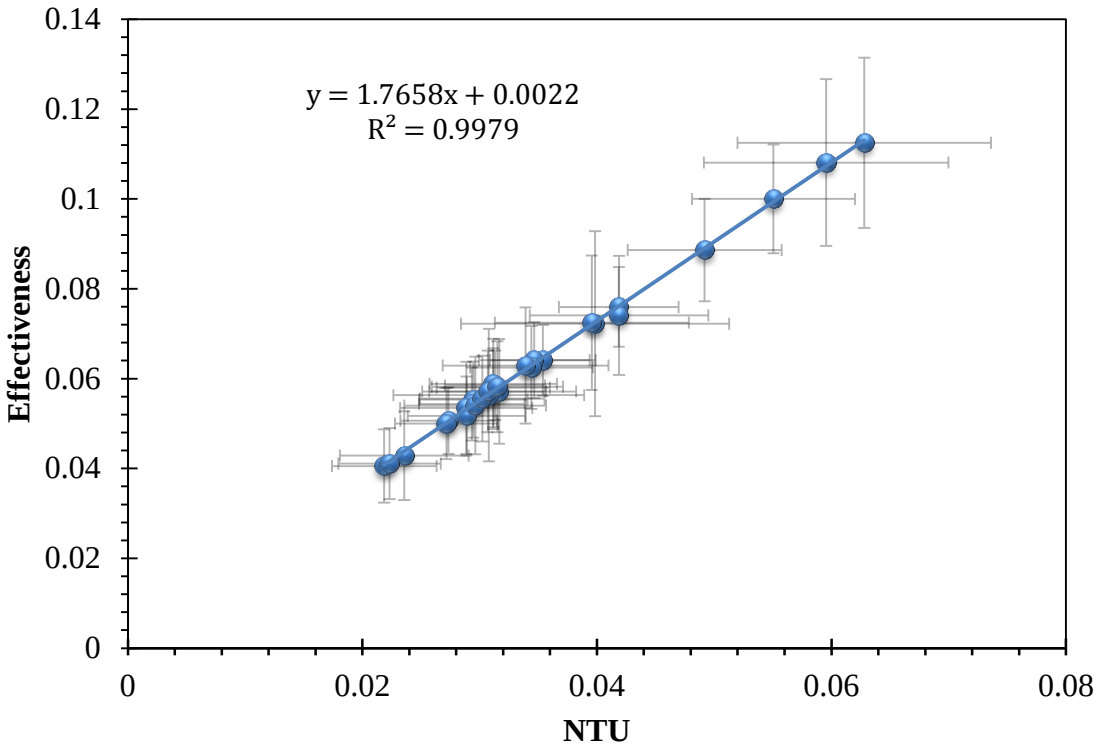

Figure 50: Variation of effectiveness of HPHE with NTU at low temperature difference

From the graph, a linear relationship was found between effectiveness and NTU. It was because NTU is directly proportional with heat transfer coefficient and as heat transfer co-efficient increases with increasing air flow rates, NTU is also increased and when NTU increases, effectiveness of HPHE is also increased as the nature of their relationship described in theory. Here the effectiveness varying from 0.04 to 0.117, and the relationship could be expressed as $\varepsilon = 1.765\ \text{NTU} + 0.002$ from the best fit straight line.

Financial Analysis

Financial analysis of the designed HPHE was performed as presented in the table below.

5.8.1 Financial Analysis for Moderate Temperature Application

Considering the application of the HPHE in a moderate temperature waste heat recovery, a financial analysis has been performed. Following experimental data and cost estimation was used to calculate the financial analysis as presented in the table below:

Table 11 : Data used for the financial analysis for moderate temperature application

Cold Air Inlet Temperature, ($T_{c,in}$)	27.2℃
Cold Air Outlet Temperature, ($T_{c,out}$)	31.2 ℃
Hot Air Inlet Temperature, ($T_{h,in}$)	63.5℃
Hot Air Outlet Temperature ($T_{h,out}$)	55.3℃
Cold Air Mass Flow Rate, (m_c)	0.25 kg/s
Hot Air Mass Flow Rate, ($m_{\square}$)	0.123 kg/s
Cold Air Specific Heat, ($C_{p,c}$)	1006 J/kg.K
Hot Air Specific Heat, ($C_{p,\square}$)	1008 J/kg.K
Natural Gas Price	7.45 taka/SCM
Heating Value of 1SCM	12940 K Cal/kg
Density of Natural Gas	0.718 kg/m^3

Table 12 : Financial analysis for moderate temperature application

Energy Available in the Hot Air Stream, $Q_A = m_{\square} C_{p,\square}(T_{h,in} - T_{c,in})$	Energy Recovered by the Cold Air Stream, $Q_{rec} = m_c C_{p,c}(\Delta T)_c$	% of Energy Recovered ($\frac{Q_{hot}}{Q_A}$)*100	Electrical Energy Saving Per year, (MJ)	Natural Gas Savings (SCM)	Monetary Saving	Investment (Taka)	Payback Period, year
4530 W	1006 W	22.20 %	26437.8	488	3642	12000	3.3

5.8.2 Financial Analysis for Low Temperature Application

Considering the application of the HPHE in a HVAC waste heat recovery, a financial analysis has been performed. Following experimental data and cost estimation was used to calculate the financial analysis as presented in the table below:

Table 13 : Data used for the financial analysis for moderate temperature application

Cold Air Inlet Temperature, $(T_{c,in})$	23.0℃
Cold Air Outlet Temperature, $(T_{c,out})$	24.3℃
Hot Air Inlet Temperature, $(T_{h,in})$	36.1℃
Hot Air Outlet Temperature, $(T_{h,out})$	34.3℃
Cold Air Mass Flow Rate, (m_c)	0.15 kg/s
Hot Air Mass Flow Rate, $(m_{\square})$	0.17 kg/s
Cold Specific Heat, $(C_{p,c})$	1006 J/kg.K
Hot Specific Heat, $(C_{p,\square})$	1007 J/kg.K
Cost of Electricity	9.45 taka/unit
EER of refrigeration system	12

Table 14 : Financial analysis for moderate temperature application

Energy Available in the Hot Air Stream, $Q_A = m_{\square} C_{p,\square}(T_{h,in} - T_{c,in})$	Energy Recovered $Q_{cold} = m_c C_{p,c}(\Delta T)_c$	% of Energy Recovered $(\frac{Q_{hot}}{Q_A})$*100	Electrical Energy Saving Per year, $\frac{Q_{cold} * 365}{EER}$	KW-h/year	Monetary Saving	Investment (Taka)	Payback Period, year
2242 W	197 W	9 %	154082	154	1456	12000	8.2

Chapter 6

Conclusions

In this thesis, experimental study was conducted to evaluate the performance of heat pipe heat exchanger (HPHE) for low grade waste heat recovery application. The study starts from constructing and evaluating performance of the heat pipe with an objective to optimize its parameters to be used in the HPHE at lower and moderate temperature applications. A heat pipe heat exchanger (HPHE) was designed and constructed for this study with the optimized parameters of the heat pipe. From the results of the experimental investigation following conclusions can be drawn:

Study for the optimization of heat pipe:

1. Low cost heat pipe and HPHE can be constructed without any sophisticated equipment in any ordinary workshop.
2. Heat pipe constructed of copper with water as the working fluid performs better than ethanol as the working fluid at the temperature range of 30 to 60 ^{o}C
3. Volume of the working fluid inside the heat pipe also influences its performance. In this study, heat pipe with five different filling ratio of 25%, 35%, 50%, 60% and 70% of the evaporation volumewere fabricated and tested for the operating temperature range of 20℃ □ 80℃. Heat pipe with 50% filling ratio indicated maximum heat transfer performance compared to heat pipe with other filling ratios.

Study of the effect of adiabatic length:

4. Most of the heat pipe is constructed with adiabatic section; however, effect of this adiabatic section is not obvious from the literature. In this study four water-water heat pipe heat exchangers were constructed with the adiabatic section length of 32 mm, 64, mm, 96 mm and no adiabatic section. Heat transfer rate was observed to increase with the shorter adiabatic section length and best performance was observed for the HPHE without adiabatic section. For the test condition of hot water temperature of 70^{o}C and cold water temperature of 25^{o}C, heat transfer rate was measured 554 W, 443 W, 388 W and 680 W respectively for the HPHE with 32 mm, 64 mm, 64 mm adiabatic section length and no adiabatic section..
5. Position of the adiabatic section also influences the performance of the Heat pipe heat exchanger. Four heat pipe heat exchangers were constructed with 32 mm adiabatic section placing at the middle, 32 mm downward from the center and 32 mm and 64 mm upward. Moving the adiabatic section upwards from the middle of the heat pipe increases

heat transfer performance; whereas, moving the adiabatic section downward from the middle of the heat pipe decreases heat transfer performance.

6. For the water-water HPHE, maximum effectiveness of 68% was observed for the heat pipe without adiabatic section followed by 55.4%, 44.3%, 38.8% for the HPHE with adiabatic section length of 32 mm, 64 mm and 96 mm. Effectiveness of 57%, 53% and 47% was found for changing the position of adiabatic section from middle of the heat pipe to 32 mm downward and 32 mm and 64 mm upward.

Study of Air-Air HPHE:

7. The heat transfer rate increases with increasing mass flow rate of air for both moderate and low temperature waste heat recovery application. The effectiveness of HPHE was found to decrease with increasing mass flow rate and velocity of air.
8. The relation between effectiveness and NTU is linear. For moderate temperature applications, effectiveness varies from 0.08 to 0.202 and the relationship is expressed as $\varepsilon = 1.691\ \mathrm{NTU} + 0.002$. For low temperature applications, the effectiveness is varied from 0.022 to 0.14, the relationship expressed as $\varepsilon = 1.765\ \mathrm{NTU} + 0.002$.
9. The heat exchanger's performance is very sensitive to the dust accumulation.
10. HPHE is economical to install in the waste heat recovery application. With the current energy price and in continuous operation, HPHE will have a payback period of 3.3 years for the moderate temperature waste heat recovery application and 8.2 years for waste heat recovery application from air conditioned space.

References

[1] BCS, Incorporated, “Waste Heat Recovery: Technology and Opportunities in US Industry”, U.S. Department of Energy, Industrial Technologies Program, 2008.

[2] Woolnough, David, “Waste Heat Recovery”, Heat & Mass Transfer, Thermopedia, 2011.

[3] Tetra Tech ES, Inc, “Industrial Energy Efficiency Opportunities and Challenges in Bangladesh”, Technical Assistance Consultant’s Report powered by Asian Development Bank (ADB), Project Number: 45916, 2014.

[4] Dr Hussam (Sam) Jouhara, “Heat Pipe Heat Exchangers for Industrial Heat Recovery”, Heat pipe based systems for waste heat recovery and renewable energy, Brunel University London, 2016.

[5] Perkins, Angier March (A.M.), “Hermetic Heating Tubes”, A.K.A. Perkins System, UK Patent 6146, 1831.

[6] Perkins, Jacob, “Perkins Tube”, UK Patent 7059, April 1936.

[7] Gaugler, Richard, "Heat Transfer Devices". Dayton, Ohio: U.S. Patent Office: 4. 2350348, 1944.

[8] Grover, G. M., Cotter, T. P. and Erikson, G. F., “Structures of Very High Thermal Conductivity”, J. Appl. Phys., 35, 1990.

[9] Mcntosh, R., Ollendorf, S. and Harwell, “The International Heat Pipe Experiment”, Proceedings of International Heat Pipe Conference, Bolgana, 589-592, April 1976.

[10] A.S.A. Mohamed, “A Review: on the Heat Pipe and Its Applications” 4th International Conference on Energy Engineering, 2017.

[11] Srimuang, P. Amatachaya, “A Review of the Applications of Heat Pipe Heat Exchangers for Heat Recovery”, Renewable and Sustainable Energy Reviews P-16, 4303–4315, 2012.

[12] MD Anwarul Hasan *et al.,* “Performance of a Gravity Assisted Heat Pipe”, International Conference on Mechanical Engineering (ICME2003), 26- 28 December 2003.

[13] Md Shahidul Haque, “Thermal Characteristics of an Alumunum Closed-Loop Pulsating Heat Pipe Charged with Ammonia”, M.Sc. Engg. Thesis, Department of Mechanical Engineering, Bangladesh University of Engineering Technology, 2011-2012.

[14] Dough Lynch, “Samsung may Introduce Vapor Chambers for Better Heat Dissipation in 2019”, Samsung Corporation Lmt., November 2017.

[15] Matt Connors, “Cooling High-Power Electronic Components in Small Packages”, Application Engineering Manager, Thermacore, Inc., Lancaster, PA, 2010.

[16] Tarau, C., W. Anderson, and C. Peters, “Thermal Management System for Long-Lived Venus Landers*”,* Advanced Cooling Technologies, Inc., Lancaster, Pennsylvania, 17601, U.S.A, 2011.

[17] John R. Hartenstine *et al.,* "Pressure Controlled Heat Pipe Solar Receiver for Regolith Oxygen Production with Multiple Reactors", Advanced Cooling Technologies, Inc. January, 2010.

[18] Calin Tarauet *et al*., "Diode Heat Pipes for Venus Landers", 9th Intersociety Energy and Conversion Engineering Conference, August 2012.

[19] Qimin J. Dong, Chung-Lung Chen, "Motor Rotor Cooling with Rotation Heat Pipes", Reliance Electric Technologies LLC, USA, 2004.

[20] Triem T. Hoang, "Loop Heat Pipe Method and Apparatus", TTH Research Inc.,USA, 2001.

[21] Silva, Marcelino, and Riehl R.,"Thermal Performance Comparison between Water-Copper and Water-Stainless Steel Heat Pipes," 13th International Energy Conversion Engineering Conference, TFESC 2015.

[22] P. Sivakumar *et al.,* "Performance Analysis of Flat Plate Solar Water Heater by Changing the Heat Pipe Material", Advanced Materials Research, ISSN: 1662-8985, Vol. 768, pp 64-69, 2013.

[23] Jouhara H. *et al.,* "Heat Pipe Based Systems - Advances and Applications", Energy, 128: p. 729-754, 2017.

[24] Peyghambarzadeh *et al.,* "Thermal Performance of Different Working Fluids in a Dual Diameter Circular Heat Pipe", Journal of Thermal Engineering, 4(4): p. 855-861, 2013.

[25] Harikrishnan, Vinod Kotebavi, "Performance Study of Solar Heat Pipe with Different Working Fluids and Fill Ratios", IOP Conf. Ser.: Material Science and Engineering, 149-012224, 2016.

[26] A. K. Mozumder *et al.*, "Performance of Heat Pipe for Different Working Fluids and Fill Ratios", Journal of Mechanical Engineering, 41(2), April 2011.

[27] M. Kannan and E. Natarajan, "Thermal Performance of a Two-Phase Closed Thermosyphon for Waste Heat Recovery System", Journal of Applied Sciences, 10: 413-418, 2010.

[28] Zhang, M. Z. Liu, and G. Ma, "The Experimental Investigation on Thermal Performance of a Flat Two-Phase Thermosyphon", International Journal of Thermal Sciences, 47(9): p. 1195-1203, 2008.

[29] Md. Moeenul Haque, "Heat Transfer Characteristics of Miniature Heat Pipes", M.Sc. Engg. Thesis, Department of Mechanical Engineering, Bangladesh University of Engineering Technology, 2005.

[30] Yu-Hsing Lin, Shung-Wen Kang, and Hui-Lun Chen, "Effect of Silver Nano-Fluid on Pulsating Heat Pipe Thermal Performance", Applied Thermal Engineering, 28: 1312 131, 2008.

[31] Paisarn Naphon, Dithapong Thongkum, and Pichai Assadamongkol, “Heat Pipe Efficiency Enhancement with Refrigerant Nanoparticles Mixtures”, Energy Conversion and Management, p.50: 772- 776, 2009.

[32] M. Arab, M. Soltanieh, and M.B. Shafii, “Experimental Investigation of Extra-Long Pulsating Heat Pipe Application in Solar Water Heaters”, Experimental Thermal and Fluid Science, p.42: 6-15, 2012.

[33] E. Ibrahim, M. Moawed, and N. S. Berbish, “Heat Transfer Characteristics of Rotating Triangular Thermosyphon”, Heat and Mass Transfer, 48: 1539-1548, 2012.

[34] S.H. Noie, “Heat Transfer Characteristics of a Two-Phase Closed Thermosyphon”, Applied Thermal Engineering, p.25: 495- 506, 2005.

[35] A. Kumar Mozumder *et al.*, “Experimental Investigation of a Heat Pipe for Different Working Fluids and Fill Ratios”, International Conference on Mechanical Engineering (ICME2009), 26- 28 December 2009.

[36] T. N. Sreenivasa *et al.,* “Working Fluid Inventory in Miniature Heat Pipe”, International Conference on Mechanical Engineering (ICME2005), 28- 30 December 2005.

[37] Mashaei and M. Shahryari, “Effect of Nanofluid on Thermal Performance of Heat Pipe With Two Evaporators; Application to Satellite Equipment Cooling”, Acta Astronautic, 111: p. 345-355, 2015.

[38] Salehi, Saeed Zeinali Heris, “Experimental Study of a Two-Phase Closed Thermosyphon with Nanofluid and Magnetic Field Effect”, Journal of Enhanced Heat Transfer, Volume 18-issue 3, 2011.

[39] Zeinali Heris *et al.,* “Experimental Study of Two Phase Closed Thermosyphon Using Cuo/Water Nanofluid in the Presence Of Electric Field”, Journal of Enhanced Heat Transfer, 18(3):261-269, · July 2011.

[40] S.H. Noie *et al.,* “Heat Transfer Enhancement Using Al2O3/Water Nanofluid in a Two-Phase Closed Thermosyphon”, International Journal of Heat and Fluid Flow, **30**(4): p. 700-705, 2009.

[41] Midwest Research Institute, Heat Pipes, NASA Report NASA CR-2508, pg. 19, Jan 1, 1975.

[42] Kew, David Anthony Reay,“Heat pipes (5th ed.)” Oxford: Butterworth-Heinemann, P. 309 ISBN 978-0-7506-6754-8, 2006.

[43] Wyoming S.E, “Vintage Meat Pin Thermal Magic Cooking Pin NOS Cook Meat in 1/2 the Time”. Energy Conversion System Inc, 1982.

[44] Tanvir Reza Tanim *et al.,* “Cooling of Desktop Computer Using Heat Pipes”, International Conference on Mechanical Engineering, (ICME2007), 29- 31 December 2007.

[45] Kwang-Soo Kim *et al.,* “Heat Pipe Cooling Technology for Desktop PC CPU”, Applied Thermal Engineering”, 23(9):1137-1144, June 2003.

[46] Sarvenaz Sobhansarbandi, “Evacuated Tube Solar Collector Integrated with Multifunctional Absorption-Storage Materials”, Ph.D. Thesis, University of Texas at Dallas, 2017.

[47] S.H. Noie-Baghban, G.R. Majideian, “Waste Heat Recovery Using Heat Pipe Heat Exchanger (HPHE) for Surgery Rooms in Hospitals”, Applied Thermal Engineering, Vol. 20 pp; 1271-82, 2000.

[48] Huang Wei and You Hongjun, “Recovery Energy from the Separated and Gravity Type of Heat Pipe Exchanger in China”, Journal of Petroleum and Gas Engineering, Vol. 2 (1), pp. 1-6, January 2011.

[49] Mathur and Gursaran, “Using Heat-Pipe Heat Exchangers for Reducing High Energy Costs of Treating Ventilation Air”, Journal of Energy, 2. 1447 - 1452 vol.2. 10.1109/IECEC.1996.553938, 1996.

[50] Gan and Riffat, “Determination of Effectiveness of Heat-Pipe Heat Recovery for Naturally-Ventilated Buildings”, Applied Thermal Engineering, 18. 121-130. 10.1016/S1359-4311(97) 00033-1, 1998.

[51] M.Ahmad zadehtalatapeh, “An Air-Conditioning System Performance Enhancement by Usingheat Pipe Based Heat Recovery Technology”, Department of Marine Engineering, Chabahar Maritime University, 99717-56499, Chabahar, Iran, 21 January 2013.

[52] Nikhil S. Chougule *et al.,* “A Review on Heat Pipe for Air Conditioning Applications”,Msc Engg. Thesis, Department of Mechanical Engineering, Maeer’s Mitcoe, Pune 411038, Maharashtra, India, 15 March 2016.

[53] Hongting Ma *et al*., “Assessment of the Optimum Operation Conditions on a Heat Pipe Heat Exchanger for Waste Heat Recovery in Steel Industry”, Renewable and Sustainable Energy Reviews, 79: 50–60, 2017.

[54] Jouhara *et al*.,“Experimental and Theoretical Investigation of a Flat Heat Pipe Heat Exchanger for Waste Heat Recovery in the Steel Industry”, Journal of Energy Engineering, 141: 1928-1939, 2017.

[55] Tian and W.-Q. Tao, “Waste Heat Recovery by Gravity Heat Pipe Exchanger”, Journal of Applied Energy, 188: p. 586-594, 2017.

[56] Hong Gao *et al*., “Performance Analysis and Working Fluid Selection of a Supercritical Organic Rankine Cycle for Low Grade Waste Heat Recovery”, Journal of Energies, 5, 3233-3247; doi:10.3390/en5093233, 2012.

[57] Shodhganga, “Design and Manufacturing of Wickless Heat Pipe”, Journal of Thermal Engineering, 2014.

[58] Dunn, P. D., and Reay, D. A., “Heat Pipes”, 3rd ed., Pergamon Press, Oxford, U.K., 1994.

[59] Z. R. Gorbis, and G.A. Savchenkov, “Low Temperature Tow-phase Closed Thermosyphon Investigation”, Proc. 2nd International Heat pipe Conf. Bologna, Italy, pp.37-45, 1967.

[60] A. Faghri, “Heat Pipe Science and Technology”, Taylor & Francis, Washington, D.C., 1995.

[61] M. Shiraishi, M. Yoneya, and A. Yabe, “Visual Study of Operating Limit in the Tow-Phase Closed Thermosyphone”, Proc. 5th International Heat Pipe Conf., 14-17 May, Tsukuba, Japan, pp. 11-17, 1984.

[62] M. Shiraishi, K. Kikuchi, T. Yamanishi, “Investigation of Heat Transfer Characteristics of a Two-Phase Closed Thermosyphon”, Journal of Heat Recover System 1, 287at R, 1981.

[63] H. Jouhara, A.J. Robinson, “Experimental Investigation of Small Diameter Two Phase Closed Thermosyphons Charged with Water, FC-84, FC-77 and FC-3283, Appl. Therm. Eng. 30,201Opera, 2010.

[64] A. Faghri, “Heat Pipe Science and Technology”, Taylor & Francis Group, Washington, DC, 1995.

[65] Carvajal-Mariscal *et al.,* “Development of High Efficiency Two-Phase Thermosyphons for Heat Recovery”, Heat Exchangers – Basics Design Applications, National Polytechnic Institute of Mexico, 2012.

[66] Faghri, A. and Thomas S., “Performance Characteristics of a Concentric Annular Heat Pipe: Part I—Experimental Prediction and Analysis of the Capillary Limit”, Journal of Heat Transfer, 11, 844–850, 1989.

[67] Buchko M., “Experimental and Numerical Analysis of Low Temperature Heat Pipes with Multiple Heat Sources,” ASME J. Heat Transfer, 113(3), pp. 728–734, 1991.

[68] Thanaphol Sukchana and Chaiyun Jaiboonma, “Effect of Filling Ratios and Adiabatic Length on Thermal Efficiency of Long Heat Pipe Filled with R-134a”. Energy Procedia, 34: 298 – 306, 2013.

[69] François Ternet *et al.*,“Impact of Microgroove Shape on Flat Miniature Heat Pipe Efficiency”, Entropy 20, 44, 2018.

[70] Rakesh Hari and Chandrasekharan Muraleedharan,“Analysis of Effect of Heat Pipe Parameters in Minimizing the Entropy Generation Rate”, Journal of Thermodynamics, P.8 , Article ID 1562145, 2016.

[71] Shuangfeng Wang *et al.*,“Effect of Evaporation and Condensation Length on Thermal Performance of Flat Plate Heat Pipes”, Applied Thermal Engineering, 31, 2011.

[72] P.G.Anjankar and Dr.R.B.Yarasu, “Experimental Analysis of Condenser Length Effect on the Performance of Thermosyphon”, International Journal of Emerging Technology and Advanced Engineering, ISSN 2250-2459, Volume 2, Issue 3, March 2012.

[73] Yunus A. Cengel and Afshin J. Ghajar, “Heat and Mass Transfer: Fundamentals & Applications”, 5th Edition, 2015.

Appendix

Appendix-A: Experimental data

Table 15: Description of water to water HPHE

Heat pipe	
Length	280 mm
Outer diameter	13 mm
Inner diameter	11.5 mm
Thickness	0.75 mm
Working fluid	Distilled Water
No. of fins per pipe	2
Fin dimensions	25 mm × 25 mm

Separator plate	
Plate radius	76.2 mm
Thickness	5 mm
Total no. of heat pipes	24

No. of pipe per HPHE	6
Total number of fins	12
Arrangement	Triangular

Table 16: Measured data for thermal performance of HPHE without adiabatic section

Obs. No.	**Cold water mass flow rate (L/s)**	**Inlet** (℃)	**Outlet** (℃)	ΔT_{cold} (℃)	**Cold water heat transfer rate (kW)**	**Hot water heat transfer rate (W)**	**Effectiveness**
1	0.005	27.0	39	12.0	0.252	1000	0.68
2	0.010	27.0	35	8.0	0.336		
3	0.023	27.0	33	6.0	0.580		
4	0.030	27.0	32	5.0	0.630		
5	0.033	26.5	31	4.5	0.624		
6	0.042	26.5	30	3.5	0.620		
7	0.054	26.0	29	3.0	0.680		

Table 17: Measured data for thermal performance of HPHE with adiabatic section 1/9th of heat pipe

Obs. No.	Cold water mass flow rate (L/s)	Inlet (℃)	Outlet (℃)	ΔT_{cold} (℃)	Cold water heat transfer rate (kW)	Hot water heat transfer rate (W)	Effectiveness
1	0.005	27.0	34.0	7.0	0.147	1000	0.55
2	0.010	27.0	33.5	6.5	0.273		
3	0.023	27.0	32.0	5.0	0.483		
4	0.030	26.7	31.0	4.3	0.542		
5	0.033	26.5	30.5	4.0	0.554		
6	0.042	26.0	29.0	3.0	0.529		
7	0.054	26.0	28.2	2.2	0.500		

Table 18: Measured data for thermal performance of HPHE with adiabatic section 1/4 th of heat pipe

Obs. No.	Cold water mass flow rate (L/s)	Inlet (℃)	Outlet (℃)	ΔT_{cold} (℃)	Cold water heat transfer rate (kW)	Hot water heat transfer rate (W)	Effectiveness
1	0.005	27.0	32.0	5.0	0.105	1000	0.44
2	0.010	27.0	31.5	4.5	0.190		
3	0.023	27.0	31.0	4.0	0.386		
4	0.030	26.5	30.0	3.5	0.441		
5	0.033	26.0	29.0	3.0	0.443		
6	0.042	26.0	28.5	2.5	0.441		
7	0.054	25.8	27.5	1.7	0.386		

Table 19 : Measured data for thermal performance of HPHE with adiabatic section 1/3th of heat pipe

Obs. No.	Cold water mass flow rate (L/s)	Inlet (℃)	Outlet (℃)	ΔT_{cold} (℃)	Cold water heat transfer rate (W)	Hot water heat transfer rate (W)	Effectiveness
1	0.005	27.0	31.0	4.0	0.084	1000	0.39
2	0.010	27.0	30.0	3.0	0.126		
3	0.023	27.0	30.0	3.0	0.290		
4	0.030	26.5	29.5	3.0	0.378		
5	0.033	26.2	29.0	2.8	0.388		
6	0.042	26.0	28.2	2.2	0.388		
7	0.054	26.0	27.5	1.5	0.340		

Table 20: Measured data for thermal performance of HPHE with adiabatic section 32 mm downward from the middle

Obs. No.	Cold water mass flow rate (L/s)	Inlet (℃)	Outlet (℃)	ΔT_{cold} (℃)	Cold water heat transfer rate (W)	Hot water heat transfer rate (W)	Effectiveness
1	0.005	27.0	35.5	8.5	0.178	1000	0.57
2	0.010	27.0	34.0	7.0	0.294		
3	0.024	27.0	32.3	5.3	0.512		
4	0.030	26.5	31.0	4.5	0.567		
5	0.033	26.2	30.3	4.1	0.568		
6	0.042	26.0	29.1	3.1	0.547		
7	0.054	26.0	28.4	2.4	0.544		

Table 21: Measured data for thermal performance of HPHE with condensation section 32 mm upward from the middle

Obs. No.	Cold water mass flow rate (L/s)	Inlet (℃)	Outlet (℃)	ΔT_{cold} (℃)	Cold water heat transfer rate (kW)	Cold water heat transfer rate (W)	Effectiveness
1	0.005	27.0	33.5	6.5	0.136	1000	.53
2	0.010	27.0	33.0	6.5	0.273		
3	0.023	27.0	32.0	5.0	0.483		
4	0.030	26.8	31.0	4.2	0.529		
5	0.033	26.5	30.3	3.8	0.527		
6	0.042	26.0	28.8	2.8	0.494		
7	0.054	26.0	28	2.0	0.454		

Table 22: Measured data for thermal performance of HPHE with condensation section 64 mm upward from the middle

Obs. No.	Cold water mass flow rate (L/s)	Inlet (℃)	Outlet (℃)	ΔT_{cold} (℃)	Cold water heat transfer rate (kW)	Cold water heat transfer rate (W)	Effectiveness
1	0.005	27.0	33.0	6.0	0.126	1000	.50
2	0.010	27.0	33.0	6.0	0.252		
3	0.023	27.0	31.5	4.5	0.435		
4	0.030	26.5	30.5	4.0	0.504		
5	0.033	26.0	29.5	3.5	0.485		
6	0.042	26.0	28.8	2.8	0.494		
7	0.054	26.0	28.0	2.0	0.454		

Table 23: Description of Air to Air HPHE

Heat pipe	
Length	558 mm
Outer diameter	13 mm
Inner diameter	11.5 mm
Thickness	0.75 mm
Working fluid	Distilled Water
Percentage of fill	50%
No. of fins per pipe	7
Fin dimensions	38 mm × 38 mm

Separator plate	
Length	609.5 mm
Width	330 mm
Thickness	3 mm

Duct cross section	305 mm × 305 mm
Total no. of heat pipes	38
Total number of fins	266
Arrangement	Triangular

Table 24: Measured data for waste heat recovery

Obs. No.	**Cold air velocity (m/s)**	**Inlet** (℃)	**Outlet** (℃)	**Hot air velocity (m/s)**	**Inlet** (℃)	**Outlet** (℃)
1	2.24	27.7	29.7	1.20	62.75	55.3
2	2.24	31.5	34.0	0.84	79.75	71.7
3	2.24	31.5	34.0	0.58	94.5	82.7
4	2.08	29.0	30.2	0.36	76.25	64.0
5	1.81	30.0	31.0	0.25	80.25	70.3
6	1.81	28.0	29.2	0.41	72.5	62.3
7	1.70	28.2	29.5	0.66	61.33333	54.5
8	1.75	28.5	30.0	0.84	65.5	58.8
9	1.30	29.2	31.5	0.84	64.75	60.0
10	1.40	28.0	29.7	0.76	75	67.7
11	1.40	29.5	31.0	0.48	72	62.7
12	1.40	30.2	31.5	0.36	75.25	64.2

13	1.011	28.2	31.5	0.80	72.0	63.00
14	1.011	29.5	33.0	0.57	83.75	73.25
15	1.011	30.2	33.5	0.46	76.5	65.50
16	1.011	24.5	27.2	0.33	72.75	59.50

Table 25: Calculated data for waste heat recovery

Obs No.	**Cold air mass flow rate (kg/s)**	**Hot air mass flow rate (kg/s)**	ΔT_{cold} (℃)	ΔT_{hot} (℃)	**Cold side heat transfer rate (W)**	**Hot side heat transfer rate (W)**	**LMTD**	**Overall heat transfer co-efficient**	**Effectiveness**	**NTU**
1	0.24	0.12	2.0	7.5	586.16	1003.7	30.17	13.80	0.13	0.145
2	0.24	0.08	2.5	8.0	732.71	754.36	42.94	12.1	0.16	0.181
3	0.24	0.05	2.5	11.8	732.71	757.09	55.75	9.32	0.18	0.204
4	0.23	0.03	1.2	12.3	339.25	470.55	40.25	5.97	0.19	0.219
5	0.19	0.02	1.0	10.0	236.53	284.99	44.60	3.76	0.16	0.186
6	0.19	0.04	1.2	10.3	295.66	469.93	38.58	5.43	0.15	0.167
7	0.18	0.06	1.2	6.8	270.36	499.56	28.95	6.62	0.11	0.128
8	0.18	0.08	1.5	6.7	341.67	635.65	32.81	7.38	0.09	0.111
9	0.14	0.08	2.2	4.7	362.34	447.31	31.98	8.03	0.10	0.120
10	0.15	0.07	1.7	7.2	319.99	610.87	42.44	5.34	0.08	0.089
11	0.15	0.04	1.5	9.2	274.27	492.85	36.99	5.26	0.12	0.139
12	0.15	0.03	1.2	11.0	228.56	436.16	38.67	4.19	0.12	0.149
13	0.11	0.08	3.2	9.0	429.14	802.93	37.55	8.10	0.10	0.128
14	0.11	0.05	3.5	10.5	462.15	663.53	47.16	6.95	0.13	0.155
15	0.11	0.04	3.2	11.0	429.14	558.83	39.00	7.80	0.18	0.217

16	0.11	0.03	2.7	13.3	363.12	492.54	40.02	6.43	0.2025	0.244

Table 26: Measured data for air conditioning system

Obs. No.	**Cold air velocity (m/s)**	**Inlet** (℃)	**Outlet** (℃)	**Hot air velocity (m/s)**	**Inlet** (℃)	**Outlet** (℃)
1	0.32	20.5	22.7	0.96	40.5	38.7
2	0.51	20.0	22.0	0.96	40.0	38.5
3	0.73	20.7	22.2	0.96	40.5	38.5
4	1.06	20.7	22.0	0.96	40.2	38.0
5	1.36	21.0	22.0	0.96	40.7	39.0
6	0.32	21.7	23.7	1.42	40.2	39.0
7	0.50	21.0	22.7	1.42	40.7	38.7
8	0.74	21.0	22.2	1.42	40.5	39.0
9	1.06	20.7	21.7	1.42	40.2	39.0
10	1.37	20.7	21.7	1.42	40.5	39.2
11	0.33	21.7	23.2	1.16	42.0	39.0
12	0.53	21.2	22.5	1.16	41.2	39.0
13	0.71	21.0	21.7	1.16	41.0	39.0
14	1.06	21.0	22.0	1.16	41.0	39.2
15	1.39	21.5	22.0	1.16	41.2	39.2
16	0.34	22.0	23.0	0.61	39.5	37.2
17	0.53	21.0	22.0	0.61	41.0	38.0
18	0.72	21.0	21.7	0.61	40.5	38.0
19	1.00	21.5	22.2	0.61	40.7	38.2
20	1.37	21.7	22.7	0.61	40.7	38.0
21	0.38	22.7	23.5	1.62	40.2	38.0

22	0.51	22.5	23.5	1.62	40.5	38.7
23	0.71	22.5	23.25	1.62	41.0	39.2
24	0.93	23.0	24.0	1.62	40.2	39.0
25	1.38	22.7	23.5	1.62	41.2	39.2
26	0.29	23.5	24.7	1.70	40.7	39.2
27	0.52	24.0	25.0	1.70	41.0	40.2
28	0.70	24.0	25.0	1.70	41.5	40.2
29	1.0	23.0	23.7	1.70	41.0	39.2
30	1.32	23.0	23.5	1.70	41.0	39.2

Table 27: Calculated data for air conditioning system

Obs No.	**Cold air mass flow rate (kg/s)**	**Hot air mass flow rate (kg/s)**	ΔT_{cold} (℃)	ΔT_{hot} (℃)	**Cold side heat transfer rate (W)**	**Hot side heat transfer rate (W)**	**LMTD**	**Overall heat transfer co-efficient**	**Effectiveness**	**NTU**
1	0.036	0.10	2.2	1.7	97.25	190.73	18.00	3.83	0.11	0.12
2	0.05	0.10	2.0	1.5	137.77	163.48	18.25	5.35	0.10	0.11
3	0.08	0.10	1.5	2.0	147.90	217.97	18.00	5.82	0.07	0.08
4	0.11	0.10	1.2	2.2	178.97	245.22	17.75	7.15	0.08	0.09
5	0.15	0.10	1.0	1.7	183.70	190.73	18.37	7.09	0.08	0.09
6	0.03	0.14	2.0	1.2	86.44	201.51	16.87	3.63	0.10	0.11
7	0.05	0.14	1.7	2.0	118.19	322.42	17.87	4.69	0.08	0.09
8	0.08	0.14	1.2	1.5	124.94	241.81	18.12	4.89	0.06	0.06
9	0.11	0.14	1.0	1.2	143.18	201.51	18.37	5.52	0.05	0.05
10	0.15	0.14	1.0	1.2	185.05	201.51	18.62	7.04	0.05	0.06
11	0.03	0.12	1.5	3.0	66.86	395.08	17.99	2.63	0.07	0.08

12	0.05	0.12	1.2	2.2	89.48	296.31	18.25	3.48	0.06	0.07
13	0.07	0.12	0.7	2.0	71.92	263.38	18.62	2.74	0.03	0.04
14	0.11	0.12	1.0	1.7	143.18	230.46	18.62	5.45	0.05	0.07
15	0.15	0.12	0.5	2.0	93.87	263.38	18.49	3.60	0.03	0.04
16	0.03	0.06	1.0	2.2	45.92	155.82	15.87	2.05	0.05	0.06
17	0.05	0.06	1.0	3.0	71.58	207.76	17.98	2.82	0.05	0.05
18	0.08	0.06	0.7	2.5	72.93	173.13	17.86	2.89	0.05	0.056
19	0.11	0.06	0.7	2.5	101.30	173.13	17.61	4.08	0.07	0.08
20	0.15	0.06	1.0	2.7	185.05	190.44	17.11	7.67	0.14	0.17
21	0.04	0.17	0.7	2.2	38.49	413.81	15.99	1.71	0.04	0.04
22	0.05	0.17	1.0	1.7	68.88	321.85	16.62	2.94	0.05	0.06
23	0.07	0.17	0.7	1.7	71.92	321.85	17.25	2.96	0.04	0.04
24	0.10	0.17	1.0	1.2	125.62	229.89	16.12	5.52	0.05	0.06
25	0.15	0.17	0.7	2.0	139.80	367.83	17.12	5.79	0.04	0.04
26	0.03	0.17	1.2	1.5	48.96	289.50	15.87	2.19	0.07	0.08
27	0.05	0.17	1.0	0.7	70.23	144.75	16.12	3.09	0.05	0.06
28	0.07	0.17	1.0	1.2	94.55	241.25	16.37	4.09	0.05	0.06
29	0.11	0.17	0.7	1.7	101.30	337.74	16.75	4.29	0.04	0.04
30	0.14	0.17	0.5	1.7	89.14	337.74	16.87	3.75	0.02	0.03

Table 28: Percentage uncertainty in different parameters for waste heat recovery

Obs. No.	Cold air mass flow rate	Hot air mass flow rate	Cold side heat transfer rate	Hot side heat transfer rate	LMTD	Overall heat transfer co-efficient	$\dot{Q}_{max}$	Effectiveness	NTU
1	2.2	4.1	7.4	4.590	0.33	7.83	0.40	07.4	8.21
2	2.2	5.9	6.0	6.18	0.23	6.58	0.29	06.1	7.03
3	2.2	8.6	6.0	8.74	0.18	6.58	0.22	06.0	7.03
4	2.4	14.5	11.6	14.6	0.25	11.80	0.30	11.6	12.1
5	2.7	19.6	14.4	19.6	0.23	14.60	0.28	14.4	14.8
6	2.7	12.2	11.7	12.20	0.26	11.90	0.32	11.7	12.2
7	3.0	7.6	11.7	7.91	0.35	12.00	0.43	11.7	12.2
8	3.0	6.0	9.8	6.29	0.31	10.20	0.38	09.8	10.5
9	4.0	56.0	7.5	6.64	0.31	7.89	0.40	07.5	8.27
10	3.6	6.6	8.8	6.91	0.24	9.18	0.30	08.8	9.51
11	3.6	10.5	10.1	10.60	0.27	10.40	0.33	10.1	10.7
12	3.6	14.1	11.9	14.10	0.26	12.10	0.31	11.9	12.4
13	4.9	6.3	6.6	6.45	0.27	7.05	0.32	06.6	7.47
14	4.9	8.8	6.4	8.93	0.21	6.86	0.26	06.4	7.29
15	4.9	11.0	6.6	11.10	0.26	7.05	0.31	06.6	7.47
16	4.9	15.0	7.1	15.00	0.25	7.56	0.29	07.1	7.96

Table 29: Percentage uncertainty in different parameters for air conditioning system

Obs. No.	Cold air mass flow rate	Hot air mass flow rate	Cold side heat transfer rate	Hot side heat transfer rate	LMTD	Overall heat transfer co-efficient	$\dot{Q}_{max}$	Effectiveness	NTU
1	15.6	5.22	16.8	9.62	0.56	17.0	0.71	16.9	17.2
2	9.8	5.22	12.1	10.8	0.55	12.4	0.71	12.1	12.6
3	6.8	5.22	11.7	8.79	0.56	11.9	0.72	11.7	12.2
4	4.7	5.22	12.3	8.17	0.56	12.5	0.73	12.3	12.8
5	3.7	5.22	14.6	9.62	0.54	14.8	0.72	14.6	15.0
6	15.6	3.54	17.2	11.90	0.59	17.3	0.76	17.2	17.5
7	10.0	3.54	12.9	7.91	0.56	13.1	0.72	12.9	13.3
8	6.7	3.54	13.2	10.10	0.55	13.4	0.73	13.2	13.6
9	4.7	3.54	14.9	11.90	0.54	15.1	0.73	14.9	15.3
10	3.6	3.54	14.6	11.90	0.54	14.8	0.72	14.6	15.0
11	15.2	4.32	17.8	6.40	0.56	18.0	0.70	17.9	18.2
12	9.4	4.32	14.7	7.63	0.55	15.0	0.71	14.8	15.2
13	7.0	4.32	20.1	8.29	0.54	20.3	0.71	20.1	20.4
14	4.7	4.32	14.9	9.16	0.54	15.1	0.71	14.9	15.3
15	3.6	4.32	28.5	8.29	0.54	28.6	0.72	28.5	28.7
16	14.7	8.20	20.4	10.30	0.63	20.6	0.81	20.4	20.7
17	9.4	8.20	17.0	9.46	0.56	17.2	0.71	17.0	17.4
18	6.9	8.20	20.1	9.96	0.56	20.3	0.73	20.1	20.4
19	5.0	8.2	19.5	9.96	0.57	19.7	0.73	19.5	19.8
20	3.6	8.2	14.6	9.68	0.59	14.8	0.74	14.6	15.0
21	13.2	3.1	23.0	7.01	0.63	23.1	0.81	23	23.3
22	9.8	3.1	17.2	8.66	0.6	17.4	0.79	17.2	17.6

23	7.0	3.1	20.1	8.66	0.58	20.3	0.76	20.1	20.4
24	5.4	3.1	15.1	11.70	0.62	15.3	0.82	15.2	15.5
25	3.6	3.1	19.2	7.72	0.58	19.4	0.76	19.2	19.5
26	17.2	2.96	20.6	9.88	0.63	20.8	0.82	20.6	20.9
27	9.6	2.96	17.1	19.10	0.62	17.3	0.83	17.1	17.5
28	7.1	2.96	15.8	11.70	0.61	16.1	0.81	15.9	16.2
29	5.0	2.96	19.5	8.61	0.6	19.7	0.79	19.5	19.8
30	3.8	2.96	28.5	8.61	0.59	28.7	0.79	28.5	28.8

Appendix-B

Sample Calculation

Measured Data for water-to-water HPHE

Dimensions of heat pipe:

Outer diameter, $D_o = 13\ mm$

Inner diameter, $D_i = 11.5$ mm

Fin Dimension = 25 mm × 25 mm

Number of fin per tube = 2

Total no. of fins = 12

Total no. of tubes = 6

Length of heat pipe, $L = 280$ mm

Radius of plate, $R_p = 76.2$ mm

Thickness of plate, $T_p = 5$ mm

Calculated Data for water-to-water HPHE

Heat pipe cross section area:

$$A_c = \frac{\pi {D_o}^2}{4}$$

$$= \frac{3.1416 \times 0.013^2}{4}$$

$$= 1.32 \times 10^{-4}\ m^2$$

Plate area:

$$A_{pl} = \pi r^2 - 6A_c$$

$$= 3.1416 \times 0.0726^2 - 6 \times 1.33 \times 10^{-4}$$

$$= 0.0174\ m^2$$

Heat pipe surface area:

$$A_s = 6\pi D_o L_c$$

$$= 6 \times 3.1416 \times 0.013 \times 0.280$$

$$= 0.011435\ m^2$$

Total fin area:

$A_f = 12 \times (0.025 \times 0.025 - A_c)$

$= 12 \times (0.038 \times 0.038 - 1.32 \times 10^{-4})$

$= 0.0059\ m^2$

Total heat transfer area:

$A = A_{pl} + A_s + A_f$

$= 0.0174 + 0.011435 + 0.0059$

$= 0.092\ m^2$

OBSERVATION OF RESULT WITHOUT ADIABATIC SECTION

1. <u>For mass flow rate of 0.005 L/s</u>

Cold or condensation side parameters:

Inlet temperature, $T_{c,in} = 27$ ℃

Outlet temperature, $T_{c,out} = 39$ ℃

Temperature gradient = 12 ℃

Specific heat, $C_{p,cold} = 4.2$ kJ/kg. K

Mass flow rate, $\dot{m}_{cold} = 0.005\ l/s$

Hot or evaporation side parameters:

Constant heat input, $\dot{Q}_{hot}$ = 1000 W

Heat transfer rate, $\dot{Q}_{cold} = \dot{m}_{cw} Cp_{cw} (T_{cw,in} - T_{cw,out})$

$= .005 * 4.2 * 12$

$= 0.252$ kW

Heat transfer coefficient, $U = \dot{Q}_{cold} / A\ \Delta T$

$= 252/0.092 * 12$

$= 228.26\ W/m^2K$

2. For mass flow rate of 0.01 L/s:

Inlet temperature = 27 ℃

Outlet temperature = 35 ℃

Temperature gradient = 8 ℃

Specific heat, Cp = 4.2 kj/kg.k

Heat transfer rate $\dot{Q}_{cold} = \dot{m}_{cw} Cp_{cw} (T_{cw,in} - T_{cw,out})$

= .01* 4.2*8

= 0.336 kW

Heat transfer coefficient, U = $\dot{Q}_{cold}$ /A ΔT = 336/0.092*8 = 456.52 W/m^2K

3. For mass flow rate of 0.023 L/s:

Inlet temperature = 27 ℃

Outlet temperature = 33 ℃

Temperature gradient = 6 ℃

Specific heat, Cp = 4.2 kj/kg.k

Heat transfer rate, $\dot{Q}_{cold} = \dot{m}_{cw} Cp_{cw} (T_{cw,in} - T_{cw,out})$

= 0.023*4.2*6

= 0.5796 W

Heat transfer coefficient, U = $\dot{Q}_{cold}$ /A ΔT = 579.6 / 0.092*6 = 1050 W/m^2K

4. For mass flow rate of 0.03 L/s:

Inlet temperature = 27 ℃

Outlet temperature = 32 ℃

Temperature gradient = 5 ℃

Specific heat, Cp = 4.2 kj/kg.k

Heat transfer rate, $\dot{Q}_{cold} = \dot{m}_{cw} Cp_{cw} (T_{cw,in} - T_{cw,out})$

= .03* 4.2*5

= 0.63 kW

Heat transfer coefficient, U = $\dot{Q}_{cold}$ /A ΔT = 630 / 0.092*5 = 1369.56 W/m^2K

5. For mass flow rate of 0.033 L/s:

Inlet temperature = 26.5 ℃

Outlet temperature = 31 ℃

Temperature gradient = 4.5 ℃

Specific heat, Cp = 4.2 kj/kg.k

Heat transfer rate, $\dot{Q}_{cold} = \dot{m}_{cw} Cp_{cw} (T_{cw,in} - T_{cw,out})$

= 033* 4.2*4.5

= 0.6237 kW

Heat transfer coefficient, $U = \dot{Q}_{cold} / A \Delta T$ = 623.7/0.092*4.5 =1506.52 W/m^2K

6. For mass flow rate of 0.042 L/s:

Inlet temperature = 26.5 ℃

Outlet temperature = 30 ℃

Temperature gradient = 3.5 ℃

Specific heat, Cp = 4.2 kj/kg.k

Heat transfer rate $\dot{Q}_{cold} = \dot{m}_{cw} Cp_{cw} (T_{cw,in} - T_{cw,out})$

= .042* 4.2*3.5

= 0.6174 kW

Heat transfer coefficient, $U = \dot{Q}_{cold} / A \Delta T$ = 617.4/0.092*3.5 =1917.4 W/m^2K

7. For mass flow rate of 0.054 L/s:

Inlet temperature = 26 ℃

Outlet temperature =29 ℃

Temperature gradient =3 ℃

Specific heat, Cp =4.2 kj/kg.k

Heat transfer rate, $\dot{Q}_{cold} = \dot{m}_{cw} Cp_{cw} (T_{cw,in} - T_{cw,out})$

= 0.054* 4.2*3

= 0.6804 kW

Heat transfer coefficient, $U = \dot{\mathbf{Q}}_{cold} / A \Delta T$ = 680.4/0.092*3 =2465.2 W/m^2

Effectiveness, □ = $\dot{Q}_{cold} / Q_{max}$

= 680.4 /1000

= 0.6804 = 68.04 %

Measured Data for Air-to-Air HPHE

Dimensions of heat pipe:

Outer diameter, $D_o = 13mm$

Inner diameter, $D_i = 11.5$ mm

Fin Dimension = 38 mm × 38 mm

Number of fin per tube = 7

Total no. of fins = 266

Total no. of tubes = 38

Length of condenser/evaporator section, $L_c = 558$ mm

Length of plate, $L_p = 0.6095$ m

Width of plate, $W_p = 0.330$ m

For **observation no. 9** at waste heat recovery application

Cold side air flow:

Velocity, $V_{cold} = 1.233$ m/s

Inlet temperature, $T_{c,in} = 29.25$ ℃

Outlet temperature, $T_{c,out} = 31.5$ ℃

Density, $\rho_{cold} = 1.17$ kg/m3

Specific heat, $C_{p,cold} = 1.2$ kJ/kg. K

Hot side air flow:

Velocity, $V_{hot} = 0.84$ m/s

Inlet temperature, $T_{h,in} = 64.75$ ℃

Outlet temperature, $T_{h,out} = 60$ ℃

Density, $\rho_{hot} = 1.11$ kg/m^3

Specific heat, $C_{p,hot} = 1.08$ kJ/kg. K

Calculated Data for Air-to-Air HPHE

Heat pipe cross section area:

$$A_c = \frac{\pi {D_o}^2}{4}$$

$$= \frac{3.1416 \times 0.013^2}{4}$$

$$= 1.33 \times 10^{-4}\ m^2$$

Plate area:

$$A_{pl} = L_p W_p - 38A_c$$

$$= 0.6095 \times 0.330 - 38 \times 1.33 \times 10^{-4}$$

$$= 0.196\ m^2$$

Heat pipe surface area:

$$A_s = 38\pi D_o L_c$$

$$= 38 \times 3.1416 \times 0.013 \times 0.558$$

$$= 0.866\ m^2$$

Total fin area:

$$A_f = 266 \times (0.038 \times 0.038 - A_c)$$

$$= 266 \times (0.038 \times 0.038 - 1.33 \times 10^{-4})$$

$$= 0.3498\ m^2$$

Total heat transfer area:

$$A = A_{pl} + A_s + A_f$$

$$= 0.196 + 0.866 + 0.349$$

$$= 1.411\ m^2$$

$$\Delta T_{hot} = \Delta T_{h,in} - \Delta T_{h,out}$$
$$= 64.75 - 60\ ℃$$
$$= 4.75\ ℃$$

$$\Delta T_{cold} = \Delta T_{c,out} - \Delta T_{c,in}$$
$$= 31.5 - 29.25\ ℃$$
$$= 2.25\ ℃$$

$$A_{duct} = 0.305 \times 0.305\ m^2$$
$$= 0.093025\ m^2$$

Mass flow rate:

$\dot{m}_{hot} = \rho_{hot} A_{duct} V_{hot}$

$= 1.11 \times 0.093025 \times 0.84\ kg/s$

$= 0.0872\ kg/s$

$\dot{m}_{cold} = \rho_{cold} A_{duct} V_{cold}$

$= 1.17 \times 0.093025 \times 1.233\ kg/s$

$= 0.1342\ kg/s$

Heat capacity:

$C_{hot} = m_{hot} C_{p,hot}$

$= 0.0872 \times 1080$

$= 94.17\ J/k$

$C_{cold} = m_{cold} C_{p,cold}$

$= 0.135 \times 1200$

$= 161.04\ J/k$

Here,

$C_{min} = C_{hot} = 94.17\ J/k$

$C_{max} = C_{cold} = 161.04\ J/k$

Heat transfer rate:

$\dot{Q}_{cold} = m_{cold} C_{p,cold} \Delta T_{cold}$

$= 0.1342 \times 1200 \times 2.25$

$= 362.34\ W$

$\dot{Q}_{hot} = m_{hot} C_{p,hot} \Delta T_{hot}$

$= 0.0872 \times 1080 \times 4.75$

$= 447.31\ W$

$\dot{Q}_{max} = C_{min}(T_{h,in} - T_{c,in})$

$= 94.17 \times (64.75 - 29.25)$

$= 3343.07\ W$

Effectiveness:

$$\varepsilon = \frac{\dot{Q}_{cold}}{\dot{Q}_{max}}$$

$$= \frac{362.34}{3343.07}$$

$= 0.1084$

$= 10.84\ \%$

LMTD:

$$\Delta T_{lm} = \frac{\{(T_{h,in} - T_{c,out}) - (T_{h,out} - T_{c,in})\}}{\ln\left\{\frac{T_{h.in} - T_{c,out}}{T_{h,out} - T_{c,in}}\right\}}$$

$$= \frac{\{(64.75 - 31.5) - (60 - 29.25)\}}{\ln\left\{\frac{64.75 - 31.5}{60 - 29.25}\right\}}$$

$$= 31.98\ ℃$$

Overall heat transfer coefficient:

$$U = \frac{\dot{Q}_{cold}}{A \times LMTD}$$

$$= \frac{362.34}{1.411 \times 31.98}$$

$$= 8.03\ W/m^2K$$

Number of transfer units:

$$NTU = \frac{U \times A}{C_{min}}$$

$$= \frac{8.03 \times 1.411}{94.17} = 0.1203$$

Uncertainty Analysis

Separator plate area:

Plate length, $a = 609.5 \pm 0.5\ mm$

Plate width, $b = 330 \pm 0.5\ mm$

Hole diameter, $d_o = 13 \pm 0.5\ mm$

Plate area, $A_p = ab - \left(\frac{\pi {d_o}^2}{4}\right) \times 38 = 609.5 \times 330 - \left(3.1416 \times \frac{13^2}{4}\right) \times 38$

$$= 196091.2\ mm^2$$

$$\frac{\partial A_p}{\partial a} = b = 330\ mm$$

$$\frac{\partial A}{\partial b} = a = 609.5\ mm$$

$$\frac{\partial A}{\partial d_o} = 19 \times \pi \times d = 19 \times 3.1416 \times 13 = 775.97$$

$w_{A_p} = \sqrt{(330 \times 0.5)^2 + (609.5 \times 0.5)^2 + (775.97 \times 0.5)^2} = 520.22\ mm^2$

$\therefore A_p = 196091.2 \pm 520.22\ mm^2$

Fin area:

Fin length, $a = 38 \pm 0.5\ mm$

Total fin area, $A_f = \left(a^2 - \frac{\pi {d_o}^2}{4}\right) \times 266$

$= \left(382 - \frac{3.1416 \times 132}{4}\right) \times 266$

$= 348797.21\ mm^2$

$\frac{\partial A_f}{\partial a} = 532a = 532 \times 38 = 20216$

$\frac{\partial A}{\partial d_o} = 133\pi d_o = 133 \times 3.1416 \times 13 = 5431.81$

$\therefore w_{A_f} = \sqrt{(20216 \times 0.5) + (5431.81 \times 0.5)} = 10466.51\ mm^2$

$\therefore A_f = 348797.21 \pm 10466.51\ mm^2$

Pipe surface area:

Pipe length, $L = 558 \pm 0.5\ mm$

Pipe surface area, $A_s = \pi d_o L \times 38$

$= 3.1416 \times 13 \times 558 \times 38$

$= 865986.3\ mm^2$

$\frac{\partial A_s}{\partial d_o} = 38 \times \pi \times L = 38 \times 3.1416 \times 558 = 66614.33\ mm$

$\frac{\partial A_s}{\partial L} = 38 \times \pi \times d_o = 38 \times 3.1416 \times 13 = 1551.95\ mm$

$w_{A_s} = \sqrt{(66614.33 \times 0.5)^2 + (1551.95 \times 0.5)^2} = 33316.2\ mm^2$

$\therefore A_s = 865986.3 \pm 33316.2\ mm^2$

Flow area:

Duct width, $a = 305 \pm 0.5\ mm$

Flow area, $A = a^2 = 305^2 = 93025\ mm^2$

$\frac{\partial A}{\partial a} = 2\text{a} = 2 \times 305 = 610\ \text{mm}$

$w_A = \sqrt{(610 \times 0.5)} = 305\ mm^2$

$\therefore \text{A} = 93025 \pm 305\ mm^2$

Cold air mass flow rate:

Density, $\rho = 1.17\ kg/m^3$

Flow area, $A = 93025 \pm 305\ mm^2$

Velocity, $V = 1.233 \pm 0.05\ m/s$

$\therefore \dot{m} = \rho \times A \times V = 1.17 \times 0.093025 \times 1.233 = 0.13420\ kg/s$

$\frac{\partial \dot{m}}{\partial A} = \rho \times V = 1.17 \times 1.233 = 1.4426$

$\frac{\partial \dot{m}}{\partial V} = \rho \times A = 1.17 \times 0.093025 = 0.1088$

$w_{\dot{m}} = \sqrt{(1.4426 \times 0.000305)^2 + (0.1088 \times 0.05)^2} = 0.00546\ kg/s$

$\therefore \dot{m} = 0.1340 \pm 0.00546\ kg/s$

Percentage of uncertainty $= \frac{0.00546}{0.1340} \times 100\% = 4.07\%$

Hot air mass flow rate:

Density, $\rho = 1.11\ kg/m^3$

Flow area, $A = 93025 \pm 305\ mm^2$

Velocity, $V = 1.443 \pm 0.05\ m/s$

$\therefore \dot{m} = \rho \times A \times V = 1.11 \times 0.093025 \times 1.443 = 0.08719\ kg/s$

$\frac{\partial \dot{m}}{\partial A} = \rho \times V = 1.11 \times 1.443 = 0.9373$

$\frac{\partial \dot{m}}{\partial V} = \rho \times A = 1.11 \times 0.093025 = 0.1033$

$w_{\dot{m}} = \sqrt{(0.9373 \times 0.000305)^2 + (0.1033 \times 0.05)^2} = 0.00517\ kg/s$

$\therefore \dot{m}_h = 0.08719 \pm 0.00517\ kg/s$

Percentage of uncertainty $= \frac{0.00517}{0.08719} \times 100\% = 5.93\%$

Cold air temperature rise:

$T_{c.in} = 29.25 \pm 0.1℃$

$T_{c.out} = 31.5 \pm 0.1℃$

$\Delta T_c = T_{c,out} - T_{c,in} = 31.5 - 29.25 = 2.25$

$\frac{\partial \Delta T_c}{\partial T_{c,in}} = -1$

$\frac{\partial \Delta T_c}{\partial T_{c,out}} = 1$

$\therefore w_{\Delta T_c} = \sqrt{(-1 \times 0.1)^2 + (1 \times 0.1)^2} = 0.1414$

$$\therefore \Delta T_c = 2.25 \pm 0.1414℃$$

Percentage of uncertainty $= \frac{0.1414}{2.25} \times 100\% = 6.28\%$

Hot air temperature reduction:

$T_{c.in} = 64.75 \pm 0.1℃$

$T_{c.out} = 60 \pm 0.1℃$

$\Delta T_h = T_{h,in} - T_{h,out} = 64.75 - 60 = 4.75℃$

$\frac{\partial \Delta T_h}{\partial T_{h,in}} = 1$

$\frac{\partial \Delta T_c}{\partial T_{h,out}} = -1$

$\therefore w_{\Delta T_h} = \sqrt{(1 \times 0.1)^2 + (-1 \times 0.1)^2} = 0.1414$

$$\therefore \Delta T_c = 4.75 \pm 0.1414℃$$

Percentage of uncertainty $= \frac{0.1414}{4.75} \times 100\% = 2.98\%$

Cold side heat transfer:

Mass flow rate, $\dot{m}_c = 0.1340 \pm 0.00546\ kg/s$

Specific heat capacity, $C_{p,c} = 1200\ J/kgK$

Temperature rise, $\Delta T_c = 2.25 \pm 0.1414℃$

$\dot{Q}_c = \dot{m}_c C_{p,c} \Delta T_c = 0.13420 \times 1200 \times 2.25 = 362.337\ W$

$\frac{\partial \dot{Q}_c}{\partial \dot{m}_c} = C_{p,c} \Delta T_c = 1200 \times 2.25 = 2700$

$\frac{\partial \dot{Q}_c}{\partial \Delta T_c} = \dot{m}_c C_{p,c} = 0.13420 \times 1200 = 161.04$

$\therefore w_{\dot{Q}_c} = \sqrt{(2700 \times 0.00546)^2 + (161.04 \times 0.1414)^2} = 27.129$

$$\therefore \dot{Q}_c = 362.337 \pm 27.129\ W$$

Percentage of uncertainty $= \frac{27.129}{362.337} \times 100\% = 7.49\%$

Hot side heat transfer:

Mass flow rate, $\dot{m}_h = 0.08719 \pm 0.00517 kg/s$

Specific heat capacity, $C_{p,h} = 1080\ J/kgK$

Temperature rise, $\Delta T_h = 4.75 \pm 0.1414℃$

$$\dot{Q}_h = \dot{m}_h C_{p,h} \Delta T_h = 0.08719 \times 1080 \times 4.75 = 447.313\ W$$

$$\frac{\partial \dot{Q}_h}{\partial \dot{m}_h} = C_{p,h} \Delta T_h = 1080 \times 4.75 = 5130$$

$$\frac{\partial \dot{Q}_h}{\partial \Delta T_h} = \dot{m}_h C_{p,h} = 0.08719 \times 1080 = 94.171$$

$$\therefore w_{\dot{Q}_h} = \sqrt{(5130 \times 0.00517)^2 + (94.171 \times 0.1414)^2} = 29.632$$

$$\therefore \dot{Q}_c = 447.313 \pm 29.632\ W$$

Percentage of uncertainty $= \frac{29.632}{447.313} \times 100\% = 6.64\%$

LMTD:

$$\Delta T_1 = T_{h,in} - T_{c,out} = 64.75 - 31.5 = 33.25℃$$

$$\Delta T_2 = T_{h,out} - T_{c,in} = 60 - 29.25 = 30.75℃$$

$$LMTD = \frac{\Delta T_1 - \Delta T_2}{\ln\left(\frac{\Delta T_1}{\Delta T_2}\right)} = \frac{33.25 - 30.75}{\ln\left(\frac{33.25}{30.75}\right)} = 31.98℃$$

$$\frac{\partial (LMTD)}{\partial \Delta T_1} = \frac{\left(\ln\frac{\Delta T_1}{\Delta T_2}\right) \times 1 - (\Delta T_1 - \Delta T_2) \times \frac{1}{\Delta T_1}}{\left(\ln\frac{\Delta T_1}{\Delta T_2}\right)^2}$$

$$= \frac{\left(\ln\frac{33.25}{30.75}\right) \times 1 - (33.25 - 30.75) \times \frac{1}{33.25}}{\left(\ln\frac{33.25}{30.75}\right)^2} = 0.48722$$

$$\frac{\partial (LMTD)}{\partial \Delta T_2} = \frac{\left(\ln\frac{\Delta T_1}{\Delta T_2}\right) \times -1 - (\Delta T_1 - \Delta T_2) \times \frac{1}{-\Delta T_2}}{\left(\ln\frac{\Delta T_1}{\Delta T_2}\right)^2}$$

$$= \frac{\left(\ln\frac{33.25}{30.75}\right) \times -1 - (33.25 - 30.75) \times \frac{1}{-30.75}}{\left(\ln\frac{33.25}{30.75}\right)^2} = 0.51329$$

$$\therefore w_{LMTD} = \sqrt{(0.48722 \times 0.1414)^2 + (0.51329 \times 0.1414)^2} = 0.1001$$

$$\therefore LMTD = 31.98 \pm 0.1001℃$$

Percentage of uncertainty $= \frac{0.1001}{31.98} \times 100\% = 0.31\%$

Overall heat transfer coefficient:

$$U = \frac{\dot{Q}_{cold}}{A \times LMTD} = \frac{362.337}{1.4109 \times 31.98} = 8.0296\ W/m^2K$$

$$\frac{\partial U}{\partial \dot{Q}_{cold}} = \frac{1}{A \times LMTD} = \frac{1}{1.4109 \times 31.98} = 0.02216$$

$$\frac{\partial U}{\partial A} = \frac{-\dot{Q}_{cold}}{A^2 \times LMTD} = \frac{-362.337}{1.4109^2 \times 31.98} = -0.25105$$

$$\frac{\partial U}{\partial (LMTD)} = \frac{-\dot{Q}_{cold}}{A \times LMTD^2} = \frac{-362.337}{1.4109 \times 31.98^2} = -5.69124$$

$$\therefore w_U = \sqrt{(0.02216 \times 27.129)^2 + (-0.25105 \times 0.034925)^2 + (-5.69124 \times 1.001)^2}$$

$$= 0.63370$$

$$\therefore U = 8.0296 \pm 0.63370\ W/m^2K$$

Percentage of uncertainty $= \frac{0.63370}{8.0296} \times 100\% = 7.89\%$

$\dot{Q}_{max}$:

$$\dot{Q}_{max} = C_{min} \times \Delta T_{in} = 94.171 \times [(64.75 - 29.25) \pm 0.1414]\ W$$

$$= 3343.073 \pm 13.318\ W$$

Percentage of uncertainty $= \frac{13.318}{3343.073} \times 100\% = 0.40\%$

Effectiveness:

$$\dot{Q}_c = 447.313 \pm 29.632\ W$$

$$\varepsilon = \frac{\dot{Q}_c}{\dot{Q}_{max}} = \frac{362.337}{3343.073} = 0.1084$$

$$\frac{\partial \varepsilon}{\partial \dot{Q}_c} = \frac{1}{\dot{Q}_{max}} = \frac{1}{3343.073} = 0.000299$$

$$\frac{\partial \varepsilon}{\partial \dot{Q}_{max}} = \frac{\dot{Q}_c}{\dot{Q}_{max}{}^2} = \frac{362.337}{3343.073^2} = -3.24 \times 10^{-5}$$

$$\therefore w_\varepsilon = \sqrt{(0.000299 \times 27.129)^2 + (-3.24 \times 10^{-5} \times 13.318)^2} = 0.008126$$

$$\therefore \varepsilon = 0.1084 \pm 0.0081$$

Percentage of uncertainty $= \frac{0.0081}{0.1084} \times 100\% = 7.50\%$

Number of transfer units:

$$NTU = \frac{U \times A}{C_{min}} = \frac{8.0296 \times 1.40875}{94.171} = 0.12030$$

$$\frac{\partial(NTU)}{\partial U} = \frac{A}{C_{min}} = \frac{1.40875}{94.171} = 0.014982$$

$$\frac{\partial(NTU)}{\partial A} = \frac{U}{C_{min}} = \frac{8.0296}{94.171} = 0.085266$$

$$\therefore w_{NTU} = \sqrt{(0.014982 \times 0.6337)^2 + (0.085266 \times 0.034925)^2} = 0.00995$$

$$\therefore NTU = 0.12030 \pm 0.00995$$

Percentage of uncertainty $= \frac{0.00995}{0.12030} \times 100\% = 8.27\%$